12-2018

The Effects of Seasonal Variations In Chemistry and Hydrology on the Microbial Community and Its Sulfide Oxidation Potential In a Naturally Acidic Maine Stream

Raymond C. Kahler III
University of Maine, raymond.kahler@maine.edu

THE EFFECTS OF SEASONAL VARIATIONS IN CHEMISTRY AND HYDROLOGY ON THE MICROBIAL COMMUNITY STRUCTURE AND ITS SULFIDE OXIDATION POTENTIAL IN A NATURALLY ACIDIC MAINE STREAM

By

Raymond C Kahler III

B.S. University of South Carolina, 2014

A THESIS

Submitted in Partial Fulfillment of the

Requirements for the Degree of

Master of Science

(in Earth and Climate Sciences)

The Graduate School

University of Maine

December 2018

Advisory Committee:

Amanda Albright Olsen, Associate Professor, School of Earth and Climate Sciences, Co-Advisor

Jean D. MacRae, Associate Professor, Department of Civil and Environmental Engineering, Co-Advisor

Andrew Reeve, Professor, School of Earth and Climate Science

THE EFFECTS OF SEASONAL VARIATIONS IN CHEMISTRY AND HYDROLOGY ON THE MICROBIAL COMMUNITY STRUCTURE AND ITS SULFIDE OXIDATION POTENTIAL IN A NATURALLY ACIDIC MAINE STREAM

By Raymond C Kahler III

Thesis Co-Advisors: Dr. Amanda Olsen & Dr. Jean MacRae

An Abstract of the Thesis Presented
In Partial Fulfillment of the Requirements for the
Degree of Master of Science
(in Earth and Climate Sciences)
December 2018

Sulfide minerals oxidize through interaction with water and oxygen, releasing hydrogen ions. The process often occurs naturally near metal sulfide deposits, and can be accelerated through mining. Microorganisms accelerate the rate of sulfide oxidation. Acidified streams typically contain high metal concentrations (e.g. aluminum) and microbes in these systems may develop resistances to metal toxicity. Stream flow can affect sulfide oxidation and microbial community structure. Baseflow can influence stream chemistry from interactions with the surrounding bedrock, while stormflow affects stream chemistry and the local microbial community through dilution and addition of microbes transported by runoff. Microbial community composition is affected by seasonal shifts in water chemistry and climate conditions like temperature and precipitation. Little work has addressed the effects of acidification upon the biogeochemistry in streams located near sulfide deposits in northern New England and similar ecosystems. Maine has numerous metallic sulfide deposits. It is important to understand what microbes are present in aqueous systems near these deposits, the effects of chemistry

and climate on their structure, and their sulfide oxidation potential within acidifying conditions in case one of these deposits were ever to be mined. We conducted a field study to assess community structure and its relationships with changing seasonal chemistry and hydrology within a naturally acidic stream Blood Brook. In the field, Blood Brook chemistry and microbial community was sampled and studied across an 8-month period of seasonal transition. We found that the community was resembled a typical community, with a small population of circumneutral iron-oxidizing bacteria. Changes in the microbial community structure were primarily driven by changes in stream flow throughout the study period, with stormflow overall increasing diversity.

A series of three, five-week, batch reactor experiments were also conducted to assess changes within the experimental community exposed to increased amounts of pyrite, and to assess how its sulfide oxidation potential changed from differing sampling conditions. Experiments were conducted using an abiotic and biotic treatment. During the experiments, we found no significant differences between abiotic and biotic sulfate concentration changes, but there were significant differences in pH changes between treatments. Microbial community analyses of the experimental solutions revealed that there were limited classified sulfide or iron oxidizing bacteria, despite precipitate evidence of circumneutral iron oxidizing bacteria. These data suggest that there is limited bacterial sulfide oxidation occurring, and that something else was driving biological pH changes. Dominant in the final communities were genera *Acidocella* and *Acidisoma*, indicating the acidic conditions drove the microbial community to become an acidophilic one. Precipitate observations revealed structures resembling those produced by previously identified circumneutral iron oxidized bacteria. The final experimental communities

resembled those that have been observed in circumneutral iron-rich groundwater and surface water communities.

We concluded that the Blood Brook microbial community is primarily a stream community, whose structure is primarily influenced in changes in hydrologic flow conditions. We also conclude that under experimental acidifying conditions, changes in the community are primarily driven by decreases in pH and increases in specific conductance.

ACKNOWLEDGEMENTS

I'd like to thank my advisors Amanda Olsen and Jean MacRae. I would have been a flounder gasping for water without all their continuous wisdom and assistance they have given me the entire time I've been here at UMaine. I'd also like to thank Andy Reeve for his vast knowledge of hydrologic principles and without him the triumvirate ruling committee would not be complete. Gratitude must also be given to the UMaine Graduate Student Government for the funding they helped to provide towards this project. I also must thank the numerous friends who have helped with my project or even just listened to me rant about bacteria endlessly. Specific names I must throw out include Jason Lively, Brian Morra, Andrew Newcomb, and Brett Gerard. There's also my parents Vickie and Ray Kahler, who find the strength to continuously support me from a distance and not berate me for spending way too much time in graduate school. Lastly, I must thank the woman of the hour, my lovely wife Emily, without whom this thesis would never have been completed. When I had nights of hopelessness, and countless endless stresses where I thought I was going to fail, her support and love kept me going even through sleepless nights. Without her, I would have been lost. Oh, I almost forgot, thanks TK, for putting up with my endless stress hugs. You're the best cat.

TABLE OF CONTENTS

LIST OF TABLES

LIST OF FIGURES

LIST OF EQUATIONS

LIST OF ABBREVIATIONS

A	Area (km^2)
AB	Abiotic
AMD	Acid Mine Drainage
ARD	Acid Rock Drainage
Aug	August
B	Biotic
BB	Blood Brook
C	Celsius
cm	Centimeter
Conc.	Concentration
Δt	Change in time
Dec	December
DO	Dissolved Oxygen
DOC	Dissolved Organic Carbon
DNA	Deoxyribose Nucleic Acid
EPA	Environmental Protection Agency
Eq.	Equation
Exp.	Experiment
Feb	February
FeOB	Iron-oxidizing bacteria
ft	Feet

g	Gram
GIS	Geographic Information Systems
GSAF	Genomic Sequencing and Analysis Facility
[H+]	Hydrogen ion concentration
$[H+]_f$	Final hydrogen ion concentration
$[H+]_I$	Initial hydrogen ion concentration
hr	Hour
HV	High vacuum
ICP-OES	Inductively Coupled Plasma Optical Emission Spectrophotometry
Jan	January
km^2	Kilometers squared
L	Liter
ME	Maine
µL	Microliter
µS	Microsiemen
µS/cm	Microsiemen per centimeter
m	Meter
max	Maximum
mg	Milligram
min	Minimum
mL	Milliliter

mg/L	Milligram per liter
mol	Mole
mol/L	Mole per liter
mol/L/s	Mole per liter per second
mmol	Millimole
mmol/L	Millimole per Liter
N	Normality
N	Number of days
n/a	Not applicable
NCBI	National Center for Biotechnology Information
ng	Nanogram
ng/µL	Nanogram per microliter
nm	Nanometer
NOAA	National Oceanic and Atmospheric Administration
Nov	November
Oct	October
PCA	Principal components analysis
pH	Decimal logarithm of the reciprocal of hydrogen ion concentration
R^2	Residual value squared
RDA	Redundancy Analysis
rpm	Rotations per minute

S	Siemen
s	Second
SEM	Scanning electron microscope
Sep	September
SOP	Standard operating procedure
$[SO_4^{2-}]_f$	Final sulfate concentration
$[SO_4^{2-}]_I$	Initial sulfate concentration
$[SO_4^{2-}]_{t24}$	Sulfate concentration at 24 hours
t	Time
Temp.	Temperature
USGS	United States Geologic Survey
WBPR	West Branch of the Pleasant River
XRF	X-ray Fluorescence
#	Number
’15	2015
’16	2016

CHAPTER 1. THE PROCESSES OF SULFIDE MINERAL OXIDATIVE DISSOLUTION, NATURALLY OCCURING ACIDIC STREAM ECOLOGY, AND THE IMPLICATIONS FOR MAINE

1.1 Introduction

In aqueous systems, sulfide minerals can break down through processes known as oxidative dissolution. Acid rock drainage (ARD) occurs when sulfide minerals oxidize through interaction with water and oxygen during oxidative dissolution. Hydrogen ions are released during oxidation, lowering the pH of water (Nordstrom 1982, Lowson 1982). This occurs naturally, with stream hydrology affecting both stream chemistry and the associated community through groundwater and surface water interactions, but mining increases oxidation rate by exposing an increased amount of sulfide rock to the atmosphere (Caissie et al. 1996, Londry and Sherriff 2005, Mamaar et al. 2015). Microorganisms can increase the production of ARD by increasing the rate of sulfide oxidation by up to five orders of magnitude relative to abiotic oxidation (Edwards et al. 1999, Nordstrom and Southam 1997). Evolution of water chemistry during the acid producing processes will affect the bacterial community present in the streams.

Maine has not had an active metal mine since 1977 (LePage et al. 1991, Marvinney 2015). In recent years, the possibility of opening a new metal mine in Maine has become a topic of discussion and proposed legislation. The state has multiple unmined metal deposits, one of the largest being the Bald Mountain deposit, which contains approximately 36 million tons of copper and zinc containing ore (LePage et al. 1991). There has been little research in New England on naturally acidic stream microbial communities, or how these communities change with the varying weather that accompanies New England's seasons. With this project,

we seek to better understand microbial communities that occur in naturally acidic streams, how they relate to stream chemistry, and how these communities and their sulfide oxidation potential would change seasonally from differing water chemistry and hydrology when subjected to increased acid producing conditions through the addition of pyrite to the aqueous system.

1.2 Stream Hydrology

Streams are created from the excess accumulation of water on the land surface, which runs downhill due to gravity (Harvey and Wagner 2000). The water within streams can come from two sources; exchange with groundwater aquifers or surface runoff from precipitation. Groundwater occurs when rainfall and snowmelt infiltrates into the ground where it is stored within aquifers. It enters streams when a saturated aquifer naturally intersects with the ground surface at a stream channel (Packman and Bencala 2000, Hill 2000). Groundwater can transport solutes dissolved from surrounding bedrock or soil into the stream channel, which affects stream chemistry (Harvey and Wagner 2000, Packman and Bencala 2000, Hill 2000) When the rate of precipitation is greater than the rate of infiltration into the ground, excess precipitation runs down slopes due to gravity into stream and river channels (Harvey and Wagner 2000). This can occur whether the ground is saturated or unsaturated. Influxes of surface runoff into the stream can dilute the present stream chemistry, as well as carry sediment and new microbes into the stream (Londry and Sherriff 2005, Mamaar et al. 2015).

Groundwater plays a major role in stream behavior, ecosystem function, and stream chemistry. Groundwater is one of the major sources of streamflow, and since the influence of groundwater is prominent during normal conditions it is specifically referred to as baseflow

(Buttle 1994). Groundwater plays an important part in influencing stream chemistry and temperature, which in turn can result in changes in microbial composition at points where groundwater enters from the stream bed (Holmes 2000, Constantz et al. 1994). Groundwater within aquifers dissolves solutes from the local bedrock. These solutes are then transported into the stream channel through interactions with the surface water within what is known as the hyporheic zone (Buttle 1994, Findlay 1995, Hill 2000, Packman and Bencala 2000).

The hyporheic zone is a channel of water that runs in conjunction and adjacent to the stream or river slightly below the bed (Findlay 1995). Here, there are constant exchanges between ground and surface water, which can create microenvironments due to temperature differences between the stream and the inflowing groundwater (Findlay 1995). Incoming groundwater is typically cooler in the summer months and warmer in the winter than the surface water (Findlay 1995). Hyporheic flowpaths constantly interchange water between the stream and geochemically and microbially active sediments. This provides a constant exchange of nutrients in and out of the stream for microorganisms to use both in the sediments and in the stream (Caissie et al. 1996, Findlay 1995, Hendricks 1996). Figure 1 demonstrates the constant exchanges between stream waters, groundwaters, and the hyporheic zone.

The riparian zone is part of the stream system where the environment transitions between terrestrial and aquatic, and is distinguished by vegetation, topography, and specific soil types (Naiman and Decamps 1997). The riparian zone can control chemistry and hydrology of a stream's base flow during both normal and storm conditions. During storm events, it acts as an important source of runoff and helps to control interactions between this runoff and the soil slopes. There are preferred macropore flowpaths that account for the exchange of solutes

and microorganisms from the soil into the runoff (McDonnell et al. 1990, Peters et al. 1995). This process is more important in open hillslopes than in undisturbed forested woodlands. Riparian zones also control biogeochemistry within groundwater flows through hydrologic flowpaths and water table fluctuations (Baker et al. 2000). Changes in these flowpaths lead to changes in oxidation reactions for local microbial communities based on the amount of electron donors and acceptors present (Hedin et al. 1998).

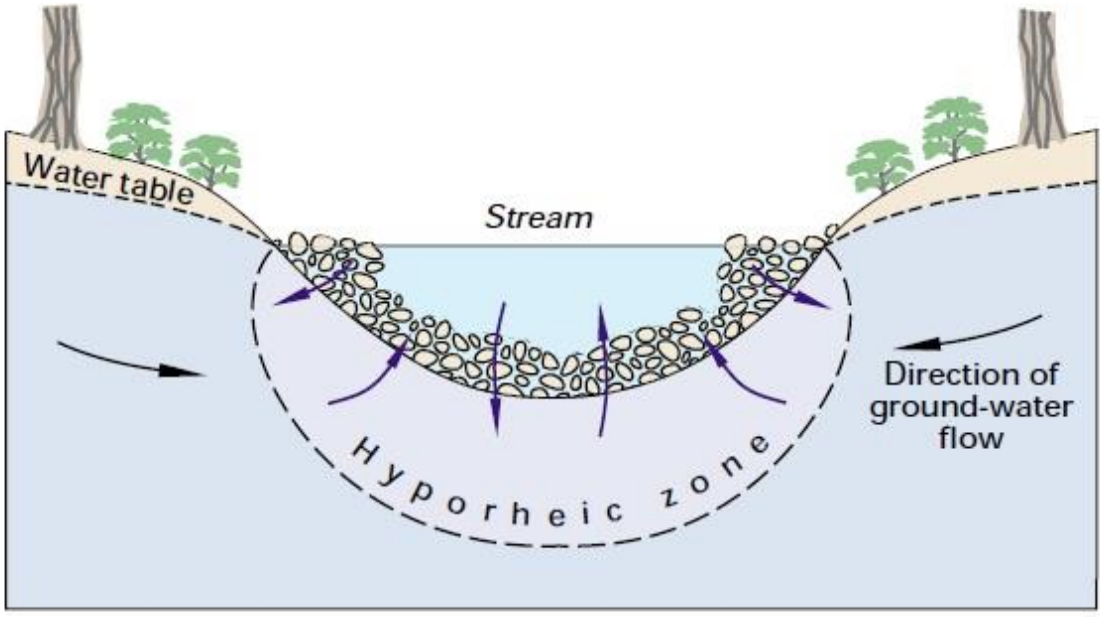

Figure 1. Simple Hyporheic Exchange Model (Winter et al. 1998). The hyporheic zone, located beneath and adjacent to the stream bed, is a zone of constant exchange between groundwater and surface water.

1.3 Microbial Community Structure and Variation

Microbial community composition can vary in both time and space. Communities can be very distinct despite being only meters apart from one another. While there are differences there is still likely to be some overlap. These variations make it difficult to establish what is "normal" for a microbial community, in either surface water or groundwater systems. The

following information is the best representation found in the literature of what can be considered a standard community composition for both surface and groundwater individual environments.

For surface water communities, both lake and stream studies were used to identify common community structure patterns. The most common class of bacteria to appear throughout all studies is Betaproteobacteria. Typically, Betaproteobacteria comprise at least of 1/3 of the surface freshwater community. Betaproteobacteria includes many bacterial genera and species that are planktonic, which accounts for the high abundance in surface waters (Fierer et al. 2007, Lindstrom et al. 2005). Actinobacteria are usually the next largest group (Fierer et al. 2007, Lindstrom et al. 2005, Van der Gucht et al. 2005). It some cases, it has been observed that Actinobacteria can become the dominant class in freshwater communities, typically in high nutrient (phosphorous concentration > 100 µg/L) and non-turbid waters (Van der Gucht et al. 2005).

Groundwater microbial communities are driven by the availability of electron donors and acceptors. Due to the low concentrations of organic carbon that are found in hard rock aquifers, electron donors and acceptors usually come from inorganic sources (Beaton et al. 2016, Mamaar et al. 2015, Santelli et al. 2001, Stevenson 1997). Many groundwater microorganisms form biofilms on inorganic sediments, and potentially differ from those free-floating within the aquifer (Stevenson 1997). Mamaar and colleagues (2015) found that groundwater microbial community structure is independent of the type of bedrock aquifer. They also found that structure is dependent upon water residence time within the aquifer and the community's place within groundwater hydrogeological loops. They also saw variations in

the community population based on the depth of sampled communities, with deep wells down to 100 meters exhibiting a large proportion of iron-oxidizing bacteria belonging to Gallionellaceae. Iron-oxidizing bacteria are common in groundwater communities at circumneutral pHs (Santelli et al. 2001).

Hyporheic sediments also contain unique microbial communities, which is due to constant mixing of groundwater and surface water. These communities can be different depending upon whether they are growing in an upwelling or downwelling zone within the hyporheic zone, which can lead to differences in biologic production and chemical exchange (Hendricks 1996). Communities in downwelling zones have been found to have higher metabolic activity, such as electron transport activity and thymidine uptake into DNA, due to these zones having greater hydrologic exchange and higher DOC quality derived from surface sources (Hendricks 1996). Bacterial population density has been observed to decrease with depth in both groundwater and hyporheic systems (Fischer et al. 1996, Hendricks 1996). Generally, hyporheic sediments tend to have lower microbial productivity than that of other aquatic sediments, presumably due to reduced amounts of organic content. However, production is not lower per unit organic matter, which implies that the organic matter which is present in the hyporheic zone is of high quality (Findlay and Sobczak 2000).

1.4 Sulfide Oxidation

Acid rock drainage (ARD) is the acidified runoff resulting from the decrease in pH caused by the release of hydrogen ions during the oxidation of sulfide minerals in water. The oxidation of sulfide minerals is the rate determining step of ARD production (Williamson et al. 2006). The most common ARD producing mineral is pyrite (FeS_2). Pyrite can be oxidized via two primary

mechanisms; dissolved oxygen (DO) and iron (Fe) III (Blowes et al. 2003). DO is the dominant oxidant at circumneutral pHs because Fe (III) has a low solubility, but at acidic pHs (<3.5) Fe (III) is the dominant mechanism of pyrite oxidation (Blowes et al. 2003, Williamson et al. 2006). DO oxidizes pyrite via the reaction:

$$FeS_{2(s)} + \frac{7}{2}O_2 + H_2O \rightarrow Fe^{2+} + 2SO_4^{2-} + 2H^+ \textbf{ (Eq. 1)}$$

Fe (II) that is released during pyrite oxidation can be further oxidized to Fe (III) via the reaction:

$$Fe^{2+} + \frac{1}{4}O_2 + H^+ \leftrightarrow Fe^{3+} + \frac{1}{2}H_2O \textbf{ (Eq. 2)}$$

At circumneutral pHs, Fe (III) primarily complexes with hydroxide ions from water to form iron hydroxides:

$$Fe^{3+} + 3H_2O \leftrightarrow Fe(OH)_3 + 3H^+ \textbf{ (Eq. 3)}$$

At more extreme pHs, Fe (III) can remain soluble and can oxidize additional pyrite which releases more hydrogen ions into solution via the reaction:

$$FeS_{2(s)} + 14Fe^{3+} + 8H_2O \rightarrow 15Fe^{2+} + 16H^+ + 2SO_4^{2-} \textbf{ (Eq. 4)}$$

The Fe (III) mechanism releases eight times more hydrogen ions, thus decreasing pH at a faster rate. Solution pH influences which oxidation mechanism dominates.

The process of pyrite oxidation is exothermic. In enclosed systems such as mine galleries or waste pile, this heat is dissipated into the surrounding medium causing temperatures to rise such as at Iron Mountain, in California, a massive sulfide mine that produces gold, zinc, copper, and silver ore (Edwards et al. 1999). Here, ARD temperatures can reach upwards of 60 ˚C. These temperatures are unlike those occurring in streams. Schoonen et al. (2000) performed an experiment that investigated the effects of visible light and its thermal activation on the mechanism of abiotic oxidation of pyrite. They found that direct visible light increases the rate

of pyrite oxidation by less than a factor of two. This information suggests that pyrite oxidation rates in surface environments where there is light should be slightly faster than those contained underground in mines where there is little light exposure.

Other sulfides oxidize via similar reactions to pyrite. Pyrrhotite can also be oxidized using DO and Fe (III) as oxidants; the dominant mechanisms depend on pH (Blowes et al. 2003). However, pyrrhotite can also be dissolved via a non-oxidative mechanism that occurs when there is no DO present and the mineral is in a highly acidic solution. Fe (II) is released while the sulfide ions combine with hydrogen ions to form hydrosulfuric acid (Janzen et al. 2000, Jones et al. 1992, Thomas et al. 2001). In this case, hydrogen ions are consumed, raising pH via the reaction

$$Fe_{(1-x)}S_{(s)} + 2H^+ \rightarrow (1-x)Fe^{2+} + H_2S \text{ (\textbf{Eq. 5})}.$$

Oxidation mechanisms and rates for other sulfide minerals are summarized in Table 1.

The processes described here occur naturally both in the subsurface when groundwater reacts with a sulfide bearing aquifer, or on the surface where sulfide bearing rocks are exposed to surface water, precipitation, and the atmosphere (Gleisner and Herbert 2002, Nordstrom 1982). Groundwater and hyporheic exchange can release acidified water and dissolved chemicals into streams and rivers, creating naturally acidified and impaired stream environments. These processes are accelerated by mining, when a greater surface area of sulfide rock is given easier accessibility to water and oxygen (Blowes et al. 2003, Williamson et al. 2006).

Table 1. Oxidation Rates of Various Sulfide Minerals

Mineral	Formula	Mechanism	Dissolution Rate ($mol/m^2/s$ unless noted)	Microbial Rate ($mol/m^2/s$ unless noted)	Conditions	Source
Pyrite	FeS_2	Dissolved O_2	5×10^{-10}	8×10^{-8}	pH < 2, 25 ˚C	Weisener 2002, Nicholsan 1994
Pyrite	FeS_2	Fe (III)	2.7×10^{-7}	10^{-5}	pH < 2, 25 ˚C	Rimstidt et al. 1994
Pyrite	FeS_2	Fe (II)	3×10^{-12} mol/L/s	3×10^{-7} mol/L/s	pH < 2, 25 ˚C	Singer and Stumm 1968, 1970
Pyrite	FeS_2	Non-Oxidative	1.9×10^{-10}		pH < 2, 25 ˚C	Weisener 2002
Pyrrhotite	$Fe_{(1-x)}S$ (x=0-0.2)	Dissolved O_2	4×10^{-9}		pH < 2, 25 ˚C	Janzen et al. 2000
Pyrrhotite	$Fe_{(1-x)}S$ (x=0-0.2)	Fe (III)	3.5×10^{-8}		pH < 2, 25 ˚C	Janzen et al. 2000
Pyrrhotite	$Fe_{(1-x)}S$ (x=0-0.2)	Non-Oxidative	5×10^{-10}		pH < 2, 25 ˚C	Janzen et al. 2000
Sphalerite	(Zn, Fe)S	Fe (III)	3×10^{-7} to 7×10^{-7}		pH < 2, 25 ˚C	Rimstidt et al. 1994
Sphalerite	(Zn, Fe)S	Dissolved O_2	1×10^{-8} to 3×10^{-8}		pH < 2, 25 ˚C	Weisener 2002
Chalcopyrite	$CuFeS_2$	Fe (III)	9.6×10^{-9}		pH < 2, 25 ˚C	Rimstidt et al. 1994
Galena	PbS	Fe (III)	1.6×10^{-6}		pH < 2, 25 ˚C	Rimstidt et al. 1994

1.5 Sulfide Oxidizing Microbiology

The presence of chemoautotrophic and chemoheterotrophic acidophilic microorganisms can increase the rate of sulfide oxidation which is shown in Table 1 (Baker and Banfield 2003, Blowes et al. 2003, Johnson and Hallberg 2003). These types of organisms prefer acidic environments and use the energy released by the oxidation reactions of sulfides as described in section 1.4. Autotrophs can use carbon dioxide as their carbon source, while the heterotrophs must obtain carbon from organic matter such as proteins, carbohydrates, and sugars. Microbes play various roles in the chemical cycling that occurs in ARD, including sulfur oxidation and reduction and metal oxidation and reduction (Baker and Banfield 2003, Johnson and Hallberg 2003). Some species can oxidize sulfur and reduce metals like iron anaerobically (Baker and Banfield 2003). Bacteria are the most common sulfide oxidizers, but Archaea can also be found in sulfide oxidation systems. The structure of the sulfide oxidizing microbial community is pH dependent, with different organisms taking different roles in the system as the pH changes in both natural and laboratory settings (Chen et al. 2014, Liu et al. 2014). Temperature can also influence the community structure, but at lower temperatures the community becomes less variable (Baker and Banfield 2003). Figure 2 shows how different species of bacteria can take similar roles in sulfide oxidation at different temperatures.

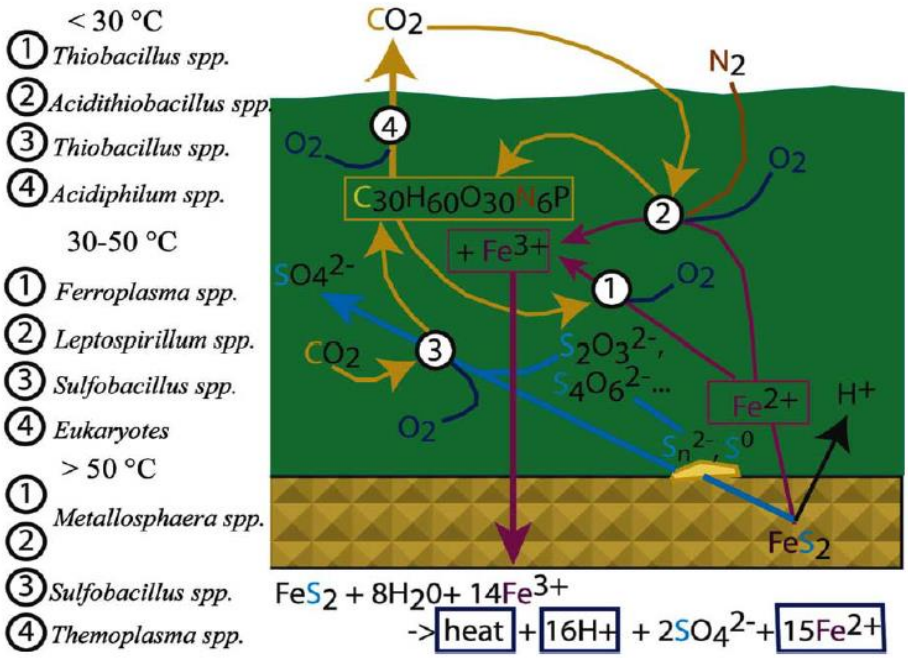

Figure 2. Common Roles of Microorganisms During Pyrite Oxidation at Varying Temperatures (Baker and Banfield 2003). Different microorganisms can substitute into similar roles within a sulfide oxidizing system depending on the environmental conditions.

The most common bacterial genera found in extreme sulfide oxidation systems are *Thiobacillus* and *Acidithiobacillus*. The most well-known species of sulfide oxidizing bacterium, *A. ferrooxidans*, is part of the *Acidithiobacillus* genus (Baker and Banfield 2003). *A. ferrooxidans* oxidizes both sulfur and iron from pyrite via direct and indirect methods (Baker and Banfield 2003, Sand et al. 2001, Tributsch 2001). In the direct mechanism, *A. ferrooxidans* attaches directly to the pyrite and enzymatically solubilizes the pyrite for its constituents while absorbing DO and water. In the indirect mechanism, the microbe catalyzes reactions near the mineral which allows further chemical oxidation, such as microbial oxidation of Fe (II) to Fe (III) (Baker and Banfield 2003, Sand et al. 2001, Tributsch 2001). At low pHs, the Fe (III) produced from this

will then in turn be used as for the abiotic mechanism as described in the section 1.4. During these processes, iron and sulfur serve as electron donors in the energy generating reactions of *A. ferrooxidans* (Baker and Banfield 2003, Sand et al. 2001, Tributsch 2001). *A. ferrooxidans*' ideal growth conditions are in a solution at pH 2.0-2.5 and a temperature of 15-35 degrees Celsius (Baker and Banfield 2003, Sand et al. 2001). However, it can survive over a pH range of 1.5-6.0 (Schrenk et al. 1998). Common microorganisms found in ARD and other environments that oxidize sulfide minerals and their ideal growth conditions are summarized in Table 2.

Table 2. Common Sulfide and Iron Oxidizing Bacteria

Genus	Species	Temperature (˚C)	pH (Optimal)	Inorganic Energy Source(s)	Special Notes
Acidithiobacillus	ferrooxidans	15-30, ideal 25-28	1.0-6.0 (1.3-4.5)	H_2S, Sulfides, S(0), $S_2O_3^{-2}$, $S_4O_6^{-2}$, Fe(II)	Nitrogen fixer
Acidithiobacillus	thiooxidans	18-37, ideal 28-30	(<4)	S(0), $S_2O_3^{-2}$, $S_4O_6^{-2}$	
Thiobacillus	neopolitanus	15-30	(2.8-3.5)	H_2S, Sulfides, S(0), $S_2O_3^{-2}$, $S_4O_6^{-2}$	
Thiobacillus	thermophilica	15-45, ideal 30-35	1-3.5 (2.5-3.0)	H_2S, Sulfides, S(0)	
Thiobacillus	thioparus	15-30	(3.5-4.0)	H_2S, Sulfides, S(0), $S_2O_3^{-2}$, $S_4O_6^{-2}$	
Leptospirillum	ferrooxidans	>14, ideal 35-40	1.3-4.0 (1.6-2.0)	Fe(II), Sulfides	Nitrogen fixer
Sideroxydans	lithotrophicus	20-25	(6.0-8.0)	Fe(II)	

Extensive research on interactions between extreme sulfide oxidation and microorganisms has taken place at Iron Mountain, California (Baker-Austin et al. 2010, Druschel et al. 2004, Edwards et al. 1999a, 1999b, Edwards et al. 2000, Jamieson 2011, Johnson 2012, Schrenk et al. 1998, Tan et al. 2009, Williams et al. 2016). At Iron Mountain, it has been observed that the pH and the microbial community vary seasonally, with the summer microbial community being dominated by Archaea, whereas the winter community is dominated by bacteria (Edwards et al. 1999, Schrenk et al. 1998). Increased precipitation can affect both abiotic and biotic oxidation of sulfides. It increases dissolution of the mineral, but the increased water volume also dilutes the microbial and solute concentrations.

While microbial communities and biogeochemistry are understood well in extreme (pH 1-3.5) sulfide oxidizing conditions, weaker acidic conditions (pH 3.5-5.5) are still poorly understood (Jones et al. 2017). Recently in 2014, reactor experimentation has been conducted at the Duluth Complex in Minnesota (Jones et al. 2017). The Duluth Complex has relatively low metal sulfide content and higher acid-neutralizing content compared to mines and deposits that have been extensively studied (i.e. Iron Mountain). It's leachate rarely reaches extreme pHs and when the sulfide content of the complex is 1% or less it typically is between pHs of 4-6. Moderately acidic taxa are often characterized by the presence of microbes such as *Thiobacillus denitrrificans* and *Thiobacillus thioparus*, along with many unclassified taxa (Korehi et al. 2014, Lindsay et al. 2009, Mendez et al. 2008).

1.6 Acid Neutralization by Dissolution

Dissolution of non-sulfide minerals occurs simultaneously with sulfide oxidation in aqueous environments. Within these aqueous systems, most neutralization occurs via calcium

carbonate dissolution and silicate dissolution (Jambor et al. 2003, Nordstrom et al. 1990, Stromberg and Banwart 1994). Most silicate and carbonate mineral dissolution reactions consume hydrogen ions from solution, thus raising the solution pH. Dissolution and oxidation reactions occur simultaneously with the net reaction and solution pH determined by their relative rates (Jambor et al. 2003, Stromberg and Banwart 1994, Nordstrom et al. 1990, Weber et al. 2005). While the oxidation reactions are producing the hydrogen ions, the carbonate and silicate dissolution reactions are consuming them. Which reaction has a faster rate will determine how pH is affected. If oxidation is stronger, more hydrogen ions are produced than consumed, causing pH to decrease. If dissolution has a faster rate, the opposite occurs, and pH increases. The amount of neutralization varies depending on the mineralogy of the host rock.

Calcium carbonate dissolution can be represented by the following reaction:

$$CaCO_{3(s)} + 2H^{+} \rightarrow Ca^{2+}_{(aq)} + CO_{2(aq)} + H_2O_{(l)}$$ **(Eq. 6)**

This reaction consumes hydrogen ions and releases calcium ions, carbon dioxide, and water into the system. Neutralization capacity is dominated by the dissolution of carbonate minerals, but there are a few exceptions (Weber et al. 2005). For the minerals siderite and ankerite, the net release of hydrogen ions is balanced to the consumption of hydrogen ions during dissolution. The iron in the minerals is oxidized, releasing hydrogen, while the carbonate consumes the same amount of hydrogen during its dissolution (Jambor et al. 2003, Weber et al. 2005). The effectiveness of calcium carbonate as a neutralizing agent can be seen from limestone addition being the primary means of remediating ARD affected water systems (Johnson and Hallberg 2005).

In silicate dissolution, as silicate minerals, hydrogen, and water are consumed, metal ions and silicic acid are released (Weber et al. 2005, Craw 2000). The following reaction of enstatite dissolution is an example:

$$MgSiO_{3(s)} + 2H^+ + H_2O_{(l)} \rightarrow Mg^{2+}_{(aq)} + H_4SiO_{4(aq)}$$ **(Eq. 7)**

Silicate minerals have a greater neutralization capacity per mole (Packtunc 1999), but they are typically only dominant in the long-term process of neutralization due to their slower rate of dissolution than carbonates (Stromberg and Banwart 1994). Iron containing silicates do not have an effective neutralization capacity (Plumlee 1999). Standard log K_Hs (log of the rate constant for proton-promoted dissolution) of various calcium carbonate and silicate minerals can be seen in Table 3.

Table 3. Log K_Hs of Various Carbonate and Silicate Minerals

Mineral	Formula	Log K_H	Conditions	Notes	Source
Calcite	$CaCO_3$	-8.48	None Specified		Nordstrom et al. 1990
Muscovite	$KAl_2(AlSi_3O_{10})(F, OH)_2$	-11.8	pH 1-4		Kalinowski and Schweda 1996
Hornblende	$Ca_2(Mg, Fe, Al)_5(Al, Si)_8O_{22}(OH)_2$	-10.02	pH 2-5.7		Golubev et al. 2005
Gypsum	$CaSO_4 \cdot 2H_2O$	-4.58	None Specified		Nordstrom et al. 1990
Biotite	$K(Mg, Fe)_3(AlSi_3O_{10})(F, OH)_2$	-9.49	pH 1-4		Kalinowski and Schweda 1996
Diopside	$MgCaSi_2O_6$	-9.4	25 ˚C, pH 2-10	Calculated based off Si release	Knauss et al. 1993
Dolomite	$CaMg(CO_3)_2$	-17.09	None Specified		Nordstrom et al. 1990
Augite	$(Ca, Na)(Mg, Fe, Al, Ti)(Si, Al)_2O_6$	-6.7	pH ≤ 6		Sverdrup 1990
Wollastonite	$CaSiO_3$	-7.19	pH 3.1-12.2		Golubev et al. 2005
Jadeite	$Na(Al, Fe^{3+})Si_2O_6$	-7	pH 3-6		Sverdrup 1990

1.7 Aluminum in the Environment

1.7.1 Aqueous Chemistry

Aluminum plays a lesser role in environmental processes than most other metals, but there are increased concerns about slowly elevating levels in surface water (Driscoll and Schecher 1990, Martin and McDonald 1988, Pina and Cervantes 1996, Porcal et al. 2010). In aqueous environments aluminum complexes with OH^-, F^-, SO_4^{2-}, HCO_3^-, and organic compounds, with OH^-, F^-, and the organic compounds being the most significant (Driscoll and Schecher 1990). Aqueous aluminum is the most bioavailable form of aluminum, but it represents a minute faction of the total aluminum in the environment (Driscoll and Schecher 1990). Due to aluminum's low solubility and slow dissolution kinetics, it typically is unavailable for biogeochemical reactions, but the main source of aqueous aluminum is the decomposition of aluminosilicate minerals (May et al. 1979, Bloom 1983). Lower pHs raise the solubility of monomeric and complexed aluminum in aqueous systems (Burgot 2012). Acidic solutions help to mobilize aluminum in soils, such as in the case of acid rain, which increases total aluminum concentration in soil solutions and surface water (Pina and Cervantes 1996). At circumneutral pHs, most aqueous aluminum is bound onto organic ligands, or complexed with sulfate or hydroxide. At a pH of 5 and below, the monomeric form of aluminum, Al^{3+}, becomes the predominant aqueous species (Pina and Cervantes 1996). Biologically, aluminum is quantitatively unimportant as it is not a plant or animal nutrient, but it is a toxicant (Bohn et al. 1985).

Acidified waters usually have higher aluminum concentrations due to more extreme pHs. Aluminum tends to form strong complexes with sulfate, where aluminum sulfate

comprises a much higher molar percent of the aqueous species in acidified waters compared to surface water at similar pHs (Driscoll and Schecher 1990, Espana 2007). When pH drops below 3.5, the predominant form of aluminum becomes its monomeric form, regardless of the amount of sulfate present in the system (Figure 3) (Driscoll and Schecher 1990, Pina and Cervantes 1996). Within acidified waters, aluminum and iron can act as pH buffering agents (iron: pH 2.5-3.5, aluminum: 4.5-5.0) (Espana 2007). Aluminum also can scavenge toxic trace metals out of acidified systems (Espana 2007). These characteristics allow aluminum's toxicity to be stronger at lower pHs and sulfate concentrations.

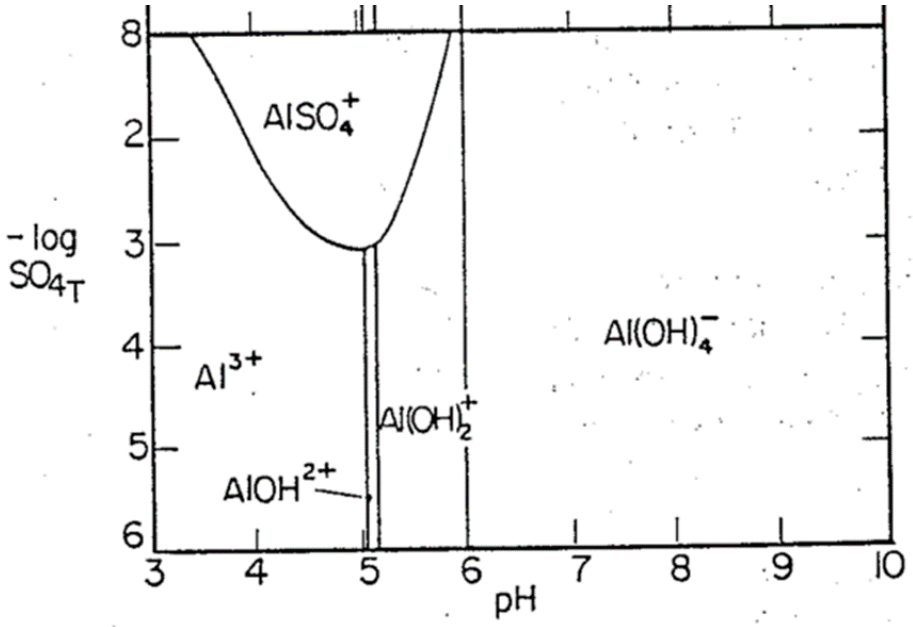

Figure 3. Speciation of Aluminum Based On pH and Sulfate Concentration (Driscoll and Schecher 1990). At lower pHs like those generated by long-term sulfide oxidation, the prevalent form of Al is its monomeric form. This is toxic to many microorganisms. At circumneutral pHs Al is complexed, rendering it non-toxic.

1.7.2 Effects on Microbiology

Inorganic aluminum is toxic to a wide variety of organisms, including microbes (Driscoll and Schecher 1990, Driscoll et al. 1980, Pina and Cervantes 1996). The toxic form of aluminum to an abundance of species is the monomeric form of Al^{3+} where it replaces other ions, usually magnesium, in critical biological functions. Aluminum has a 10^7 stronger bond with ATP than magnesium, which means that magnesium must be present in an aqueous system at a millimolar level to overcome an aluminum concentration of only nanomoles (MacDonald and Martin 1988). Different bacteria have different levels of aluminum tolerance, ranging from micromolar to millimolar levels (MacDonald and Martin 1988). Lower concentrations of iron increase Al toxicity, which suggests that aluminum uptake involves iron transport systems (Pina and Cervantes 1991, Davis et al. 1971). Most common ARD bacteria are metal-tolerant because ARD often contains high concentrations of metals, including aluminum. *A. ferrooxidans* and *A. thiooxidans* exhibit reduced growth patterns in aluminum sulfate levels of 200 mM but maintain enough resistance to Al to still double their optical density (Fischer et al. 2002).

Certain acidophilic bacterial genera exhibit enhanced growth in acidic, high-aluminum media. Wakao et al. (2002) demonstrated that members of the genus *Acidocella* exhibit enhanced growth when directly increasing the concentration of aluminum. The exact mechanism of these microorganisms' tolerance to aluminum and why they exhibit these enhanced growth rates is still unknown. *Pseudomonas fluorescens* was reported to sequester and detoxify aluminum by producing an extracellular lipid compound, but this has been disputed as this lipid compound has been identified in both aluminum-sensitive and aluminum-resistant bacteria (Appanna and St. Pierre 1994, Vargas et al. 1995).

1.8 Maine Mining and Its Potential Risks

Figure 4 shows both legacy mines and unmined major deposits in the state (Maine Geological Survey 2005). Recently, political discussions have addressed the issue of relaxing current mining regulations, which could lead to the opening of a new metal mine in Maine. The

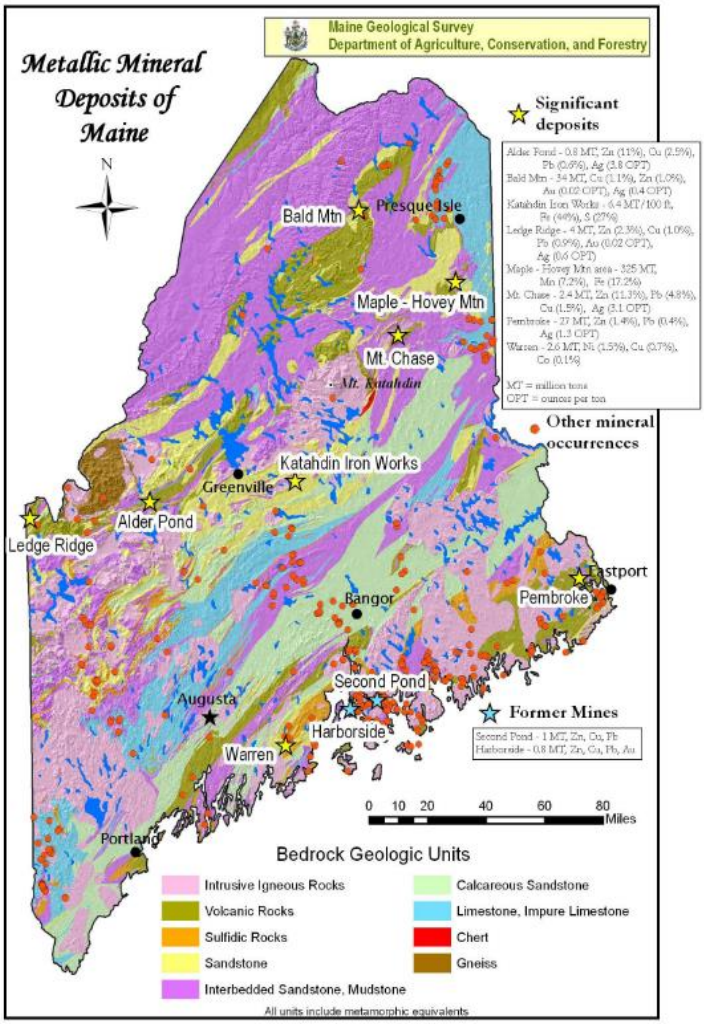

Figure 4. Mined and Unmined Metallic Deposits in Maine (Maine Geological Survey 2005). Around the state are many deposits that contain a strong sulfide presence (i.e. Katahdin Pyrrhotite Deposit). These deposits, if mined, have the risk of producing accelerated sulfide oxidation, which can result in acidified aqueous conditions and negative environmental impacts.

most recent development in the discussion comes as of May 9th, 2017. The Maine senate voted to ban larger sized open-pit mines and the underwater storage of mine wastes with bill LD 820 (Cousins 2017). Possible sites include Lead Ridge, Mount Chase, Alder Pond, and Bald Mountain (Marvinney 2015). Lead Ridge in Pamanchee contains zinc, lead, and copper ore. Mount Chase contains those as well as silver. Alder Pond is an underground deposit that has an estimated 1.5 to 3 million tons of copper-zinc sulfide ore (Marvinney 2015, Marvinney and Berry 2015). Bald Mountain contains an estimated 36 million tons of copper-zinc sulfide close to the surface (Maine Geological Survey 2005). Due to its size and accessibility Bald Mountain has been the site of major focus for exploration and debate within the public eye for the at least the past five years (Brino 2016, Cairn 2013).

The prospect of opening a new mine in Maine also comes with the potential risk of sulfide mineral deposits having increased exposure to water and oxygen, which increases the generation of ARD. Tailings are the waste material left over after the valuable materials are extracted from an ore. They are the most significant environmental concern for mines (Marvinney 2015). In the legacy mining sites, the waste sulfides are unsegregated rather than having the sulfides separated out (Marvinney 2015, Marvinney and Berry 2015). After ore processing, tailings are typically contained in impoundments to restrict access to oxygen, but water can still access and oxidize the sulfides (Blowes et al. 2003). Runoff from these tailings can enter surrounding aqueous environments, both ground and surface water. This causes numerous environment problems, including disrupting food webs and biological functions through the changing pHs (Blowes et a. 2003). Even only slight acidity has a large effect upon endangered Atlantic Salmon populations. It has been shown that changing pHs both negatively

impact the fishes' growth and the spawning of their food source insects (Sibrell et al. 2006). Since lower pHs increases the solubility of metals, when acidified water enters more neutral waters some of these metals will precipitate out as the pH rises (Burgot 2012, Johnson and Hallberg 2005). The massive amounts of precipitates can cloud water, which kills plants, and smothers fish by blocking oxygen transfer within their gills (DeNicola and Stapleton 2002).

An extreme example of the fallout that occurs when mine waste is mishandled is the Summitville Mine in Colorado. In 1992, extremely acidic (pH < 3), metal rich runoff escaped from tailings compounds, into the surrounding environment (Bigelow and Plumlee 1995). Approximately 210 million dollars has been spent by the Environmental Protection Agency to help remediate the mine (Bigelow and Plumlee 1995, Rieder et al. 2013). In recent years, remediation attempts have appeared to start to be successful. Vegetation is being restored, with the plant community beginning to shift from seeded plants to those in a reference environment (Rieder et al. 2013). While the escaped runoff was the long-term environmental concern, there is belief that natural drainage will still be a problem, even after remediation efforts are completed (Gray et al. 1994).

1.9 Project Objectives

Knowing the effects microbial populations can have on sulfide oxidation and acidification, it is important to understand how seasonal variations in stream chemistry, temperature, and precipitation will have upon their community structure in Maine waters near a sulfide bearing deposit. Maine's climate has three general zones; coastal, southern interior, and northern continental (Fobes 1946). Precipitation in all zones is generally constant, varying around 1.5-2 inches from summer to winter (US Climate Data 2018). Precipitation and storm

events can change stream chemistry through dilution. Having most precipitation stored as snow in Maine's winter creates a delayed response to precipitation events for stream chemistry and the microbiological response. Temperature patterns in Maine are related to the coastal vs. continental regions. On the coast, average seasonal temperature changes have less variation, and are overall about 3-5 degrees (F) warmer than continental temperatures (US Climate Data 2018). A majority of Maine's unmined deposits are in the northern continental part of the state (Figure 4), but there are a few located within the coastal region. These variations in climate from season to season could have an impact upon a microbial community's ability to accelerate sulfide oxidation, otherwise known as its sulfide oxidation potential.

To better understand the effects of Maine's seasonal climate changes on its microbial population, stream chemistry, and hydrology, Blood Brook, a naturally acidic and impaired stream (Whiting 2011), located near the Katahdin pyrrhotite deposit, was studied to:

1.) Characterize the microbial community present in a naturally acidic stream in Maine.
2.) Identify variations in Blood Brook's community over a period of seasonal transition while comparing this community to what has been commonly observed in surface water streams through the literature.
3.) Identify water source input for the selected field site at each time it was sampled to help explain hydrologic influence on stream chemistry and the microbial community.
4.) Identify correlations between changes in the microbial community and stream chemistry.

5.) Experimentally identify how the community changes when subjected to increased exposure to sulfide minerals.

6.) Experimentally identify changes to the communities' sulfide oxidation potential based on differences in sampling conditions (i.e. chemistry, temperature, precipitation).

To do this, water was sampled from Blood Brook, and stream chemistry measurements were taken across an 8-month period (July '15 – February '16). Blood Brook is classified as an impaired stream by the Maine Department of Environmental Protection and is naturally weakly acidic (pH of 4.5-5.5), like that of the Duluth Complex (Whiting 2011, Jones et al. 2017). By observing and understanding microbial, rock, and water interactions occurring in this naturally acidic stream we may get an idea of how acidification may look if one of Maine's deposits was cleared to be mined.

Understanding how the microbial community already present in Maine's environment changes and evolves throughout the acidification process is important to better manage mine wastes and reduce remediation efforts and costs. To do this, a series of batch reactor experiments was also performed to assess the effects of the changing seasonal conditions within Blood Brook on the sulfide oxidation potential of its microbial communities. Experiments were run using water samples taken from Blood Brook during three different sampling events of the study period (October, December, January). The acidifying conditions were created by incubating the samples with pyrite to promote sulfide oxidation conditions.

Under the experimental acidifying conditions, we hypothesized that Blood Brook's microbial communities would evolve into those containing an increased population of

acidophiles that participate in the oxidation of the pyrite and exhibit tolerance for high metal concentrations. The microbial community will respond to changes in chemistry by populations of microbes that are better adapted to the new conditions becoming more abundant. Many of the present dominant surface water bacteria like those of Betaproteobacteria, will begin exhibiting smaller populations as conditions move towards unfavorable acidic conditions. The likelihood of the community to develop a strong abundance of iron-oxidizers could push the overall community structure towards one that resembles a groundwater community and those observed in well studied acidified mine sites.

We also hypothesized that samples collected when the dominant source of flow in Blood Brook was stormflow will have decreased oxidation potential due to dilution of the bacteria within the community participating in sulfide oxidation. Stormflow water also comes from more oxidized soil environments that would contain less sulfides (Evangelou 1998). By completing the proposed research goals, we hope to understand how microbial communities from a naturally acidic stream are affected by chemical variations and hydrology within the stream water, and how this affects the communities' iron sulfide oxidation potential. This will provide a better understanding of the response of Maine microbiology to acidification and seasonal changes in stream chemistry and hydrology. The results of the field and experimental portions of this project are presented below in Chapters 2 and 3 respectively.

CHAPTER 2. NATURALLY ACIDIC STREAM MICROBIAL COMMUNITY VARIATION IN RESPONSE TO CHANGING SEASONAL CONDITIONS

2.1 Introduction

Within this chapter are the methods and results of the field examination of Blood Brook's seasonal chemistry, hydrology, and changing microbial community. To reiterate, the goals of the field portion of the project were as follows:

1.) Characterize the microbial community present in a naturally acidic stream in Maine.

2.) Identify variations in Blood Brook's community over a period of seasonal transition while comparing this community to what has been commonly observed in surface water streams through the literature.

3.) Identify water source input for the selected field site at each sampling point to help explain hydrologic influence on stream chemistry and the microbial community.

4.) Identify correlations between changes in the microbial community and stream chemistry.

By accomplishing these research goals, we will add to the understanding of the interactions between water, rock, and biology within this naturally acidic system. Understanding these dynamics will increase knowledge of Maine's ecosystems involving sulfide bearing rock deposits.

2.2 Methods and Materials

2.2.1 Field Site Selection

Water for the project was collected from Blood Brook (outlined in red in Figure 5) near Katahdin Iron Works State Park in Brownville Junction, Maine. The Katahdin pyrrhotite deposit was mined in the 1800s as an open pit site for iron ore to use in the production of pig and cast iron at the Iron Works. The deposit contains 200 million tons of pyrrhotite (Foley 2003, Whiting 2011). Pits used for mining are still present to the south of Blood Brook on the slope of Ore Mountain (Figure 5). This deposit, referred to as the Katahdin Pyrrhotite Deposit, is located on the north side of Ore Mountain within Devonian aged gabbro (Hanson and Sauchuk 1991). Many streams in this area have natural acidity due to groundwater interactions with the massive sulfide deposit within the bedrock (Whiting 2011). The most prominent of these is Blood Brook where the pH is usually around 4.5 but can range from 4-6 (Whiting 2011). Blood Brook empties into the West Branch of the Pleasant River (WBPR; Figure 5). While Blood Brook has been classified as an impaired stream with unusually high aluminum levels by the Maine Department of Environmental Protection (DEP), it has been determined that it has very little influence on the overall chemistry of the WBPR (Whiting 2011). Blood Brook is shallow and roughly 3-9 meters. wide. Samples for this project were collected from a slow-moving portion of Blood Brook approximately 150 meters upstream from where it empties into the WBPR. No macroscopic organisms were visible in the stream apart from insects occasionally on the surface. The rocks that make up the banks and base of Blood Brook are covered with a rusty red colored staining, which contributes to the source of the streams name as can be seen in the right image of Figure 6. Within the stream there is a film of precipitate that is a similar color

which covers most of the rocks on the stream base. As mentioned in Chapter 1, pyrrhotite, like that within the Katahdin deposit, can oxidize in an acidic environment in the absence of DO, in a process that gives it some neutralization capacity. However, given the stream bed of Blood Brook is composed of bedrock and the stream itself is only weakly acidic (pH 4.5-5.5), this type of dissolution is likely minimal compared to pyrrhotite oxidation.

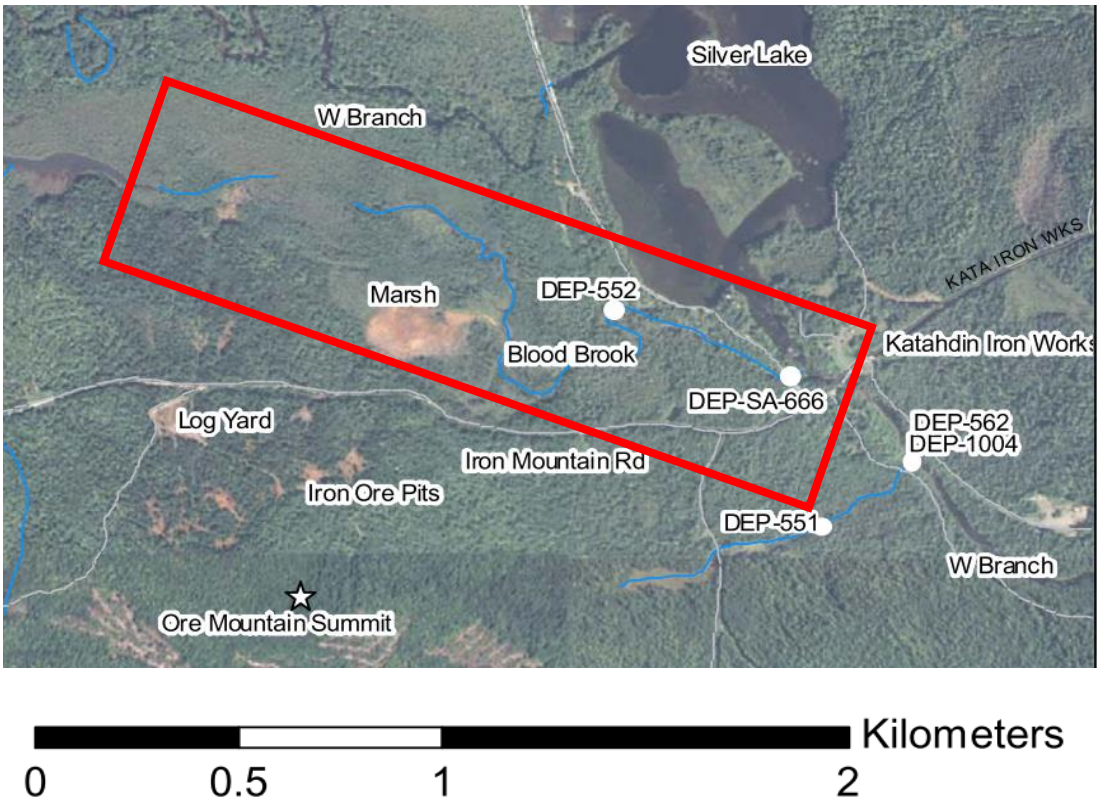

Figure 5. Map of Blood Brook and the Surrounding Area (Whiting 2011). Blood Brook is a tributary to the West Branch of the Pleasant River. Located to the southeast of Blood Brook are the ore pits where ore was extracted for use at Katahdin Iron Works.

Figure 6. Images of Blood Brook (Winter and Summer). The rusty red color from which Blood Brook gets its name can be seen in the right image. Blood Brook is a bedrock stream, with bedrock pieces comprising its base and most of the banks. Coating the rock base is a thin film of precipitate which bears the same color as the oxidized rock.

2.2.2 Sampling

Sampling of Blood Brook was conducted once roughly every month, 20-40 days apart, across an 8-month period that spanned summer through winter. This sampling was chosen to find how Blood Brook's chemistry and microbial community varied at monthly intervals. Sampling began in July and proceeded until February of the next year to see how these changes would appear across a seasonal gradient. Specific conductance, pH, and dissolved oxygen concentration were recorded using portable field meters, which were standardized prior to visiting Blood Brook. Three readings were taken for each parameter and averaged. At least 3.5 liters of water were collected during each sampling event in 3.5-liter Nalgene bottles for microbial community analysis, alkalinity titration, and sulfate concentration analysis. Bottles

used were acid washed with 10% HCl, thoroughly rinsed with deionized water, soaked in 70% ethanol, and rinsed with deionized water again at least 24 hours prior to the sampling date to avoid sample contamination. The ethanol wash was done as an alternative to autoclaving as the bottles were not made of autoclavable material. The 3.5-liter bottle was submerged in the stream without disturbing sediments and filled to the brim to reduce air exposure within the bottle. Once capped, the bottle was sealed with Parafilm and placed on ice for transport to return to the University. Samples were then stored at 5˚ C in the geochemistry laboratory until use.

2.2.3 Sulfate Analysis

Sulfate concentration was measured using a variation of the standard Hach colorimetric method using Hach Sulfaver 4 Reagent packets and a Genesys 10vis spectrophotometer (Hach Method 8051). The technique was adapted for use on a more powerful and detailed spectrophotometer. For each sample, four 2.5 mL aliquots of sample water were taken from the water collected in the field, pipetted into 10 mL sample cells and diluted to 10 mL with deionized water. One of the sample cells was set aside to be used as a blank. All sample cells were acid washed with 10% HCl and rinsed thoroughly with deionized water. Three reagent packs were emptied into the remaining three sample cells, shaken, and allowed to stand undisturbed for 5 minutes. The spectrophotometer was then zeroed with a blank, standardized with three standards, and the three samples read for absorbance at 420 nm wavelength. These absorbances were then used to calculate sulfate concentration from the following formula:

$$y = 0.0068x + 0.015 \text{ (**Eq. 7**)}$$

This formula was constructed using multiple known standards prior to measuring sample sulfate concentrations (Figure 7). The calculated sulfate concentrations were then recorded. During measurements, the standardized formula was extremely close to the original constructed standard formula, only requiring minor adjustments.

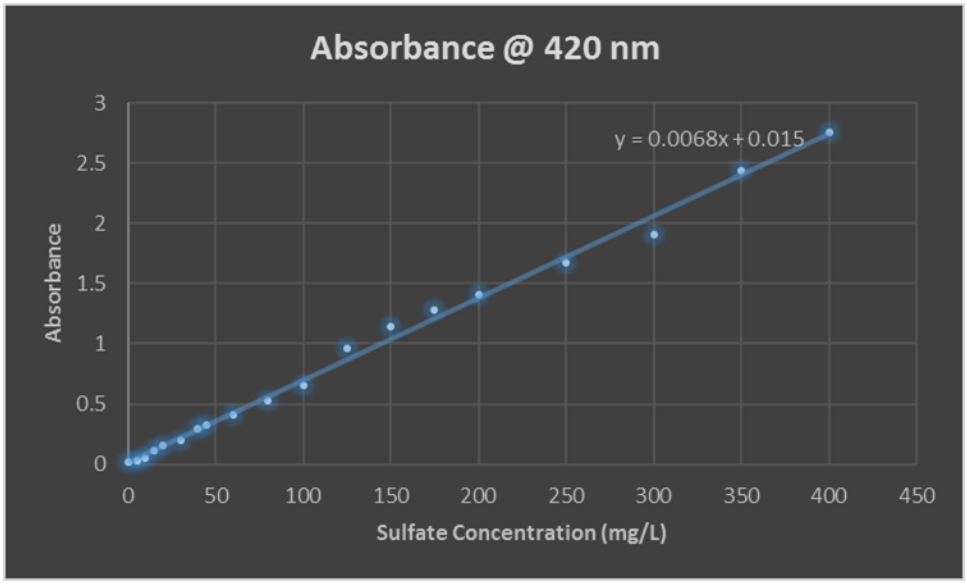

Figure 7. Constructed Standard Sulfate Curve. This trend was constructed from multiple prepared sulfate standards at various concentrations. Each time sulfate was measured in samples, the spectrophotometer was standardized using three of the prepared standards and compared back to this original curve for accuracy.

2.2.4 Microbial Community Extraction and Analysis

Following each field sampling, 1800 mL of collected sample was filtered and DNA extracted from the subsequent filtrate to find microbial community composition. Using a vacuum flask, water was filtered through a sterile 0.45-micron (HACH) pore size polycarbonate filter for a total of 600 mL or until no more water could pass through the filter. This was repeated three times. These filters were then used with MoBio PowerWater DNA extraction kits

per the manufacturer's instructions to obtain three 100 µL aliquots of DNA for each month in the study period. These DNA samples were stored at -80˚ C until further use. Concentrations (ng/µL) of the DNA samples were measured using a Thermo Scientific NanoDrop 2000 Spectrophotometer in the Deering Microbiology Lab.

Illumina MiSeq sequencing of the V4/V5 region of the 16S rRNA gene (metagenomics assay) was done by the Genomics Sequencing and Analysis Facility (GSAF) at the University of Texas at Austin. Samples were prepared for analysis by diluting all samples to a common concentration under 10 ng/µL. Aliquots of 25 µL of the normalized samples were shipped overnight on dry ice to the sequencing facility. Results for the field communities from the GSAF can be found online in the National Center for Biotechnology Information's (NCBI) GenBank database under accession number PRJNA430708.

2.2.5 Alkalinity Titration

For each sampling point in the study period 50 mL of sampled water was titrated with 0.020 N sulfuric acid to find alkalinity in mg/L of calcium carbonate ($CaCO_3$). 50 mL of sample was placed in a 100 mL Erlenmeyer flask with the probe of a benchtop pH meter. Titrant was added to the sample water dropwise from a 50 mL burette until the pH of the sample reached 4.5. The volume of titrant (mL) added to the solution was then multiplied by 20 to find total alkalinity (mg/L $CaCO_3$). Since all the samples had a starting pH of ~6 or lower, all their total alkalinities were in the bicarbonate form (Eaton et al. 2005).

2.2.6 Inductively Coupled Plasma Optical Emissions Spectrometry (ICP-OES) Analysis

Each month, immediately upon returning from field sampling, three aliquots of 5 mL were transferred to three acid washed 25 mL sample bottles from the 3.5 liters of collected

sample for analysis on the ICP-OES in the Deering Hall Analytical Lab at the University of Maine. These samples were acidified to 1% using nitric acid (HNO_3). This is for stability and comparability to the standard solutions. Samples were analyzed for the following using standard ICP-OES methods (Eaton et al. 2005); Ca, Mg, K, P, Al, B, Cu, Fe, Mn, Na, S, and Zn.

2.2.7 Stream Water Source Input

2.2.7.1 Blood Brook Watershed Area with ArcGIS

The estimated area of Blood Brook's watershed was calculated in ArcGIS. The original file was a streams and rivers shape file downloaded from the Maine Office of GIS at https://www1.maine.gov/geolib/catalog/index.shtml. This file was cut down to the area of Piscataquis County, Maine, the county where Blood Brook is located. A digital elevation model map (DEM) of Maine was also obtained, cut, and modified to match the same area as the streams and rivers shape file. From here, Watershed and Stream Network Delineation using ArcHydro Tools was partially followed (steps 1-3 as described in the rest of this section) until the step necessary to obtain an estimated watershed area for Blood Brook (Merwade 2012).

The first step of the process reconditions the DEM using the AGREE system. This method was originally developed by the Center for Research in Water Resources at the University of Texas Austin. It was created as an alternative to the "burning the streams" method, where elevation was just dropped to match that of the streams (Hellweger 1997). The DEM is reconditioned assuming that the streams and rivers shape file is more accurate than the DEM. The AGREE system adjusts the surface elevation of a DEM consistent with vector coverage, where the vector coverage is streams or ridge-line (Hellweger 1997). It does this by pushing an unaltered DEM along the linear vector. In this case, the vector is the stream shape

file. This creates a new DEM that capture a distinct profile based off the stream elevation, which is not normally captured in raw DEMs due to the lack of elevation data along streams (Hellweger 1997).

Step 2 of Watershed Delineation involves filling sinks within the newly reconditioned DEM. This step fills in incomplete hole, or sinks, in the produced DEM from step 1. If these sinks were left unadjusted, the program would interpret them as cells in the grid where water would not flow during the flow direction process (Planchon and Darboux 2002). This would create a drainage network that is discontinuous. The fill tool continues to iterate until either all sinks are filled, or a specified limit is input. This tool can also be used to remove random peaks that have a higher than normal elevation compared to the area around them (Planchon and Darboux 2002).

The third step of the procedure computes flow direction. This is done within the Flow Direction function using the following:

$$maximum\_drop = change\_in\_z - value \,/\, distance * 100 \quad \textbf{(Eq. 8)}$$

This formula determines the direction of steepest descent within a DEM, with distance between cells being measure between center points (Jenson and Domingue 1988). The function analyzes individual cells and assigns them values corresponding with various flow directions to create the output flow direction grid. The output cell numbers have the following values: 1 = East, 2 = Southeast, 4 = South, 8 = Southwest, 16 = West, 32 = Northwest, 64 = North, 128 = Northeast (Jenson and Domingue 1988).

Once the flow direction grid was obtained, the Watershed tool was used to delineate Blood Brook's watershed. By indicating the desired catchment point, where Blood Brook

empties into the West Branch of the Pleasant River, ArcGIS can calculate watershed area based off the flow direction and the threshold value (the number of cells that constitute the stream). The output is a raster of Blood Brook's stream are, which simply had to be converted to a polygon to obtain the area. Complete input steps for finding the area in ArcGIS can be found in Appendix C.

2.2.7.2 Finding N and Determining Stream Influence

To determine the ratio of surface to groundwater influence, Method 2 of Separation by Arbitrary Attrition as described by Gupta (2017) was used. The following formula is used in this method:

$$N = 0.8A^{0.2} \quad \textbf{(Eq. 9)}$$

where *A* represents the area of the watershed of interest in square kilometer, and *N* represents the number of days a sampling date must follow a discharge peak on a hydrograph to be groundwater dominant. N was calculated for both Blood Brook, as well as Black Stream since that was the hydrograph used to assist in the assessment. The area of the Blood Brook watershed was calculated through ArcGIS (Section 2.2.7.1). The necessary hydrograph was taken from the USGS Current Water Conditions web site. The Black Stream near Dover-Foxcroft gauge was used as it is spatially one of the gauges closest to Blood Brook (approximately 20 miles). Black Stream is also the closest gauge with a watershed area closest to Blood Brook's. While it's still much larger than Blood Brook's watershed size, the size will better reflect changes in Blood Brook. Watershed size affects the response time of discharge. First order streams like Blood Brook's hydrograph peaks would appear earlier and skinnier due to faster response time when compared to peaks of Black Stream. However, the frequency of storm

events would remain consistent for both surface water systems. Calculating N assists in making inferences about the source of flow within Blood Brook using the Black Stream hydrograph. Since we do not know exactly when peak discharge occurs, we assumed any sampling point that has rainfall occur 2*N prior to sampling is baseflow dominated. If a large rain or snowmelt even occurs within 2*N of sampling, it will be assumed that Blood Brook was stormflow dominated.

2.2.8 Statistical Methods

2.2.8.1 Sequence Data Processing

Once received from the GSAF, Illumina MiSeq data was processed in the program mothur to identify different microbial organisms' genetic sequences and structure the data in a usable format (Schloss et al. 2009). Preliminary files were constructed and organized, and the data processed following mothur's MiSeq standard operating procedure (SOP) (Schloss et al. 2009). This SOP included numerous actions to clean the genetic data and prepare them for analysis. Sequencing and PCR errors were reduced, with the improved sequences being processed. These improved sequences were aligned with downloaded database reference files. This allowed the system to identify the genetic sequences within the Blood Brook data and match it to known sequences of genetic bases from the SILVA database. The system would then create a file showing the matched sequences known taxonomy which could be used for analyses. Complete processing code can be found in Appendix C.

A few details in this procedure were unique to our analysis. For these data, a 16S rRNA V4/V5 primer set was used by the GSAF. This targeted genetic fragments that fell between 475 and 500 genetic bases. These numbers were used during screening of sequences to obtain that specific range. When the processed sequences were to be aligned with the reference file, the

downloaded SILVA files were used, and the boundaries for alignment were the beginning and end of the 16S V4/V5 region at 6388 and 25319 bases respectively. When classifying sequences in the SOP to obtain taxonomic OTU files, the downloaded RDP files were used for reference. The last unique thing done in this project while following the MiSeq SOP was subsampling the data. Subsampling was completed using the size of 1934 reads for the smallest reasonable sample, which was the third replicate of October. From here, the processed and subsampled community data was used to construct figures and complete statistical analyses as described in the results section below.

2.2.8.2 Diversity Indices

An inverse-Simpson's diversity index was also run using mothur on the cleaned and processed sequences. The purpose of this index was to quantify both the richness, the number of different species within a community, and evenness, the abundance of the species that are present within a community. In our microbial community samples, mothur analyzes OTU classifications and counts rather than distinct species. The Simpson's diversity index is ideal because it incorporates both evenness and richness into its measures (Simpson 1949). The inverse of the Simpson's index is used for reporting, because it comprises an easily understandable scale. The lowest index, 1, would be indicative of 1 species or OTU. As the number increases, diversity increases along with it.

The additional code needed to complete the inverse-simpson index is located within the mothur code section of Appendix C. The main argument used was calc=invsimpson which instructs the program to calculate the index during a summary function. It first was completed

on the original produced shared file of all samples before subsampling, followed by being run again within a summary of the sample subsampled to 1934 counts.

2.2.8.3 Redundancy Analysis (RDA)

To find relationships between Blood Brook's chemistry and the varying microbial community throughout the study period a redundancy analysis, or RDA, was performed in R using the vegan package (R Core Team 2013). An RDA is a constrained ordination technique that combines multiple linear regression with a principle components analysis (PCA). The RDA summarizes the variation of a set of response variables constrained to a set of explanatory variables (Borcard et al. 2011). In this study's case, the microbial communities are the response variables while Blood Brook's chemistry are the explanatory variables. To run the RDA, both the genetic and chemical data had to be transformed. The community and genus data were transformed using the Hellinger transformation, while the chemical data were normalized to a 0-1 scale by using the transformation formula

$$\boldsymbol{x} = \frac{(\boldsymbol{value}-\boldsymbol{min})}{(\boldsymbol{max}-\boldsymbol{min})}$$ (**Eq. 10**) (Borcard et al. 2011)

This transformation puts all the chemical parameters on the same scale and eliminates units to better overlay the response variables, which are the transformed genetic data.

Once the chemical and biologic data are transformed for the RDA's explanatory and response variables, the function can be run in R. The following R code was run using the function RDA from the package vegan (Oksanen et al. 2018):

$$FldRDA < -rda(BBGenera.hell, NrmFldData, scaling = 2)$$ (**Eq. 11**)

BBGenera.hell was the object name for the Hellinger transformed biological output from the mothur analysis organized by genus. NrmFldData is the object name for the normalized field

data, including both the parameters measured in the field as well as the ICP analysis results. They represent the response and explanatory variables respectively. The scaling parameter modifies the displayed relationship between the explanatory and response variable and their relationship to the axes on an outputted triplot. After an RDA model is run, each R^2 value must be adjusted due to the RDA being biased along the X-axis, like multiple regression tests (Peres-Neto et al. 2006). The R^2 was simply adjusted using the vegan function Rsquareadj(). The RDA with adjusted R^2 was placed into a new object with the following code:

$$NewObjectName < -Rsquareadj(NameofRDAObject)\$adj.r.squared \quad \textbf{(Eq. 12)}$$

Each RDA must be tested for significance to interpret it. A non-significant RDA should be discarded (Borcard et al. 2011). This is done using the anova.cca function, which implements a permutation test to calculate significance based upon the multiple axes. While the name is the name, the function is not the same as the well-known ANOVA test (Borcard et al. 2011).

2.3 Results

2.3.1 Hydrological Influence

It is important to understand during when Blood Brook's flow is influenced primarily by groundwater or surface runoff. This will allow us to better understand and interpret the relationships between changes in Blood Brook's microbial community and the stream chemistry. Once *N* is found using Equation 8, this can be used to determine whether a stream is driven by baseflow or stormflow at a certain date (Gupta 2017). With an area of approximately 0.81 km^2 for the Blood Brook watershed, *N* equals approximately 0.75 days or 18 hours for the Blood Brook watershed. When compared to the precipitation data and hydrograph, the sampling dates for three months occurred within 36 hours (2N) of a significant

amount of precipitation or snowmelt. These three sampling points were November 23rd, January 7th, and February 19th. At these points, Blood Brook was dominated by stormflow as opposed baseflow. At every other sampling point within the study period Blood Brook was dominated by baseflow. The sampling points in July and at the end of October had slight precipitation within three days of sampling, but not within 36 hours. The total precipitation that preceded each sampling point by 3 days can be found along with the other chemical data in Table 4. January and February's flow are contributed to, in part, by a large amount of melting snow. According to NOAA data, snow height changed approximately 2 inches and 6 inches within 2 days of the sampling points in January and February respectively.

2.3.2 Blood Brook Seasonal Chemistry

Blood Brook's chemistry varies considerably throughout the year. The mean temperature (Figure 8) in the summer sampling periods (July-September) remained around 20˚ C, peaking during the sampling point in August at approximately 23˚ C. In October, the temperature dropped to approximately 4˚ C. From then until the January sampling point, the temperature dropped steadily to approximately -1˚ C and remained at this temperature into February. This indicates that the probe used to measure temperature in the field had some analytical error, as water temperatures cannot drop below 0 degrees Celsius. Blood Brook's pH (Figure 8) remained relatively constant throughout the study period, fluctuating between 5 and 6, as can be seen in Table 4. Points of high pH were in August and December, with low points occurring in July, October, and February. Conductivity and sulfate concentration (Figure 9) show similar patterns throughout the study period. Both parameters vary month to month without a clear trend; conductivity varies between 100 and 200 µS/cm and sulfate concentration varies

between 60 and 120 mg/L. Sulfate concentrations do contribute to total conductivity. The biggest difference in these parameters is that conductivity remains more constant from July to October while sulfate concentration still fluctuates. Other measured chemical parameters include dissolved oxygen (DO) concentration and alkalinity. All collected field data is reported in Appendix A.

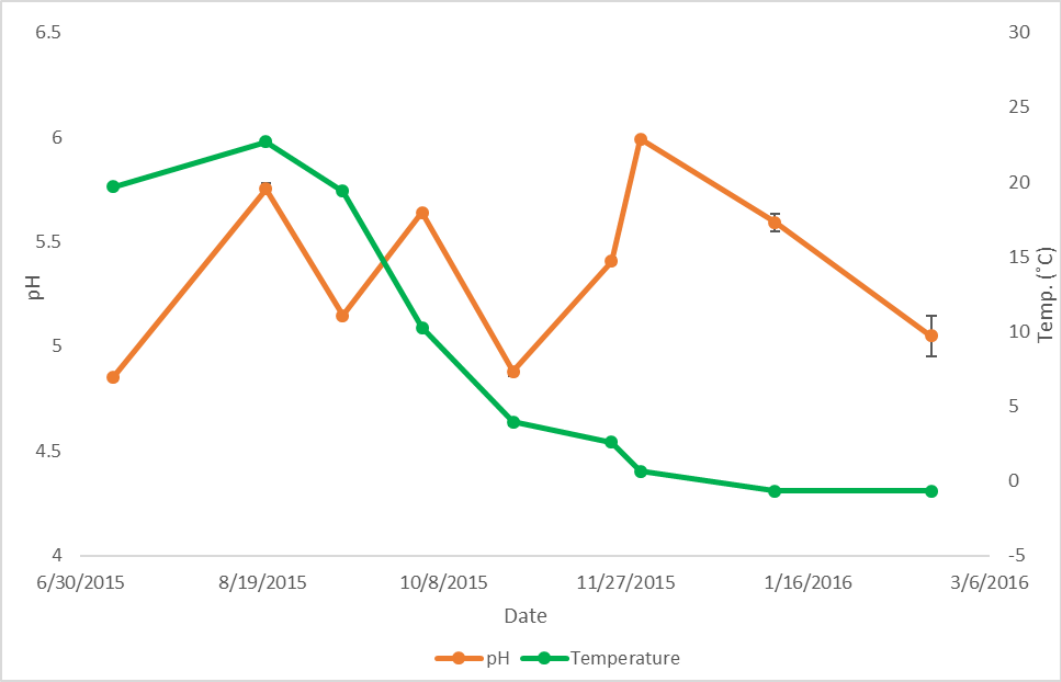

Figure 8. Blood Brook Mean Temperature and pH. Blood Brook's mean monthly pH fluctuates steadily between 4.8 and 5.6. It's mean monthly temperature is reflective of Maine averages for Summer (approximately day 175 to 250) and for winter (approximately day 335 to 410).

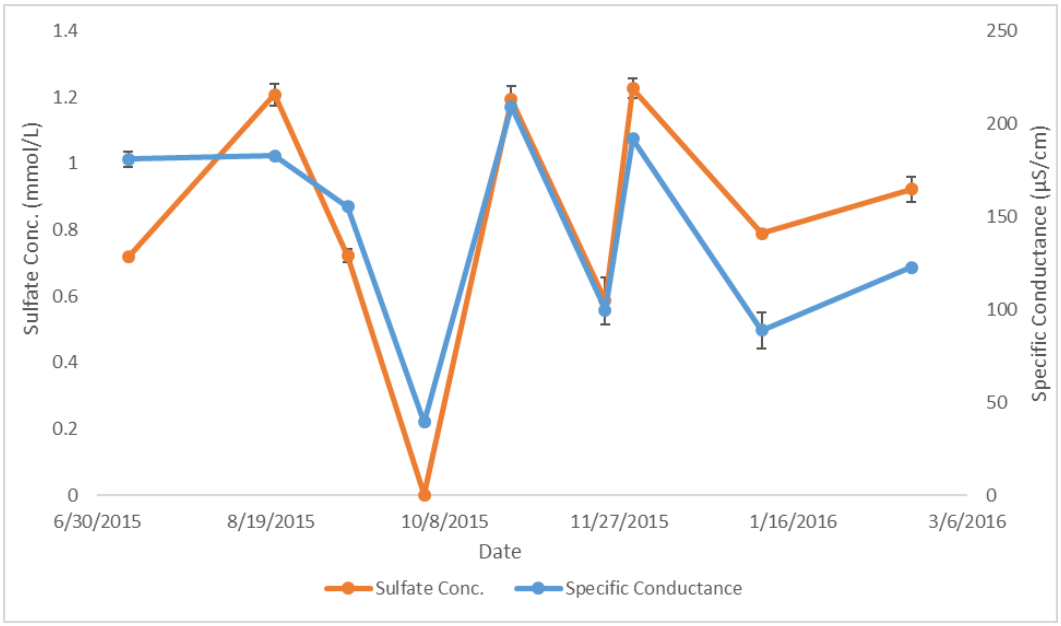

Figure 9. Blood Brook Mean Conductivity and Sulfate Concentrations. Sulfate concentrations and conductivity vary with very similar trends, with apparent low values at stormflow dominated periods.

Table 4. Collected Blood Brook Field Data

n/a = not applicable	July	August	September	October		November	December	January	February
Sampling Date	7/9/15	8/20/15	9/10/15	10/2/15	10/27/15	11/23/15	12/1/15	1/7/16	2/19/16
Calendar Day	190	232	253	275	300	327	335	7	50
Conductivity (µS/cm)	175.3	182	155.5	39.1	211	97.7	191.9	75.2	122.4
	183.3	182.9	155.3	39.6	209	100.1	192	96.2	122.9
	184.4	183.3	155.3	39.5	208	100.8	192	95	123
Mean Cond.	181	182.7	155.4	39.4	209.3	99.5	192	88.8	122.8
pH	4.84	5.78	5.14	5.68	4.9	5.41	5.99	5.64	5.16
	4.87	5.75	5.15	5.62	4.88	5.42	5.98	5.58	5.02
	4.85	5.75	5.15	5.62	4.86	5.39	6	5.56	4.97
Mean pH	4.85	5.75	5.15	5.64	4.88	5.41	5.99	5.59	5.05
Sulfate Conc. (mmol/L)	0.718	1.2076	0.7495	0	1.1559	0.5158	1.1871	0.7831	0.9198
	0.718	1.1659	0.7079	0	1.1747	0.5595	1.2368	0.7893	0.9695
	0.718	1.2492	0.7079	0	1.2492	0.6836	1.2555	0.7955	0.8763
Mean Sulfate	0.718	1.2076	0.7218	0	1.1933	0.5863	1.2265	0.789	0.9219
Temperature (˚C)	19.7	22.7	19.4	10.2	3.7	2.4	0.7	-0.6	-0.6
	19.7	22.7	19.4	10.3	4.2	2.7	0.6	-0.7	-0.7
	19.7	22.7	19.4	10.3	3.9	2.7	0.6	-0.7	-0.7
Mean Temp.	19.7	22.7	19.4	10.3	3.9	2.6	0.6	-0.7	-0.7
Dissolved O_2 Conc. (mg/L)	n/a	n/a	n/a	5.71	7.17	9.13	11.99	10.82	13.18
	n/a	n/a	n/a	5.92	7.13	9.89	12.24	10.26	12.78
	n/a	n/a	n/a	5.23	7.15	10.05	12.29	9.96	12.47
Mean DO	n/a	n/a	n/a	5.62	7.15	9.69	12.17	10.35	12.81
Alkalinity (mg/L $CaCO_3$)	n/a	n/a	n/a	n/a	2	10	4	6	6
Total Precipitation for 3 days prior to sampling (inches)	0.05	0	0	6.63	0.11	2.83	0	0	0.68

2.3.3 Metal Concentrations

Metal concentration data sampled in triplicate (Table 5) for Blood Brook were analyzed by ICP-OES in Deering Soil Analysis Lab at the University of Maine as described in Section 2.2.6. Data were not obtained for September, due to the ICP being unable to read concentrations but consuming all sample in the process. Boron and copper trends remained at or below the detection limit throughout the sampling period and were therefore not included in statistical analyses. Na, Ca, Mg, and S display similar trends as conductivity, even though some have different magnitudes of overall concentration (Figure 11). Al also has a trend that resembles conductivity but exhibits a few differences in the summer (July-September), where it has its lowest concentrations. Zn, K, and Fe have notably different trends compared to the rest of the measured elements. Zn contains a single peak that hits its maximum in November at approximately .004 mmol/L. Fe remains below the detection limit until October and then increases to a single peak in December at approximately 0.07 mmol/L. It then decreases until the end of the study period but does not reach the detection limit again. K remains relatively steady around the detection limit at 0.026 mmol/L, but then drastically increases in February to 0.21 mmol/L.

Table 5. ICP Measured Triplicate Field Concentration Data (mmol/L)

Sampling Date (Calendar Day)	Ca	K	Mg	P	Al	B	Cu	Fe	Mn	Na	S	Zn
July 9th '15 (190)	0.333	<0.0256	0.496	<0.00323	0.0324	<0.0028	<0.000315	<0.0018	0.00893	0.127	0.846	<0.000765
	0.333	<0.0256	0.486	<0.00323	0.0191	<0.0028	<0.000315	<0.0018	0.00863	0.108	0.858	<0.000765
	0.330	<0.0256	0.502	<0.00323	0.0327	<0.0028	<0.000315	<0.0018	0.00891	0.101	0.835	<0.000765
July Mean	0.332	<0.0256	0.495	<0.00323	0.0281	<0.0028	<0.000315	<0.0018	0.00882	0.112	0.846	<0.000765
Aug. 20th '15 (232)	0.352	<0.0256	0.552	<0.00323	0.0114	<0.0028	<0.000315	<0.0018	0.0108	0.123	0.897	0.00138
	0.364	<0.0256	0.567	<0.00323	0.0037	<0.0028	<0.000315	<0.0018	0.0111	0.122	0.859	0.00135
	0.333	<0.0256	0.536	<0.00323	0.0175	<0.0028	<0.000315	<0.0018	0.0106	0.135	0.823	0.00118
Aug. Mean	0.350	<0.0256	0.551	<0.00323	0.0109	<0.0028	<0.000315	<0.0018	0.0109	0.127	0.860	0.00130
Oct. 27th '15 (300)	0.420	0.033	0.649	<0.00323	0.0967	<0.0028	<0.000315	<0.0018	0.0115	0.154	1.124	0.00287
	0.341	<0.0256	0.581	<0.00323	0.0882	<0.0028	<0.000315	<0.0018	0.0102	0.121	1.008	0.00164
	0.454	0.0573	0.770	<0.00323	0.124	<0.0028	0.00045	<0.0018	0.0136	0.176	1.276	0.00280
Oct. Mean	0.405	0.0386	0.667	<0.00323	0.103	<0.0028	0.00036	<0.0018	0.0118	0.150	1.136	0.00244
Nov. 23rd '15 (327)	0.218	0.0315	0.31	<0.00323	0.041	<0.0028	<0.000315	0.0341	0.00587	0.0967	0.505	0.00550
	0.133	0.0492	0.266	<0.00323	0.0605	<0.0028	<0.000315	0.0303	0.00498	0.0490	0.422	0.00169
Nov. Mean	0.175	0.0404	0.288	<0.00323	0.0508	<0.0028	<0.000315	0.0322	0.00542	0.0729	0.463	0.00360
Dec. 1st '15 (335)	0.475	0.0429	0.586	<0.00323	0.088	<0.0028	<0.000315	0.0724	0.0113	0.183	0.942	0.00275
	0.338	<0.0256	0.547	<0.00323	0.101	<0.0028	<0.000315	0.0639	0.011	0.0871	0.871	0.00126
	0.251	<0.0256	0.388	<0.00323	0.496	<0.0028	<0.000315	0.0733	0.00802	0.0646	0.646	<0.000765
Dec. Mean	0.355	0.0313	0.507	<0.00323	0.0771	<0.0028	<0.000315	0.0699	0.0101	0.112	0.820	0.00159

Table 5. cont.

Jan. 7th '16 (7)	0.234	<0.0256	0.356	<0.00323	0.041	<0.0028	<0.000315	0.0586	0.00736	0.0536	0.606	<0.000765
	0.243	0.0424	0.361	<0.00323	0.04	<0.0028	<0.000315	0.0412	0.00754	0.166	0.603	<0.000765
Jan. Mean	0.239	0.034	0.358	<0.00323	0.0404	<0.0028	<0.000315	0.0499	0.00745	0.110	0.605	<0.000765
Feb. 19th '16 (50)	0.168	0.236	0.306	<0.00323	0.0746	<0.0028	<0.000315	0.0283	0.00637	0.139	0.545	<0.000765
	0.161	0.211	0.296	<0.00323	0.0559	<0.0028	<0.000315	0.0261	0.00617	0.139	0.524	<0.000765
	0.155	0.195	0.288	<0.00323	0.0531	<0.0028	<0.000315	0.0254	0.006	0.133	0.508	<0.000765
Feb. Mean	0.161	0.214	0.297	<0.00323	0.0612	<0.0028	<0.000315	0.0266	0.00618	0.137	0.526	<0.000765

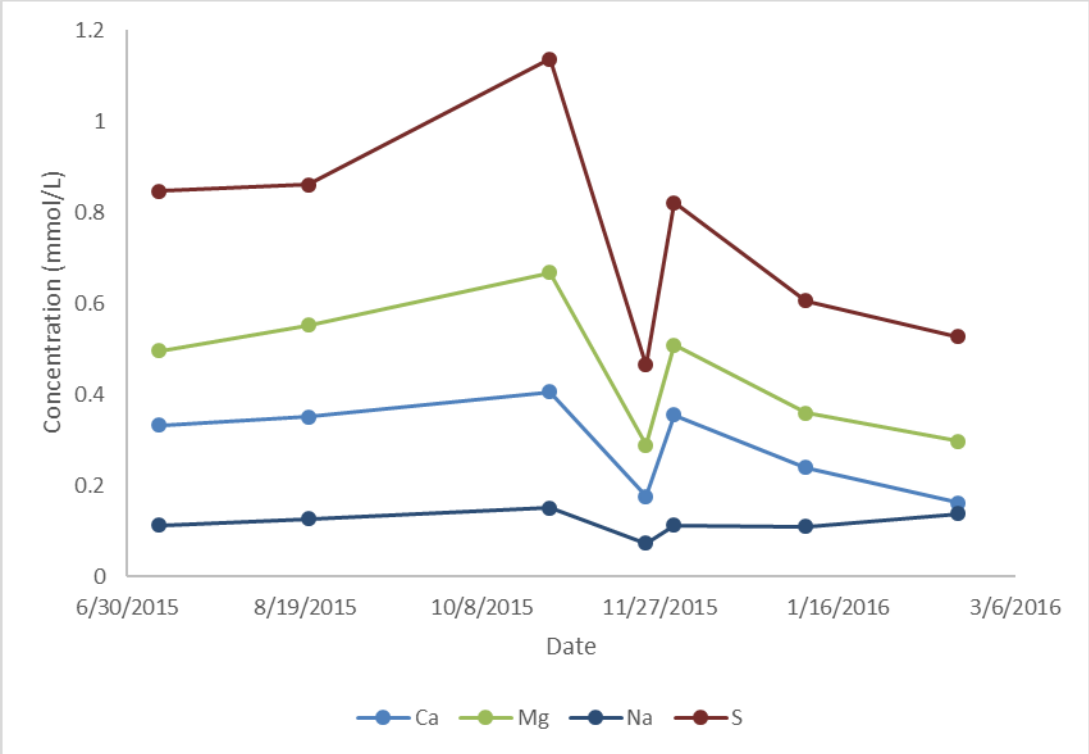

Figure 10. Concentrations of Metals in Blood Brook. The trends displayed here all strongly resemble the trend displayed by conductivity. Similar changes in concentrations are observed at the same points, even though the overall concentration levels are not the same.

2.3.4 Microbial Community

Blood Brook's microbial community changes throughout the study period (July '15 – Feb. '16). All samples were subsampled to 1934 counts, and replicates were averaged together to create one community for each sampling point of the study period (Figure 11). All calculated community percentages represent a percentage of this total read count. Since the communities displayed are averages, error bars are present on Figure 11 between category boundaries. The most abundant genera extracted from Blood Brook are *Polynucleobacter*, *Herminiimonas, Sideroxydans*, *Burkholderia*, *Sediminibacterium*, and *Novosphingobium*. The unclassified category is comprised of any microorganisms that were unable to be identified at the displayed

taxonomic level. The “Other” category is comprised of all identified microorganisms that comprise less than 1% of the total community.

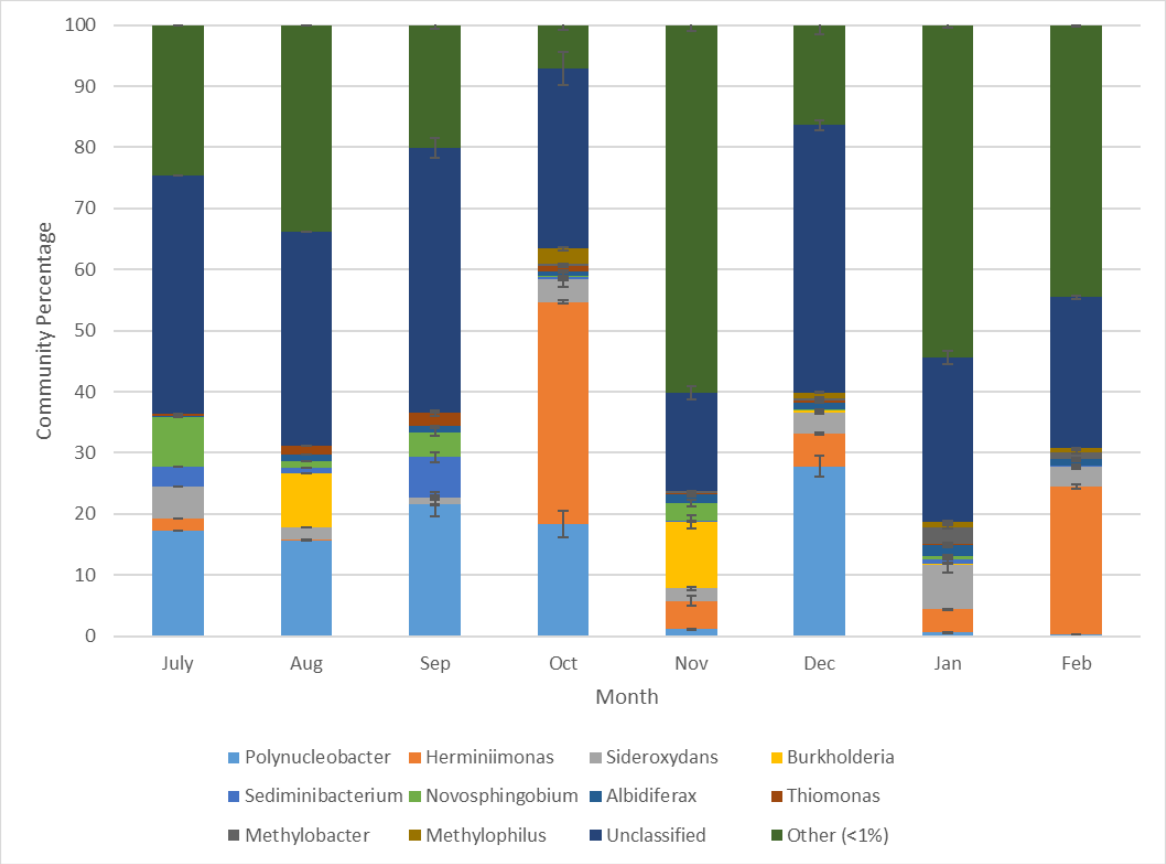

Figure 11. Blood Brook Microbial Communities Organized by Genus [NCBI Accession #: PRJNA430708]. Dominant genera present include Polynucleobacter, Herminiimonas, Sideroxydans, Burkholderia, Sediminibacterium, and Novosphingobium. There are large fluctuations in the size of the “Other” (<1%) category at certain sampling points.

2.3.5 Redundancy Analysis (RDA)

An RDA was run to find relationships between the microbial community (response variables) and the stream chemistry (explanatory variables) (Figure 12). Total microbial communities are plotted as sites and are displayed in black. Individual genera within the communities are plotted in red. The explanatory variables are plotted as linear vectors, with longer vectors having a stronger influence on the variability of the microbial community. Figure 12 is shown in Scaling 2. Scaling 2 means that to find a response variables correlation with a specific explanatory vector, one would draw a perpendicular line to the variable of choice. The closer to the tip of an explanatory vector a response variable is, the stronger the correlation

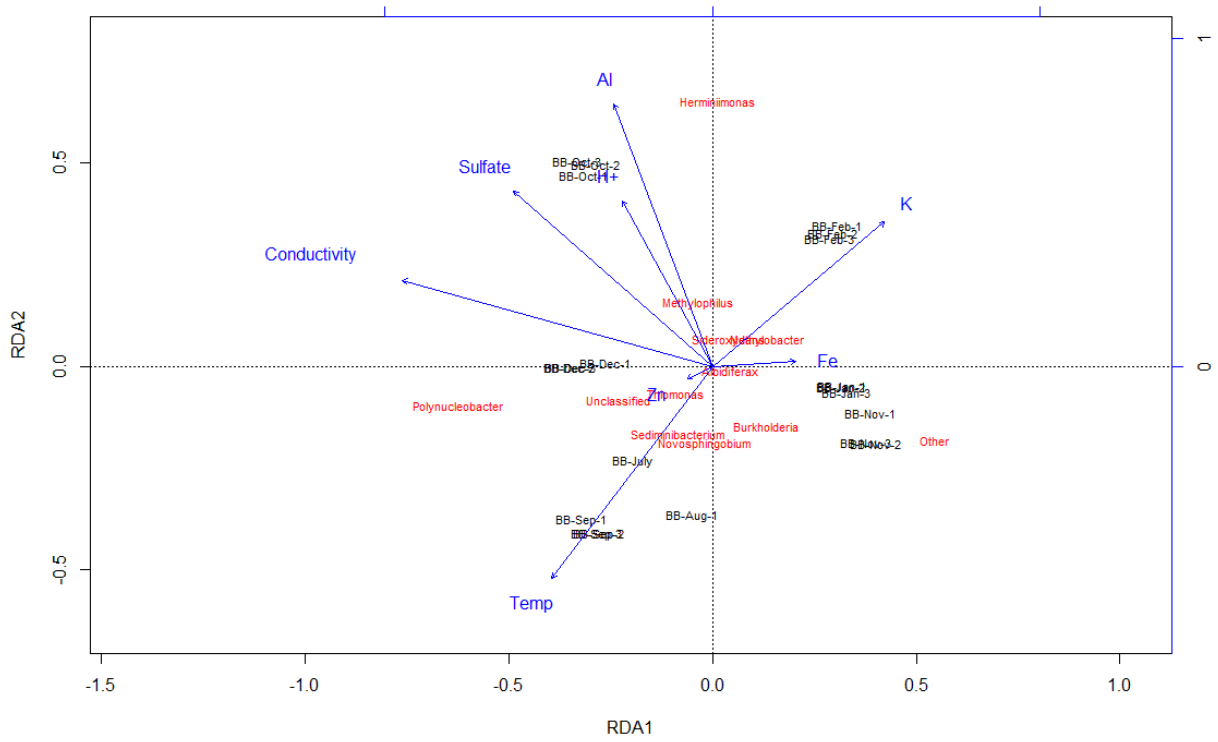

Figure 12. Triplot of RDA Results for Collected Blood Brook Field Data (Scaling 2). The stream chemistry is plotted as linear vectors, while the individual microbial communities are sites, plotted in black. Bacterial genera are also plotted in red.

between them. Response variables closer to the center of the triplot have weak correlations with any vector. Total sulfur, Mg, Ca, and Mn are not included on the figure due to their already identified correlation with conductivity. Their vectors fall within the same upper-left quadrant, but do not have as powerful an influence on the response variables as the plotted vectors. DO was excluded from the analysis as there was incomplete data for the study period. Table 6 summarizes the output of the test.

Table 6. Blood Brook Field RDA Triplot Explanatory Variables

Unadjusted R^2	Adjusted R^2	Variance Explained	Total Axes Variance Explained	X-Axis	Y-Axis
0.8911	0.8118	81.18%	78.459%	44.833%	33.626%

Sulfate concentration, conductivity, hydrogen ion concentration and aluminum concentration are strongly correlated with each other in the same quadrant. Bacterial genera and samples that appear in the upper-left quadrant will have correlations with increases in these vectors. Genera and samples that appear in the lower-right quadrant will have negative correlation with these vectors. This quadrant favors low Al and sulfate, low conductivity, low hydrogen ion concentration, and high pH. Temperature and K concentration appear opposite of each other in opposing lower-left and upper-right quadrants respectively. Genera and communities located along the negative side of the x axis are primarily influenced by temperature and conductivity. However, conductivity is the stronger influence on the two as its explanatory axis is closer to the x-axis. Genera and communities located along the positive side of the x-axis are correlated with increases in Fe and K concentrations. The positive vertical axis is a combination of Al and K, while the negative vertical is primarily influenced by pH with a secondary effect from temperature.

With conductivity being the closest vector to the primary axis, having the largest explanatory vector, and the primary x-axis explaining the largest proportion of the community variance, it appears that conductivity has the most correlation with the variance of the microbial community compositions. Sulfate and Al concentrations cluster with conductivity, do differ slightly, but bear enough of a resemblance to the overall conductivity curve to be included in that assumption. Temperature is the second largest explanatory vector, playing a large part in explaining both the horizontal and vertical axes.

By understanding the relationships between the microbial community and Blood Brook's chemistry, along with knowing how the hydrological influence varies due to precipitation for each sampling point, some inferences can be made about the circumstances in which certain bacterial genera are more abundant. Most of the bacteria present can live under changing conditions as shown by the RDA and the community data and are not strongly influenced by any extreme. However, most do gravitate slightly in a certain direction. *Thiomonas, Polynucleobacter*, and those genera that are unclassified are the genera strongly correlated with increased conductivity and temperature, while *Sediminibacterium* is associated mostly with temperature. These genera are those in the community that are correlated with conductivity. Many of the genera classified as "Other", along with *Burkholderia* are associated with lower hydrogen ion concentration (higher pH), higher Fe concentrations, and low conductivities. "Other" genera are significantly more abundant in November, January, and February as can be seen in the microbial communities in Figure 11. The increases of "Other" and *Burkholderia* are likely due to the change of flow source in Blood Brook during these months. *Herminiimonas* is correlated with Al and with K concentration. The sampling points

from late October and February where *Herminiimonas* is most abundant for the study period exhibit the highest concentrations of Al and K respectively. While *Herminiimonas* is more abundant during the fall/winter sampling points (October-February), *Novosphingobium* is most abundant in the summer sampling points (July-September). *Novosphingobium* appears in the RDA in the bottom hemisphere, opposite *Herminiimonas*, indicating that it is correlated with the lower Al and K concentrations, while also being associated with warmer temperatures. The summer sampling points are correlated with temperature, while the differences in August appear to be associated with raised pH.

2.4 Discussion

2.4.1 Microbial Preferences and Variability

Polynucleobacter is a freshwater planktonic bacterial genus as seen in the community composition breakdown (Figure 11). It represents important bacterioplankton in freshwater streams (Jezberova et al. 2010). *Herminiimonas* has multiple species, most of which are chemolithotrophs (Lang et al. 2007, Muller et al. 2006). One species is well known for oxidizing arsenic, while another is associated with lichens that are attached to rocks (Lang et al. 2007, Muller et al. 2006). Another species was isolated from a glacier and has a temperature range from 1-30 degrees C (Loveland-Curtze et al. 2009). *Burkholderia* is a large genus that contains pathogenic species as well as many that are used for bioremediation (Woods and Sokol 2006). *Sediminibacterium* is gram-negative, with both aerobic and anaerobic species that have been isolated from freshwater sediments (Kang et al. 2014, Kim et al. 2013, Qu and Yuan 2008). *Novosphingobium* is a genus whose species are known for the ability to break down aromatic

compounds, particularly aromatic hydrocarbons (Liu et al. 2005). One species is known to be halophilic (Gupta et al. 2009).

Sideroxydans is a bacterial genus with two known iron-oxidizing species. *S. paludicola* has been isolated from the rhizosphere of wetland plants, but *S. lithotrophicus* is a gram negative, neutrophilic chemolithoautotroph freshwater bacteria that oxidizes soluble Fe (II) at the cell surface (Emerson et al. 2007, Weis et al. 2007). This genus is present in the communities throughout the study period. Since we can only identify to the genus level, the abundance of each of *Sideroxydans* two identified species in Blood Brook is unknown. It is most abundant in January, and the least abundant in September. ICP data showed an increase in iron concentration in Blood Brook starting in October and peaking in December with levels at approximately .07 mmol/L, before beginning to decline again. The increases in *Sideroxydans* abundance correlates with this observed increase in iron concentrations. This correlation is confirmed by the RDA for the field data (Figure 12), where *Sideroxydans* has the strongest association with the vector for iron.

The microbial communities observed in November, January, and February were different in structure than at the other sampling times (Figure 11). Most of the bacteria common in the other months of the study period become a much smaller portion of the overall community while the “Other” (<1%) category becomes most of the community, comprising over 50% of the total reads. The calculated diversity indices (Table 8) show that at points where “Other” increases and becomes most of the community the indices also increase substantially.

2.4.2 Chemistry Variability

Many of the observed variations in chemistry can be attributed to when Blood Brook's stream flow is dependent upon surface runoff instead of groundwater. This can be observed in stormflow dominated months, November, January, and February. In the three days prior to sampling for November, 2.38 inches of rain was recorded (NOAA 2015-2016). January did not have any precipitation within 36 hours of sampling, but there was 6 inches of snow melt within that time (NOAA 2015-2016). Proceeding sampling in February was 0.68 inches of rain, along with 6-7 inches of snowmelt (NOAA 2015-2016). The drop in most of the chemical parameters (conductivity, sulfate concentration, Ca, Mg, Al, Na, etc.) is likely due to the dilution of the stream chemistry from these large influx runoff or meltwaters. This increase in stormflow is likely the cause of the large increase in the "Other" category of the microbial communities. Stormflow washed additional bacterial genera from the soil into the stream, which increased community diversity.

Iron fluctuations in Blood Brook are unusual. They exhibit positive correlation to pH, where increasing iron concentrations correlate with increasing pH. We'd expect to see the opposite, due to lower pHs increasing solubility (Burgot 2012). What is observed increasing alongside iron concentrations is the DO concentrations. These increase into the winter months, along with falling temperature (Table 4). DO is more soluble in colder water along with other gasses (Garde et al. 1999). With an increase of DO, it is likely sulfide oxidation within Blood Brook increased releasing more iron into the stream. Sulfate concentration also increases across the time iron is at its highest concentrations (October-December), other than during the dilution of Blood Brook during the stormflow period in November. This supports increased

sulfide oxidation during this period, as sulfate is also a product of those processes (Singer and Stumm 1970).

Aluminum concentrations in Blood Brook are primarily associated with pH. Overall, aluminum concentrations tend to decrease as pH increases (Figure 13). The larger concentration associated with the sampling point at the end of October is likely due to the pH being at the second lowest point of the entire study period. Here, the pH is 4.88. Al also shows a trend where concentrations increase along with increasing sulfate concentrations (Figure 14). This makes sense, as increased sulfate is also related to pH within sulfide oxidation systems (Singer and Stumm 1970, Williamson et al. 2006). As more sulfide oxidation occurs within the bedrock base of Blood Brook, sulfate will be released into the waters, and the pH will be lowered. Lowering pH increases solubility of aluminum and other metals (Burgot 2012). The RDA (Figure 12) supports these inferences, because the Al, sulfate, and H vectors are all correlated together within the same quadrant. The drops in concentration observed at the November and January sampling points can associated with the dilution from Blood Brook being dominated by stormflow at those points.

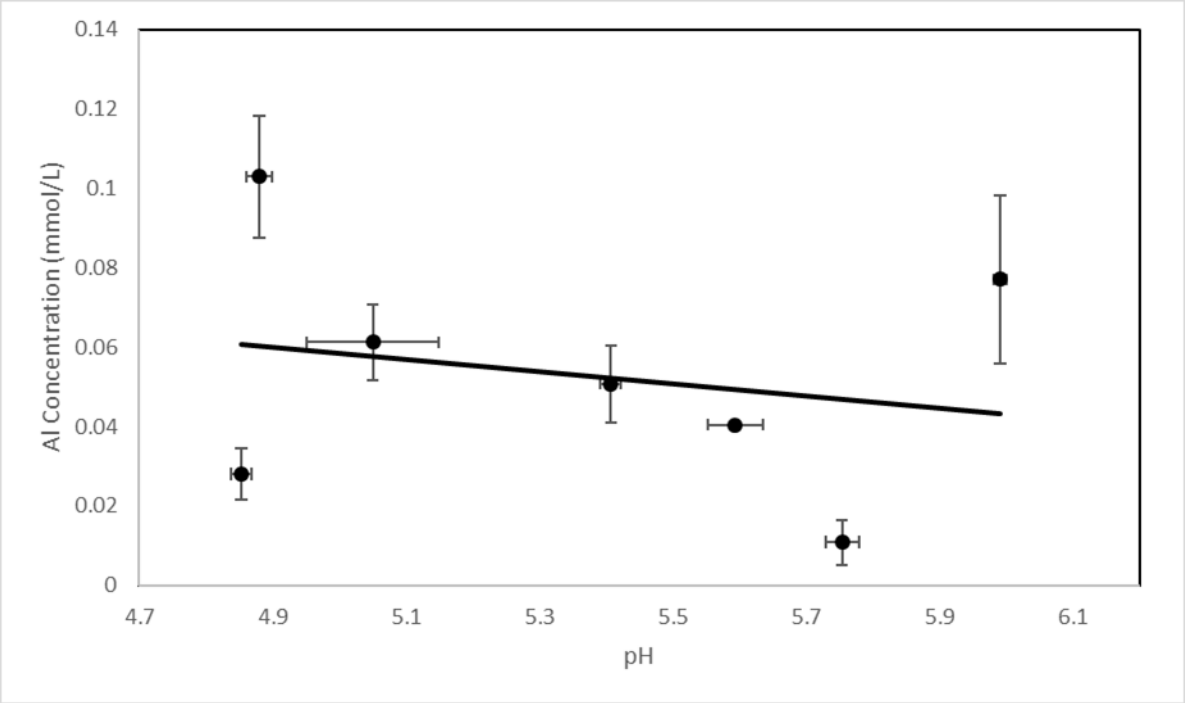

Figure 13. Blood Brook Al Concentration vs. pH. As expected, Al concentrations decrease along with pH. This is due to pH affecting solubility of metal (Burgot 2012). The November sampling point contains higher aluminum concentrations, despite being at maximum pH for the study period.

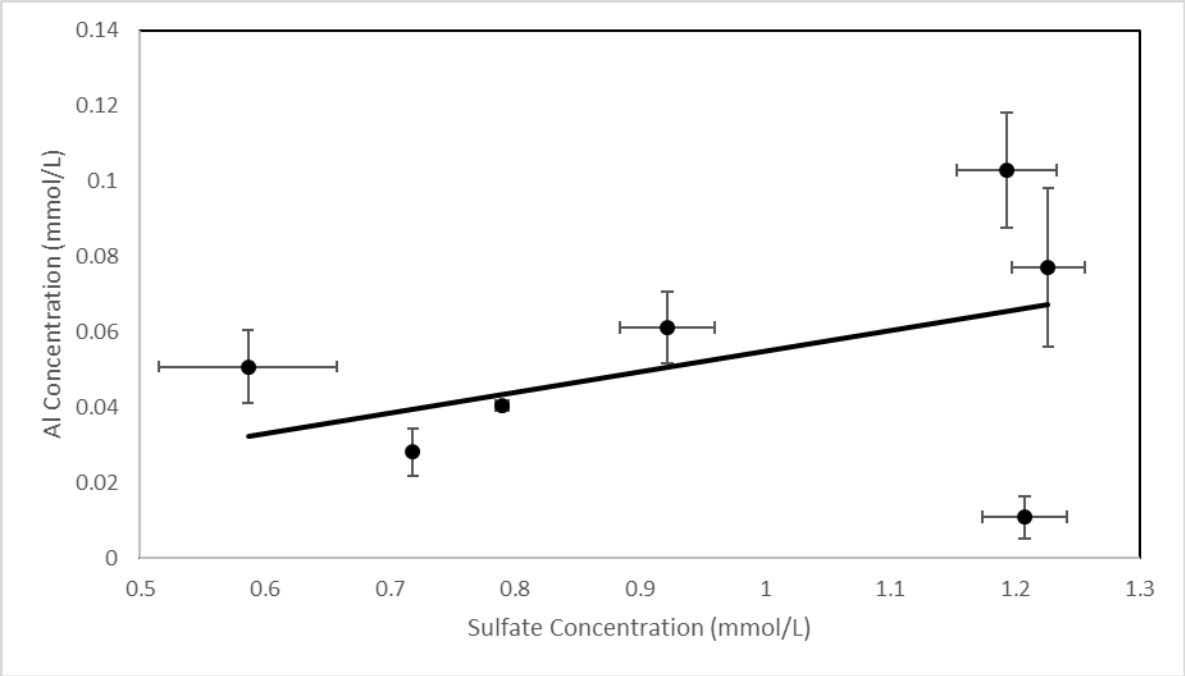

Figure 14. Blood Brook Al Concentrations vs. Sulfate Concentrations. A positive correlation is displayed between the two parameters. The data point for July contains high sulfate, but low aluminum concentrations.

The rapid increase in potassium observed in January and February (Table 5) is likely due to the element's dominance as a plant nutrient. A strong source of potassium within inland surface waters is the periodic decomposition of organic matter (Talling 2010). In January and February, the ground was covered by snow. It is likely there was decaying leaf matter trapped underneath the snow. Meltwater from the observed snow melt periods (NOAA 2015-2016) likely transported potassium from this leaf matter into Blood Brook.

2.4.3 Standard Community Comparison

As discussed in Chapter 1, have their own distinct chemistry and microbial community structure compared to groundwater aquifers (Beaton et al. 2016, Fierer et al, 2007, Lindstrom et al. 2005, Mamaar et al. 2015, Stevenson 1997, Van der Gucht et al. 2005). The microbial communities identified in Blood Brook generally follow the surface water community structure, with minimal similarities to groundwater communities. Betaproteobacteria community percentages range from approximately 45-80% of the total community (Figure 15). At two points where the Blood Brook is stormflow dominated (November and January), Betaproteobacteria drop slightly below the 33% mark that is normally seen in surface water communities, at approximately 26% of the community. In February, Betaproteobacteria still remains high, comprising 50% of the community. The iron and sulfide oxidizing bacteria present in the field community (*Sideroxydans* and *Thiomonas*) are part of the Betaproteobacteria population.

Alphaproteobacteria is usually the second most dominant class in the communities, followed by Actinobacteria. This is different from what is observed in stream communities in the literature, where Actinobacteria is usually more populous (Fierer et al. 2007, Lindstrom et

al. 2005, Van der Gucht et al. 2005). Most of the strains identified by our analysis include many unclassified genera from the orders Rhodospirallales and Rhizobiales. A large population of uncultivated strains are common in mildly acidic waters created from sulfide oxidation like Blood Brook (Jones et al. 2017). Most of the present Rhodospirallales tend to come from the family Acetobacteriaceae, which commonly produce acetic acid through respiration (Raspor and Goranovic 2008).

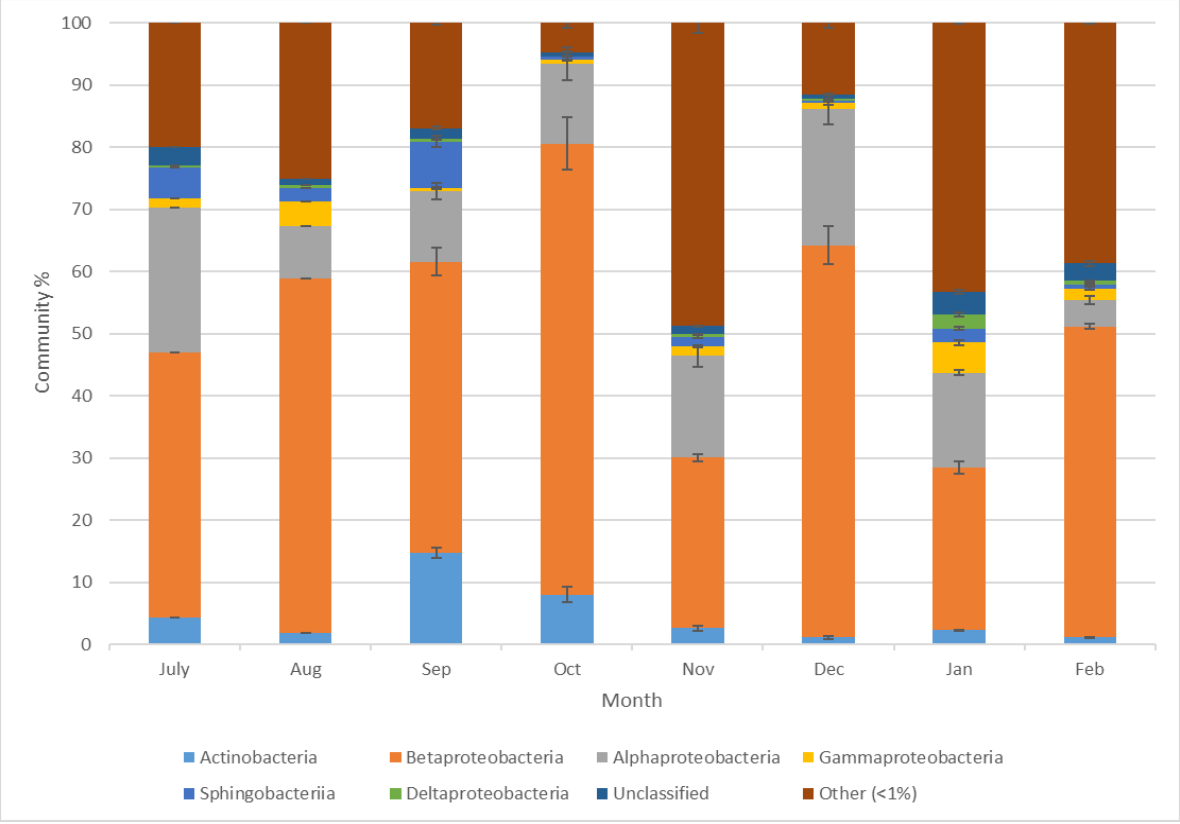

Figure 15. Blood Brook Microbial Communities Organized by Class [NCBI Accession #: PRJNA43078]. Blood Brook's microbial communities resemble what could be considered a standard stream community. Betaproteobacteria comprise 33% or more of the total community.

2.4.4 Dilution vs Diversity Within the Community Structure

Does the influence of stormflow into Blood Brook dilute the microbial community or increase diversity through the influx of soil bacteria into the stream? It would appear the diversity is increased, as shown by the increased amount of the "other" category (<1% of the total population) in November and January sampling events. By comparing the DNA concentrations in our sample water at each point, we can see when in Blood Brook microbial mass was at its highest. DNA extractions were performed using 600 mL of filtered sampled water, except in cases where the filter could no longer allow water through it (Section 2.2.4). All sampling points were able to reach 600 mL except for the samples taken in September and January. Samples at these points contained a high amount of suspended matter and were only able to filter about a third of the total volume (~225 mL). When comparing DNA yields between samples (Table 7) there are sizably greater DNA yields in the samples take in September and January. This means that there was higher bacterial mass in those two samples, but not necessarily higher diversity. Since the sampling point in September was taken during a baseflow period and the sampling in January during stormflow this isn't an indicator of flow impact. What can be concluded is that the higher turbidity is positively correlated with higher microbial mass.

The inverse-Simpson diversity indices for the samples that were calculated by mothur. (Table 8) provide a better understanding of diversity within Blood Brook's microbial communities. These results clearly show that both the January and November samples are the most diverse communities, both before and after subsampling, with post subsampling diversity indices ranging from 60-78 and 37-50 respectively. This is even with only approximately 69-

73% coverage of the original sample after subsampling. The next most diverse sample is July with a subsampled index of 15.39. The rest of the microbial communities have diversity that ranges from approximately 4-10. Even though February is a stormflow dominated sampling point, the microbial community's diversity is not comparable to November and January's diversity. It is higher than the baseflow points from fall and winter (September, October, December). The summer communities do have larger portions of "Other" and unclassified than September, October, and December (Figure 11). The largest DNA yields that were not from September and January also came from the summer months (July and August). The proportions, DNA yields, the diversity indices, and the RDA results (Figure 12) together suggest that temperature does influence bacterial activity and overall community diversity.

Table 7. Field Sample Extraction Volumes and Yields

Sample (Calendar Day)	Volume of H_2O Filtered (mL)	DNA Yield (ng/µL)	Original DNA Concentration (ng/mL)
July (190)	600	14.9	2.48
Aug-1 (232)	600	23.0	3.83
Aug-2 (232)	600	6.2	1.03
Aug-3 (232)	600	5.8	0.97
Sep-1 (253)	258	28.7	11.12
Sep-2 (253)	265	23.3	8.79
Sep-3 (253)	247	31.7	12.83
Oct-1 (300)	600	6.5	1.08
Oct-2 (300)	600	11.2	1.87
Oct-3 (300)	600	8.1	1.35
Nov-1 (327)	600	7.3	1.22
Nov-2 (327)	600	4.3	0.72
Nov-3 (327)	600	5.4	0.9
Dec-1 (335)	600	2.9	0.48
Dec-2 (335)	600	3.3	0.55
Dec-3 (335)	600	5.1	0.85
Jan-1 (7)	223	20.5	9.19
Jan-2 (7)	219	21.4	9.77
Jan-3 (7)	268	17.8	6.64
Feb-1 (50)	600	5.9	0.98
Feb-2 (50)	600	2.7	0.45
Feb-3 (50)	600	2.8	0.47

Table 8. Inv-Simpson Diversity Indices for Field Sampled Microbial Communities

Sample (Calendar Day)	Initial Read Count	Inverse-Simpson Diversity	Subsampled Reads	Subsampled Coverage (%)	Subsampled Inv-Simpson
July (190)	13888	15.22	1934	89.34	15.39
Aug-1 (232)	24861	12.57	1934	85.22	12.92
Aug-2 (232)	87	6.42	1934	N/A	N/A
Aug-3 (232)	152	9.48	1934	N/A	N/A
Sep-1 (253)	22532	8.09	1934	88.73	8.26
Sep-2 (253)	53294	8.55	1934	89.75	8.84
Sep-3 (253)	37797	8.81	1934	89.38	8.96
Oct-1 (300)	25638	4.54	1934	96.65	4.60
Oct-2 (300)	1934	5.59	1934	95.55	5.59
Oct-3 (300)	38822	4.41	1934	96.84	4.45
Nov-1 (327)	30859	35.73	1934	70.19	37.45
Nov-2 (327)	16638	35.43	1934	71.25	36.17
Nov-3 (327)	13261	49.81	1934	69.27	50.94
Dec-1 (335)	32887	5.62	1934	91.66	5.75
Dec-2 (335)	27535	4.70	1934	92.90	4.80
Dec-3 (335)	22627	6.50	1934	92.17	6.60
Jan-1 (372)	17125	59.66	1934	72.22	60.58
Jan-2 (372)	21073	75.75	1934	71.84	78.33
Jan-3 (372)	17543	69.43	1934	72.30	70.22
Feb-1 (415)	24121	9.19	1934	73.01	9.48
Feb-2 (415)	22231	10.12	1934	72.47	10.38
Feb-3 (415)	20713	9.86	1934	72.64	10.07

2.5 Field Conclusions

The results of the study show that structure of Blood Brook's microbial community resembles a standard surface water community with an atypical smaller population of circumneutral iron-oxidizers. The sequenced and observed community is comprised entirely of bacteria, with approximately 42% of total reads being unclassified at the genus level for most of the study period. Those classified bacteria that are the most abundant genera are typically chemolithotrophic and gram-negative. Also present are planktonic bacteria like *Polynucleobacter*. The only abundant genus present throughout the entire study period that is known to contribute to sulfide oxidation is *Sideroxydans* which does not directly attach to pyrite, but rather absorbs and oxidizes already dissolved Fe (II) (Emerson et al. 2007, Weis et al. 2007). This genus varies between 2-5% of the community throughout the study period. *Thiomonas*, a genus that has been often identified in ARD and contributes to sulfide oxidation is also present (Auld et al. 2013, Baler and Banfield 2003, Edwards et al. 1999, Johnson 1998, Johnson and Hallberg 2003), but is not as abundant as *Sideroxydans* and comprises over 1% of the total reads only between July and October. The most noticeable variation in the community is within the category "Other" (genera that comprise less than 1% of the total community). This group increases from approximately 17% of the community to 61%, while the other abundant genera all decrease, except for *Burkholderia* within the November sample. The class Betaproteobacteria, which contains the planktonic bacteria like *Polynucleobacter* and the present iron-sulfide oxidizing bacteria, is the dominant class in both these communities and surface water communities from the literature(Fierer et al. 2007, Lindstrom et al. 2005, Van der Gucht et al. 2005). It comprises approximately 25-70% of the total reads. Seasonally, there are

very small variations. *Thiomonas* only appears at greater than 1% for a few months. The genus *Novosphingobium* and the class Sphingobacteriia both become more abundant in the summer sampling points, ranging from July to September. Conversely, the genus *Herminiimonas* is less abundant in this time frame compared to the rest of the sampling points.

The study results also revealed correlations between the changing microbial community, and seasonally changing hydrologic, chemical, and temperature conditions. Using collected precipitation data and hydrological methods as described in Sections 2.2.7 and 2.3.5, it was determined that November, January, and February are the sampling points where Blood Brook is influenced primarily by stormflow, with the rest of the study period being dominated by baseflow. Stormflow contributes to the diversification of the microbial community through microbial transport to the stream from soil surfaces (Mamaar et al. 2015), which accounts for the observed increases of the "Other" category at these three sampling points. The large precipitation and surface water runoff events in those two months also account for the large drop in conductivity and many of the metal concentrations that can be observed. The increase in DO and iron concentrations most likely contribute to the reason *Sideroxydans* becomes the most abundant genera in January, despite the dilution influence observed by every other genus in the community. This all supports the conclusions based on the RDA, which shows the effects of precipitation and stormflow events on the microbial community. Lastly, the RDA, yield data, and diversity indices reveal that temperature may play a role in increasing the microbial diversity during baseflow periods.

CHAPTER 3. EXPERIMENTAL ASSESSMENT OF BLOOD BROOK MICROBIAL COMMUNITIES' OXIDATION POTENTIAL AND STRUCTURAL EVOLUTION WITHIN CONTROLLED ACIDIFYING CONDITIONS

3.1 Introduction

This chapter contains the methods and results for the conducted batch reactor experiments. The goal was to assess the sulfide oxidation potential of Blood Brook's microbial community, sampled at various hydrological and chemical conditions. The community was subjected to prolonged exposure to pyrite, thereby potentially created acidifying conditions. We hypothesized that;

1. Acidophilic iron and sulfide oxidizing bacteria would become dominant in Blood Brook's microbial communities in the presence of pyrite and acidifying conditions.
2. We also hypothesized that samples collected during periods dominated by stormflow will have lower oxidation potential due to the dilution of the of bacteria participating in sulfide oxidation.

We believe that the information presented in this chapter will provide insight into the response of microbial communities within these systems to increased acidification, like that produced by mining a sulfide deposit.

3.2 Methods and Materials

3.2.1 Mineral Preparation

High-grade pyrite from Huanzala, Peru was purchased from Ward's Science+. Pyrite was chosen due to it being the most commonly oxidized sulfide mineral. Pyrite was crushed, pulverized, and sieved to a grain size of 0.5-1 millimeter. Once the correct size, the grains were

washed in ethanol and subjected to ultrasonic emission from a Microsonix sonicator to remove reactive micro-particles from the mineral grains. This process was repeated until the ethanol remained clear after sonication which usually took about 45 minutes. The pyrite was then placed in a clean storage cup and placed in a drying oven at 80˚ C for 24 hours. A total of 800 grams of clean pyrite was prepared. Before addition to the reactors, the pyrite was again washed in ethanol and dried to remove any microorganisms from the mineral surface.

Using an EDAX Pegasus system, chemical data for the pyrite was analyzed by the Department of Earth and Climate Sciences' Tescan Vega II XMU tungsten filament scanning electron microscope (SEM) (Appendix A) (Goldstein et al. 2017). Pyrite grains were mounted in epoxy, sanded for exposure, and carbon coated using an EMITECH K950X to allow analysis by the EDAX system (Robinson et al. 1987) . Using energy dispersive x-ray spectrometry on high vacuum mode within the SEM, the chemical data were collected with EDAX Genesis software. The data shows that the cleaned sample contains 59.84 weight percent sulfur and 40.16 weight percent iron after recalculation from carbon omission. The atomic percent of these elements are 72.2 and 27.8 respectively. Carbon can be ignored as it is interference from the carbon coat of the sample. Sulfur is about 6 percent higher than normal, while iron is 6 percent lower than normal for both weight and atomic percentages (Fiechter et al. 2011). This is a normal fluctuation for an unstandardized sample (Goldstein et al. 2017).

3.2.2 Experimental Design

Twelve batch reactors containing waters from Blood Brook were run in five-week (840-hours) experiments. The experiment was repeated three times, once for each sample taken from Blood Brook at calendar day 300 (October), day 335 (December), and day 372 (January). In

each of these experiments, six of the flasks contained 50 mL sterilized abiotic water and the other six contained 50 mL unaltered biotic water directly from the field sites. Abiotic water was prepared by autoclaving sample water for 90 minutes. The water was then refrigerated overnight for use in the experiment the following day. The volume within the reactors was kept this low to facilitate the oxygenation of the reactors, since DO is needed for both abiotic and biotic sulfide oxidation processes. One gram of the prepared pyrite was added to all reactors. The reactors were capped with aluminum foil so that they were open systems, which also helped facilitate the addition of DO to the reactors. Reactors were placed in shaker baths which were run at a speed of 50 rpms and at a temperature of 25˚ C.

3.2.3 Sampling

Samples were collected at 0, 4, 24, 168, 336, 504, and 840 hours. At each sampling point, unfiltered 7.5 mL of water was removed from one of the replicates for sulfate and metal analysis (see Section 3.2.4). Water was removed from the reactors using a 10-mL calibrated Eppendorf pipette. Sample data for all analyses at time point 0 came from unaltered water collected in triplicate directly from the field sites before adding to the batch reactors. This data was also used in chapter 2 as the monthly sampling data for October, December, and January respectively. Because a large volume of water was needed for analyses, a different fresh, unsampled replicate was sampled each time. Sampling was done in this manner to preserve the solute to solution ratio within the reactors. For example, at 4 hrs 7.5 mL water was sampled and removed from replicate reactor 1 for each treatment, which left the reactors at a total volume of 42.5 mL after sampling. At the next time point, 24 hrs, 7.5 mL was taken from replicate reactor 2, which would leave the first two replicates in each treatment now at a volume of 42.5

mL. The procedure continued using a different replicate for each subsequent time point. This way, samples were always taken from a reactor containing the original volume of solution that would be reacting for that length of time. 2.5 mL of the unfiltered sample taken from the reactors was set aside for immediate use on the spectrophotometer. The remaining 5 mL was filtered through a sterile syringe file into 10 mL plastic sample vials, acidified to 1% with nitric acid (HNO_3), and capped. Each sample vial was labeled with Raymond Kahler Thesis (RKT), experiment replicate number (i.e. 1, 2), sampling time point (T336), field site (Blood Brook) and treatment (AB or B). Acidified ICP samples were then placed in the geochemistry lab refrigerator at 10˚ C for storage until analysis and samples for sulfate concentration were analyzed immediately. At the end of each experiment, the water and solids from three of the biotic reactors were set aside for immediate use in DNA extractions. For the remaining reactors, the water was decanted from reactors to use within alkalinity titrations immediately. The decanting for the titrations was performed for both treatments and included the remaining biotic reactors not used for DNA extractions, and all the abiotic reactors. Precipitate samples to be observed in the SEM were also taken from the decanted reactor water.

3.2.4 Chemical Analyses

All the same chemical parameters from the field study (pH, DO concentration, sulfate concentration, etc.) were tracked throughout the course of the experiments. For each experiment, pH, DO concentration, and specific conductance were taken and recorded at time 0, 4, and every subsequent 24 hours using a benchtop pH probe, a portable HACH DO meter, and a portable HACH conductivity meter respectively. These measurements are reported using the mean of all the replicates for each experimental treatment. In between each reading, the

probes were washed with 95% ethanol, followed by deionized water to minimize cross-contamination between samples. Abiotic reactors were read and recorded before biotic reactors to minimize cross-contamination as well.

Sulfate was analyzed for each of the 2.5 mL experimental samples taken using the method described in Section 2.2.3. One change, however, is the same sample was used to blank the spectrophotometer before adding the reagent to it and being read. The rest of the sample taken weekly (5 mL) was prepared for use on the ICP-OES in the Deering Hall Analytical Lab at the University of Maine. The experimental samples were prepared the same way as the field samples, as described in Section 2.2.6 (Eaton et al. 2005). Alkalinity was also recorded at the beginning and of each experiment. Alkalinity for times 0 was recorded as the same as the sampled water used in each experiment. An alkalinity titration as described in Section 2.2.5, was performed at the end of each experiment for both the abiotic and biotic treatments using 50 mL of the end experiment sample pools. If the pH of the sample pool was ultimately less than 4.5, a titration was not performed, and the alkalinity recorded as 0 mg/L of $CaCO_3$ (Eaton et al. 2005). This is because a solution with pH less than 4.5 no longer has any ability to neutralize acid (Drever 1988).

3.2.5 ICP-OES

Experimental samples were analyzed for metal content on the ICP-OES concurrently with the field samples by the Deering Soil and Water Analytics Lab at the University of Maine. Samples extracted from the reactors were immediately prepared, stored, and analyzed for ICP analysis as described in Section 2.2.6.

3.2.6 Microbial Community Extraction and Observation

The microbial communities present in the experiments' reactors were found using the same extraction and analysis techniques as described in Section 2.2.4. Samples were extracted and analyzed at the end of each experiment. The community found for the field data in the month in which the experiment occurred was used as Time 0 community for the experiment. For example, October sample was used as the water for Experiment 1. The community found for October represents the Time 0 community for Experiment 1. Three aliquots of 50 mL from the pooled biotic water at the end of each experiment was filtered and analyzed. For the experiments, the pyrite grains from three of the biotic reactors was also used in the filtering and extraction process along with the solution from the biologic reactors. Once extracted the 100 µL of DNA solution was stored at -80˚ C along with the field extractions. The experimental samples were also analyzed at the UT Austin GSAF. Samples were prepared, shipped, and analyzed as described in Section 2.2.4. Results for the experimental communities from the GSAF can be found within the NCBI's GenBank online database under accession number PRJNA430708.

Direct counts using a microscope were performed at the beginning and end of each experiment to assess microbial growth and concentration in solutions. Slides were prepared using acridine orange staining. Acridine orange is sensitive to microorganisms at mildly acidic (~4.0) pHs (Francisco et al. 1973). Slide solution was prepared in a 50-mL graduated cylinder. This solution included 40 mL of sample water from the associated timepoint, 9 mL of 4% formaldehyde, and 1 mL (2%) acridine orange stain. The water samples used were unaltered, so they included any solid precipitates. The graduated cylinder was wrapped in aluminum foil to

prevent exposure to light and the degradation of the stain. This mixture stood undisturbed for at least 10 minutes to stain and fix microorganisms within the sample solution. Once the sample was stained and fixed, the liquid solution was filtered through a black 0.22 µm (Millipore) pore size, 25 mm diameter, polycarbonate filter using an autoclaved 100 mL vacuum flask and pump. Using sterilized tweezers, the filter was transferred to a glass slide. The filter was covered with immersion oil and then a cover slip was placed on top of the now prepared slide. Counts were performed using the microscope at 40x objective magnification, along with a 10x magnification eye piece, for a total of 400x magnification.

3.2.7 Scanning Electron Microscope (SEM)

Along with the pyrite composition, the University of Maine's School of Earth and Climate Sciences' Tescan Vega II XMU tungsten filament SEM and the EDAX Pegasus apparatus within it were used to analyze post-experiment precipitates collected from the experimental reactors (Goldstein et al. 2017). Photographs were taken to observe precipitate structure, and chemical analyses performed using EDAX Genesis software to collect chemical data (Goldstein et al. 2017). Large precipitates were removed from the biological reactors using a pair of tweezers that had been washed with 95% ethanol and deionized water and sterilized with a Bunsen burner. The precipitate was placed on a slide and then flash carbon coated using an EMITECH K950X to reduce charge buildup while being observed in the SEM (Robinson et al 1987). The slide was then placed inside the SEM chamber using the slide holder. The chamber was closed, sealed, and prepared for photography. Photos were taken under high vacuum (HV), using a secondary electron detector.

3.2.8 Statistical Methods

3.2.8.1 Simple Linear Mixed-Effect Models

Simple linear mixed-effect models were used to test if there were significant differences between the trends in the amount of hydrogen ions or sulfate being released across time, measured from the abiotic and biotic treatments. These were also used to test trends for significant differences between the results across each of the three experiments. In simple linear mixed-effect models, the equation that is tested accounts for both fixed and random variables (Galecki and Burzykowski 2012). The random effect aims to account for unobserved heterogeneity within the samples and adds the assumption that observations within the random variable group are correlated. Mixed-models also add the assumption that effects associated with the random variables are uncorrelated to the fixed effects (Galecki and Burzykowski 2012). In the case of these experiments, the random variable accounts for the need to sample from a different reactor replicate at each time point to conserve volume. By adding this to the fixed linear model, we are telling the model to not relate the staggered sampling to changes within the trends when comparing for significance.

These mixed-effects models were run in R using the function lmer from the package lme4 (Bates et al. 2015). This test evaluates the input formulas and includes a significance test. Mixed-effect models were used to assess whether there were significant differences in the changes in pH between the abiotic and biotic reactors in each of the three experiments (October, December, and January) as well as to assess if there were significant differences between each of the experiments themselves for the abiotic and biotic reactors. All the following discussed R code can be found in Appendix C.

Two different formulas were used to address these different problems using the lmer function. The first, which was used simply for differences between the abiotic and biotic reactors, was written in R as follows:

$$lmer(pH{\sim}Treatment * Time + (1|Sample), data = bbexp1) \text{ (**Eq. 13**)}$$

In this formula pH represents either pH or sulfate, this would change depending on what was being tested for, and this would be the response variable. In this formula, treatment across time is the fixed effect while the sample is the random effect. This formula was run 3 times using sulfate data from each experiment and 3 times using the pH data. The data portion of the function would change from bbexp1 to bbexp2, or bbexp3 depending on which data frame representing each experiment was being used. The results reveal any significant differences between the treatments over the course of the experiment.

Sulfate tests were conducted using a similar formula that was adjusted slightly for the limited time points as well as a different data frame named bbsulf. This data frame contains sulfate data for all experiments as it is only one chemical parameter due to the different sampling structure. Linear mixed-effect models were performed for sulfate as follows:

$$lmer(Exp1{\sim}Treatment * Time + (1|Sample), data = bbexpsulf) \text{ (**Eq. 14**)}$$

Sulfate tests between treatments and experiments were all run twice, once with the initial data point, and once without. The addition of time point 0 alters the overall linear trend of the sulfate data due to a significant jump in sulfate concentration during the first 4 hours of each experiment that can be seen below in Figure 16 and Section 3.3.3. Analyzing the linear trend of the sulfate concentration data from time points 4 to the end may be a better representation of the overall data trend.

To test significant differences between the individual experiments simple linear regression (lm) was used for sulfate. The formula can be seen below:

$$lm(Exp1 \sim Exp2 * I(\frac{Time}{24}), data = bbexpsulfA) \text{ (**Eq. 15**)}$$

The mixed-effect regression model was still used for pH, DO, and conductivity due to the multiple replication and the alternative sampling. To effectively run these tests comparing treatments between experiments, the treatment data for each chemical parameter was organized into its own data frame labeled as bbexpparameter(AorB) where parameter was replaced with the appropriate name and A or B was the appropriate treatment. For pH, DO, and sulfate since their data was on a much smaller scale than time, time was adjusted using the I function within the formula to divide by 24 hours and convert time to days rather than hours. This created a better fit for those models when comparing experiments. Complete R code for all the experiments can be reviewed in Appendix A.

3.2.8.2 RDAs

Redundancy Analyses were also completed in R for the experiments (Bourcard et al. 2011). The data was analyzed and processed similarly to what is described in section 2.2.8.2. Two RDAs were completed for the experimental data, due to gaps in the ICP results. One RDA included chemical data recorded during all three of the experiments (sulfate concentration, DO, pH, etc.), but excluded the ICP data, while the other excluded Experiment 1: October from the analysis, but included the ICP data as well as the daily recorded data for the other two experiments. The coding for these RDAs was not significantly different than those run for the field data. The rda function from the vegan package was still used with similar formula structure as described in Chapter 2 (Oksanen et al. 2018). The data table contained in R had to be

manipulated into two separate data frames for use in the separate RDAs, where the ICP data was removed and labeled as a new object, NewExpChemData1. This was repeated by removing all Experiment 1 data and labeled as object, NewExpChemData2. Complete coding for this process can be seen in the included R script within Appendix C. These RDAs were run using the following formulas:

$$NewExpRDA1 \leftarrow rda(ExpGenera.hell, NrmExpChemData1, scaling = 2) \text{ (Eq. 16)}$$

$$NewExpRDA2 \leftarrow rda(ExpGenera1.hell, NrmExpChemData2, scaling = 2) \text{ (Eq. 17)}$$

In these formulas, ExpGenera.hell is the data frame with the experimental biological OTU data converted using the Hellinger transformation, which acts as the response variable set. ExpGenera1.hell, is the same data frame, albeit with the Experiment 1 data removed, since the response and explanatory sets of variables in and RDA must contain the same number of fields.

3.2.8.3 Microbial Data Analysis

Experimental microbial community data was again processed by the GSAF at University of Texas Austin. The results from the metagenomics were processed through mothur according to the standard operating procedure for MiSeq data, reference files, and the associated additional steps as described in section 2.2.8.1, except communities were subsampled to 1934.

3.3 Results

3.3.1 Summary of Starting Experimental Samples

Experiments were conducted using water samples collected from Blood Brook in October 2015, December 2015, and January 2016 (Table 9). From this point forward, the experiments will be referred to as Experiment 1, 2, or 3 (October, December, and January respectively) along with their treatment letter (A or B). For example, biotic reactors from the

December experiment will be called Experiment 2B. If treatment is not specified, both treatments are being referred to. The water used in Experiment 1 was characterized by the highest specific conductance of the study period with a mean of 209.3 µS/cm and the second lowest pH of the period with a mean of 4.88 which translates to a concentration of hydrogen atoms of $1.32x10^{-5}$ mol/L. The October sample also had the second highest sulfate

Table 9. Starting Experimental Samples Chemical Summary

	Experiment 1: October 2015	**Experiment 2: December 2015**	**Experiment 3: January 2016**
Mean pH	4.88	5.99	5.59
Mean Sampling Temperature (˚C)	3.9	0.6	-0.7
Mean Sulfate Conc. (mmol/L)	1.19	1.23	0.79
Mean Specific Conductance (µS/cm)	209.3	191.7	88.8
Mean DO Conc. (mg/L)	7.15	12.17	10.35
Alkalinity (mg/L of $CaCO_3$)	2	4	6
Mean Fe Conc. (mmol/L)	0.00179	0.0699	0.0499
Mean Al Conc. (mmol/L)	0.103	0.0771	0.0404
Dominant Microbial Genus	*Herminiimonas*	Unclassified	"Other"
Community % of iron-oxidizing *Sideroxydans*	3.619	3.413	7.325
% of community that is unclassified at genus level	29.47	43.79	26.84
% of "Other" (<1%)	7.14	16.36	54.41
Dominant Flow Source at Time of Sampling	Baseflow	Baseflow	Stormflow

concentrations, at a mean of 1.19 mmol/L. The mean water temperature averaged from three measurements at the time of sampling for the October sample was 3.9 ˚C. Iron levels were low at $1.8x10^{-3}$ mmol/L. *Herminiimonas* is the dominant genus within the microbial community, making up approximately 36% of the total microbial community, while the iron-

oxidizing genus *Sideroxydans* is present at approximately 3.6%. Unclassified bacteria make up about 29.5% of the total community. The October water sample came from a baseflow period, as determined in Chapter 2.

The starting water used in Experiment 2 has similar chemical and microbial characteristics to the Experiment 1 water. Conductivity is 191.7 µS/cm; however, pH is much higher at 5.99. This translates to a hydrogen ion concentration almost an order of magnitude lower at 1.02×10^{-6} mol/L. Sulfate concentration is 1.22 mmol/L. The major difference chemically in this sample is iron concentration is almost 40 times higher than the Experiment 1 iron concentration. This month comes from a baseflow point (Chapter 2), with evidence of increased sulfide oxidation occurring at that time. The microbial community exhibits slight increases in the proportion in the unclassified and the "Other" category (<1% of the total microbial community), and a large reduction in *Herminiimonas*. *Sideroxydans*' proportion is relatively the same as in October (Figure 11).

The final experiment (3) sample, collected in January of 2016, is the most different of all the water samples used in the experiments. This can be attributed to flow being stormflow as opposed to baseflow. Conductivity, sulfate, and iron levels have decreased to 88.8 µS/cm, 0.79 mmol/L, and 4.99×10^{-2} mmol/L respectively. pH has slightly decreased to 5.59. The "Other" category dominates the microbial community, increasing to approximately 54.4% of the total. Most other genera decrease in abundance, except for *Methylobacter* and *Sideroxydans*. *Sideroxydans* is at its highest abundance in the study period at 7.32%. This is likely due to the soluble iron concentrations seen in the sample of the previous month and this month, which

are still very high compared to October and earlier. Across all samples used in the experiment, water temperature at the time of sampling has decreased sequentially (October to January).

3.3.2 Experimental Results

3.3.2.1 pH

Within the batch reactors, pH was monitored daily (Figure 16). In Experiment 1A the initial mean pH was 4.24 and the final mean pH was 4.75. The initial mean pH in Experiment 2A was 4.96 and increased to 5.2 by the end. For Experiment 3A, there is an initial mean pH of 5.41 which decreases to 5.16. The changes within the abiotic reactors are not large, and they stay relatively similar from start to end of all the experiments.

In the biotic experiments, a greater decrease in pHs is observed. The starting pH Experiment 1B was 4.79, which decreased to 3.13. The pH of Experiment 2B started at 5.52 and decreased to 3.89. Lastly, the pH of Experiment 3B started at 5.45 and decreased to 4.09. The pH within all the biotic reactors decreased consistently throughout all the experiments, with the decrease becoming less pronounced from Experiment 1B to Experiment 3B. Complete pH data for all points throughout the experiments can be found in Appendix A.

3.3.2.2 Sulfate Concentration

Sulfate was measured at the time 0, 4, and 24 hours, as well as weekly in each experiment. For all experiments, sulfate concentration did increase (Figure 17). For Experiment 1A, the sulfate concentration was initially 1.19 mmol/L and after 840 hours had a concentration of 6.39 mol/L, for a total increase of 5.20 mmol/L. The Experiment 1B reactors had the same initial concentration but ended slightly higher with a concentration of 7.48 mmol/L of sulfate.

Experiment 2 reactors had an initial sulfate concentration of 1.23 mmol/L. Experiment 2A reactors had a final concentration of 6.28 mmol/L while Experiment 2B finished with a lower concentration of 5.38 mmol/L. For the abiotic this is an increase of 5.05 mmol/L and the biotic and increase of 4.15 mmol/L. Finally, Experiment 3 reactors started at 0.89 mmol/L of sulfate and ended at approximately the same concentration of 2.4 mmol/L. For both reactor types, this is an increase of 1.611 mmol/L. It is important to note, that for all the reactors there is a sharp increase in sulfate in the first 24 hours, while having a slower steady rate of increase for the rest of the experiment lengths (Figure 17). Complete sulfate concentration data can be found in Appendix A.

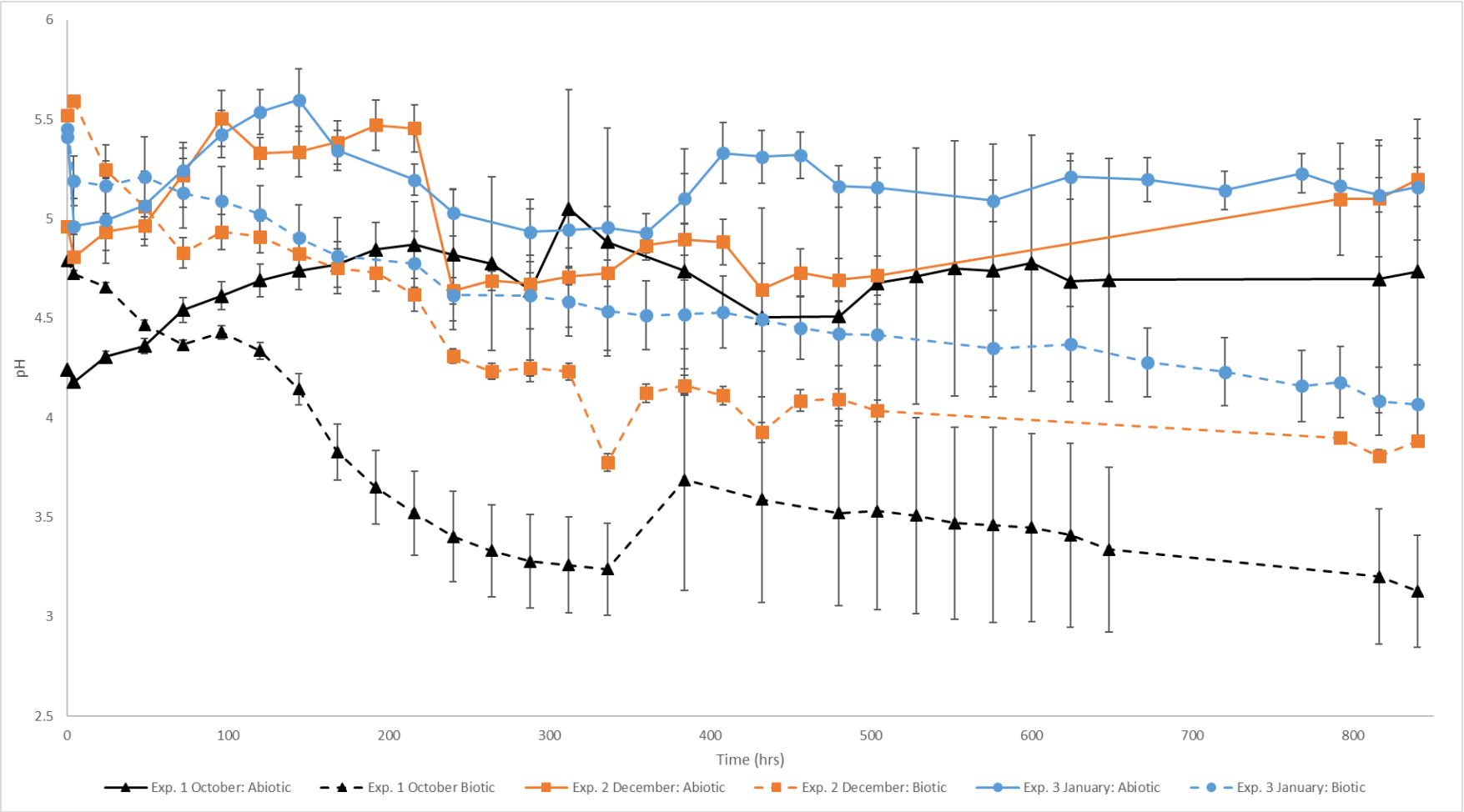

Figure 16. Experimental Mean pHs. The pHs displayed are a mean for all 6 replicates from each experimental treatment. There is a clearly visible disparity in pH trends across time between treatments for all experiments. The abiotic reactors either remain constant or pH slightly increases, while the biotic reactors pHs decrease steadily throughout the length of the experiments.

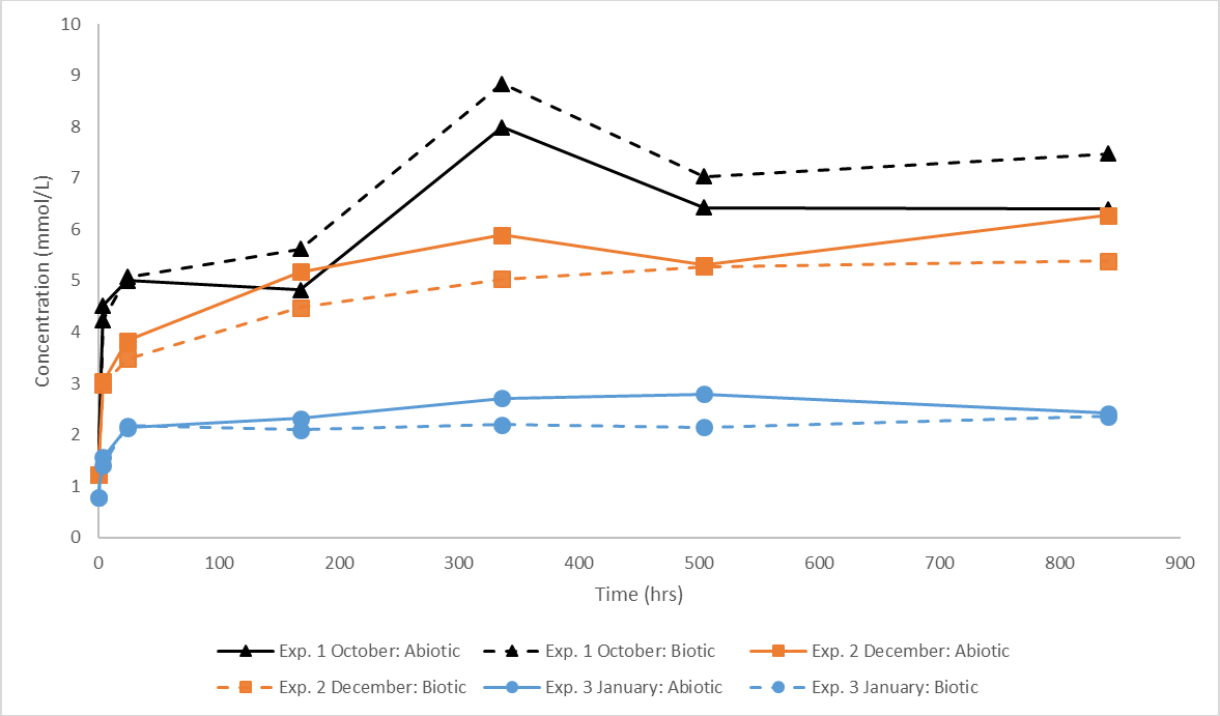

Figure 17. Experimental Sulfate Concentrations. All experiments and treatments appear to have the same trends. There are two distinct trends displayed, with a sharp increase in concentration between 0 and 24 hours, and a lower rate of increase from 24-840 hours.

3.3.2.3 Metal Chemistry

Concentrations of Ca, Mg, K, P, Al, B, Cu, Fe, Mn, Na, S, and Zn ions were measured on the ICP-OES (Tables 10-12). Data were not obtained for most samples from Experiment 1A and 1B. For these data points, the ICP-OES was unable to produce an accurate concentration. This attempt consumed all the collected sample, so the procedure was unable to be repeated to gain information for these time points.

Sulfur and iron are the most important elements in our system due to the release of sulfate and iron when pyrite is oxidized. The sulfur concentration data (Figure 18) exhibit a pattern like what is shown in sulfate concentration, with a sharp increase in the first 24 hours of

the experiments, and a much slower steady rate in the subsequent 816 hours. Experiment 3 has overall slightly lower concentrations of sulfur than Experiment 2, but the trend appears to be identical between the two experiments. There also appears to be little difference between the biotic and abiotic treatments. It is important to note that in both experiments, the abiotic reactors have a faster increase in sulfur at the beginning of the experiments, but by the end of the end the biotic reactors had higher sulfur concentrations, which is like the pattern exhibited by the recorded sulfate concentrations. Experiment 2 reactors have an initial concentration of 0.82 mmol/L and end with concentrations of 1.45 and 1.58 mmol/L for the abiotic and biotic reactors respectively. Experiment 3 starts with 0.6 mmol/L and finishes with 1.27 abiotic and

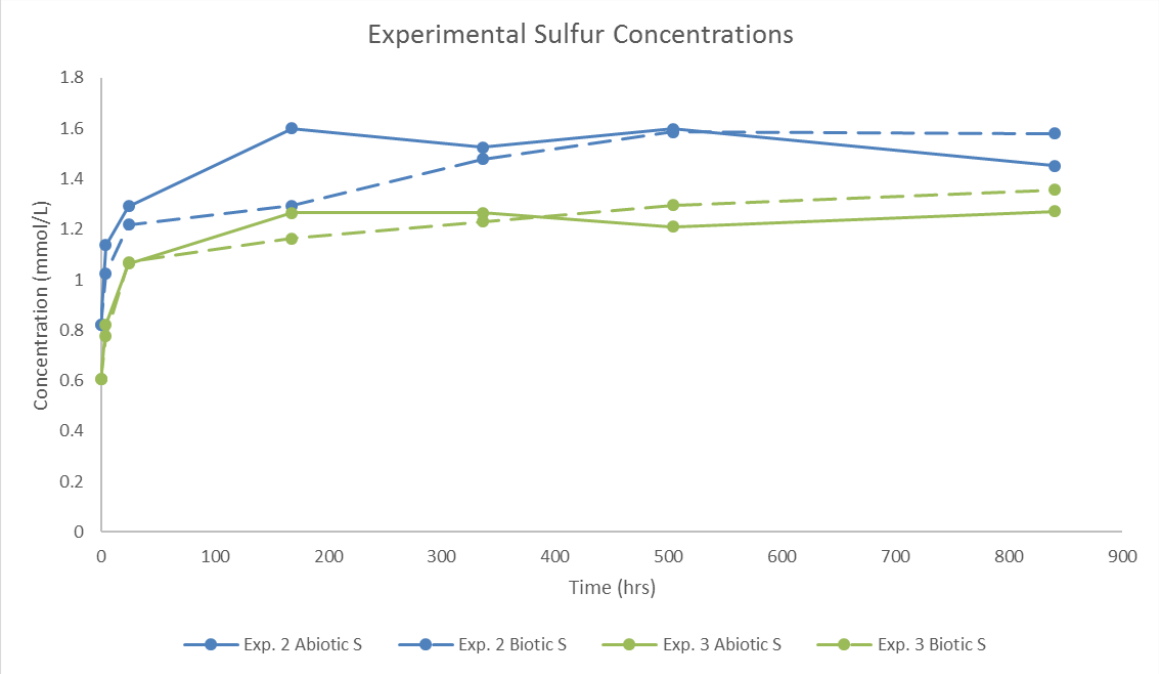

Figure 18. Blood Brook Experimental Sulfur Concentrations (mmol/L). Total sulfur concentrations exhibit trends very similar to that of sulfate. There does not appear to be a difference in trends between treatments or across experiments.

1.36 mmol/L in the biotic.

Iron concentrations throughout the experiments are more variable (Figure 19). The only consistent pattern is that the abiotic reactors end with lower concentrations then the biotic reactors. Iron levels for both treatments in Experiment 2 begin at 0.0699 mmol/L. Abiotic levels decrease slightly to 0.0523 mmol/L by the end of the experiment, while biotic levels almost double to 0.126 mmol/L. Experiment 3 concentrations begin slightly lower than experiment 2 at 0.0499 mmol/L. Abiotic levels slightly increase to 0.0995 mmol/L and biotic levels increase to levels very close to the biotic levels of Experiment 2, at 0.122 mmol/L.

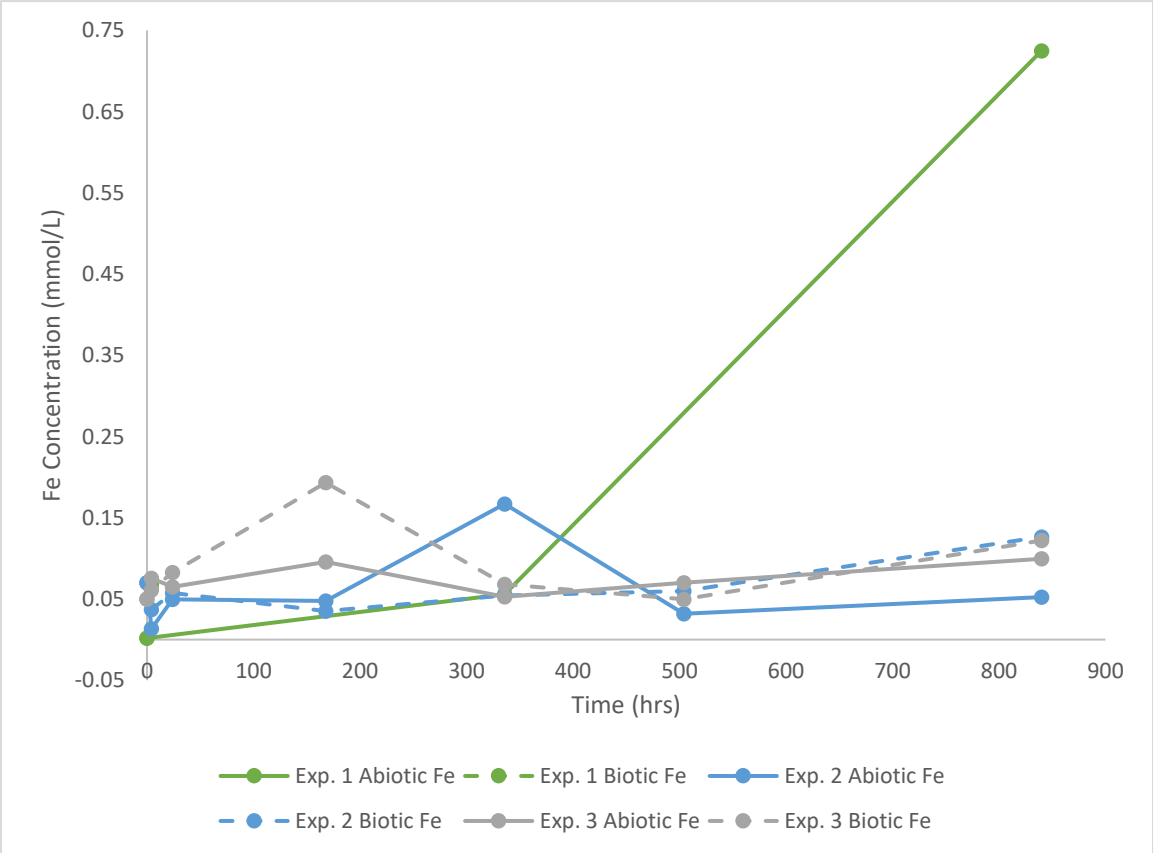

Figure 19. Blood Brook Experimental Iron Concentrations (mmol/L). Iron concentrations are relatively constant throughout the experiments. The few data points for Experiment 1 are included here.

Aluminum concentrations also do not display a distinct pattern. However, a consistent trend displayed by all treatments in both experiments is a rapid drop in aluminum concentrations in the first 4 hours of shaking (Figure 20). For Experiment 2, both abiotic and biotic treatments began at a concentration of 0.0771 mmol/L. In the first four hours, abiotic dropped to 0.0218 mmol/L and biotic dropped to 0.0246 mmol/L. From there, the abiotic increased slightly to 0.0268 mmol/L while biotic increased much more so to 0.0667 mmol/L. Neither treatment reached concentrations that were recorded for time 0 again. Experiment 3 had lower initial concentrations at 0.0404 mmol/L. Experiment 3 also experiences drops in the

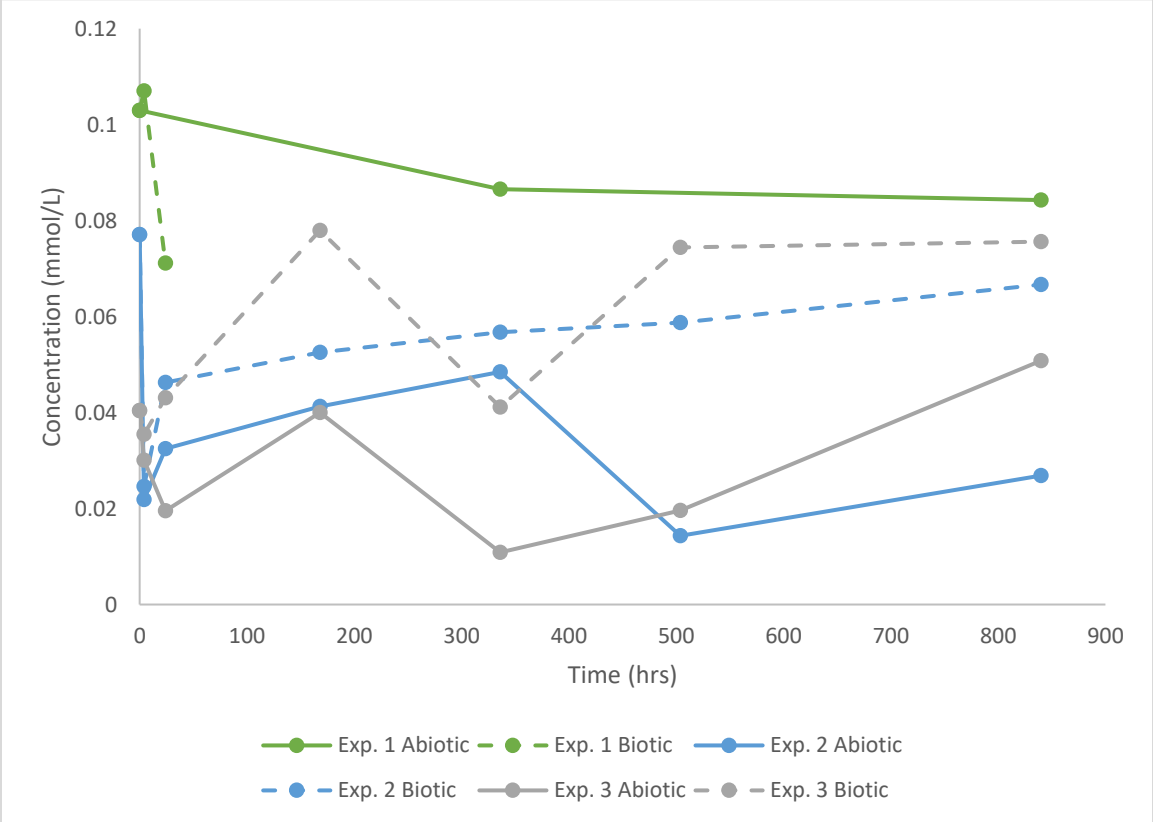

Figure 20. Blood Brook Experimental Aluminum Concentrations (mmol/L). The few data points obtained for Experiment 1 are included here. There are no discernable trends in the abiotic concentrations, but there is a small steady increase in the overall concentrations by the end of the biotic experiments.

first 4 hours, however they are not as large as recorded in Experiment 2. Abiotic reactors drop to 0.03 mmol/L while biotic reactors drop to 0.0355 mmol/L. By the end of experiment 3, abiotic reactor concentrations increase to 0.0508 mmol/L, while the biotic reactors increase to 0.0756 mmol/L. Both treatments for Experiment 3 have final concentrations higher than their initial. Experiment 1 data, while fragmented and missing points, is still displayed in Figure 19 to show the initial and final Al concentrations for this experiment. While data for the biotic treatment does not contain the final aluminum level, we can see that the final abiotic concentration is at 0.0843 mmol/L, higher than both Experiments 2 and 3. If the observed pattern of the final two experiments holds, where the final biotic Al concentrations are higher than the abiotic, we can assume that the final biotic concentration for Experiment 1 likely is was higher than the observed abiotic level.

Table 10. Experiment 1: October ICP Read Concentrations (mmol/L)

Time (hrs)	Ca	K	Mg	P	Al	B	Cu	Fe	Mn	Na	S	Zn
Abiotic 0	0.405	0.0386	0.667	0.00323	0.103	<0.00278	0.00036	<0.00179	0.0118	0.151	1.136	0.00244
AB 336	1.106	0.105	0.648	0.138	0.0865	0.00625	0.00226	0.0558	0.0123	0.229	1.72	0.00447
AB 840	1.101	0.401	0.669	0.00364	0.0843	0.0323	0.0141	0.725	0.0138	0.178	3.306	0.00505
Biotic 0	0.405	0.0386	0.667	0.00323	0.103	<0.00278	0.00036	<0.00179	0.0118	0.151	1.136	0.00244
B 4	0.678	0.128	0.758	0.0144	0.107	0.00394	0.00143	0.0677	0.0123	0.336	1.442	0.00437
B 24	0.844	0.0454	0.591	0.0187	0.0711	<0.00278	0.00162	0.0703	0.0109	0.294	1.437	0.00329

Table 11. Experiment 2: December ICP Read Concentrations (mmol/L)

Time (hrs)	Ca	K	Mg	P	Al	B	Cu	Fe	Mn	Na	S	Zn
Abiotic 0	0.355	0.0313	0.507	<0.00323	0.0771	<0.00278	<0.000315	0.0699	0.0101	0.112	0.820	0.00159
AB 4	0.553	0.108	0.585	0.0152	0.0218	<0.00278	0.00110	0.0132	0.0118	0.333	1.136	0.00329
AB 24	0.818	0.220	0.553	0.00555	0.0324	<0.00278	0.001	0.0495	0.012	0.280	1.292	0.00384
AB 168	1.139	0.261	0.576	0.00432	0.0413	<0.00278	0.00118	0.0477	0.0126	0.293	1.60	0.00645
AB 336	0.991	0.793	0.601	0.014	0.0484	0.0056	0.00144	0.167	0.012	0.236	1.525	0.00251
AB 504	1.0732	0.222	0.591	0.0273	0.0143	<0.00278	0.00164	0.0319	0.0119	0.363	1.598	0.00231
AB 840	0.96	0.342	0.569	0.00644	0.0268	<0.00278	0.00154	0.0523	0.0116	0.273	1.452	0.00242
Biotic 0	0.355	0.0313	0.507	<0.00323	0.0771	<0.00278	<0.000315	0.0699	0.0101	0.112	0.820	0.00159
B 4	0.487	0.0256	0.546	0.018	0.0246	<0.00278	0.000533	0.0368	0.0111	0.292	1.0245	0.00267
B 24	0.757	0.028	0.520	0.0224	0.0463	<0.00278	0.00108	0.0576	0.0105	0.237	1.218	0.0029
B 168	0.847	0.0787	0.531	0.0113	0.0525	<0.00278	0.001404	0.0351	0.0107	0.271	1.293	0.001702
B 336	0.955	0.0512	0.564	0.006	0.0567	<0.00278	0.00237	0.0542	0.0124	0.182	1.477	0.00232
B 504	1.010	0.138	0.573	<0.00323	0.0587	<0.00278	0.0030	0.06	0.0206	0.166	1.586	0.0113
B 840	1.0182	0.0746	0.551	0.0133	0.0667	<0.00278	0.00343	0.126	0.0153	0.15	1.579	0.00511

Table 12. Experiment 3: January ICP Read Concentrations (mmol/L)

Time (hrs)	Ca	K	Mg	P	Al	B	Cu	Fe	Mn	Na	S	Zn
Abiotic 0	0.239	0.034	0.358	<0.00323	0.0404	<0.00278	<0.000315	0.0499	0.00745	0.11	0.605	<0.000765
AB 4	0.456	0.166	0.376	0.00385	0.03	0.00707	0.000809	0.0755	0.00827	0.202	.0821	0.00186
AB 24	0.755	0.167	0.362	<0.00323	0.0195	0.00338	0.000636	0.0648	0.00856	0.154	1.0638	0.00231
AB 168	0.976	0.23	0.384	<0.00323	0.04	0.00404	0.000854	0.0955	0.00947	0.148	1.265	0.00208
AB 336	1.0507	0.389	0.375	<0.00323	0.0109	0.00326	0.000395	0.0527	0.0122	0.147	1.266	0.00141
AB 504	0.921	0.409	0.367	0.00356	0.0196	0.0034	0.000779	0.0702	0.00923	0.163	1.210	0.00228
AB 840	0.946	0.349	0.374	0.00324	0.0508	0.0038	0.00147	0.0995	0.00906	0.148	1.271	0.00274
Biotic 0	0.239	0.034	0.358	<0.00323	0.0404	<0.00278	<0.000315	0.0499	0.00745	0.11	0.605	<0.000765
B 4	0.477	<0.0256	0.350	<0.00323	0.0355	<0.00278	<0.000315	0.0609	0.00777	0.1005	0.778	0.00113
B 24	0.775	<0.0256	0.355	<0.00323	0.0431	<0.00278	0.0006	0.0827	0.00801	0.0805	1.0694	0.00177
B 168	1.0342	0.0477	0.354	0.00493	0.0779	<0.00278	0.000781	0.193	0.00353	0.0956	1.164	0.000959
B 336	0.929	0.0803	0.366	0.00143	0.0411	<0.00278	0.00119	0.0681	0.00823	0.0941	1.231	0.00197
B 504	0.963	0.119	0.359	0.00368	0.0744	<0.00278	0.00205	0.0497	0.00844	0.116	1.295	0.00194
B 840	0.948	0.182	0.354	0.00592	0.0756	<0.00278	0.00357	0.122	0.00892	0.111	1.357	0.00262

3.3.2.4 Microbial Community

DNA was extracted and sequenced to compare the final community of each experiment to that of the initial sample water that was used in each experiment (Figure 21). All samples were subsampled to 1934 counts. Replicates for the beginning and end of each experiment were averaged together to create a single community. In Experiment 1B, the community became dominated by acidophilic bacteria. The primary classified genera present are *Acidisoma* (15.94%), *Acidocella* (16.87%), *Brevibacterium* (1.65%), and *Thiomonas* (1.90%). Unclassified bacteria at the genus level comprise approximately 54% of the community and "Other" (genera comprising <1% of the total community) comprises around 8.5%. In Experiment 2B, the final community became dominated by *Burkholderia* (23.08%), *Novosphingobium* (14.03%), and *Microbacterium* (12.51%). Both unclassified bacteria and the "Other" community represent a smaller proportion of the community in December comprising 37.5% and 7.31% respectively. Finally, in Experiment 3B the final community included the primary dominant microbes *Novosphingobium* (3.19%), *Burkholderia* (7.65%), and *Acidisoma* (13.01%). In this community, most of the bacterial genera have a reduced presence in the total community than in the first two experiments. Unclassified bacteria have an approximately equal portion of the community as in the October experiment at 48.67%. "Other" represents a greater portion in the January experiment at 24.23% when compared to the first two

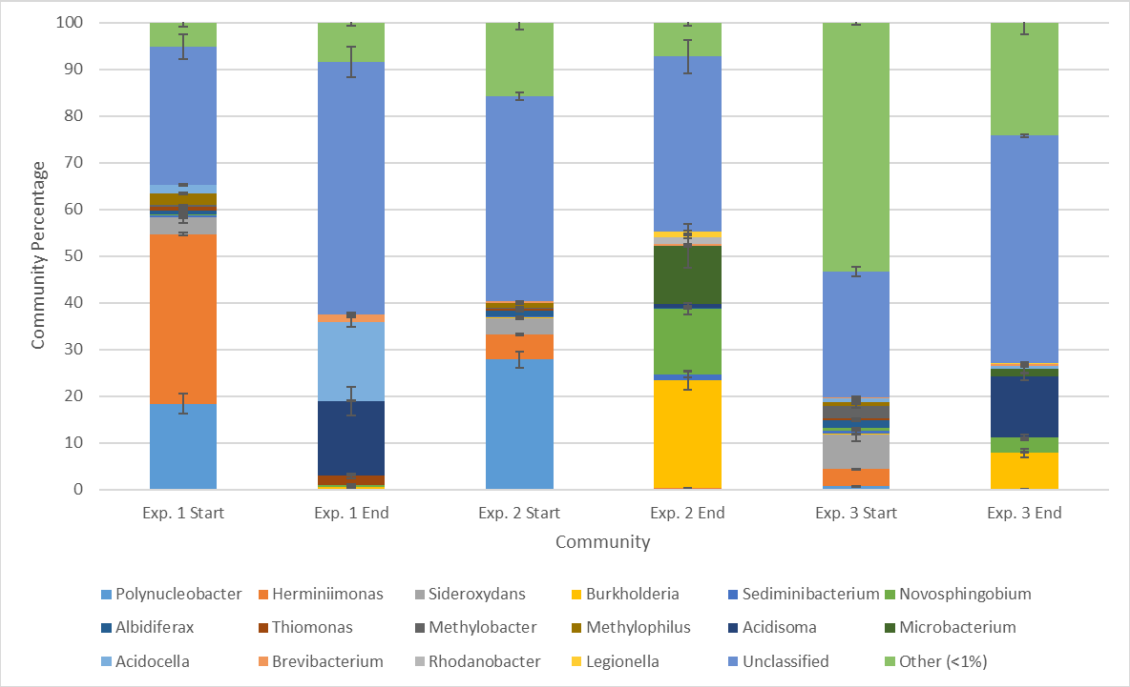

Figure 21. Blood Brook Experimental Microbial Communities Organized by Genus (NCBI Accession #: PRJNA430708). The final communities evolve to ones that are primarily acidophilic, being dominated by the genera *Acidisoma* and *Acidocella*. There appears to be a succession in the final communities, with the farthest developed being Experiment 1, followed by Experiment 3, and then Experiment 2.

experiments. Of the two genera that contain the most iron and sulfide oxidizing bacteria involved in ARD production, *Thiomonas* and *Sideroxydans*, only *Thiomonas* appears to survive into the final experimental reactors, as can be seen when comparing the initial to final communities for the experiments. *Sideroxydans* does not grow to become one of the dominant species present at the end of any of the experiments, and *Thiomonas* only is present in the final community of Experiment 1B.

3.3.2.4.1 Direct Count Results

Direct counts were performed at 40x magnification the start and finish of each experiment using a light microscope and prepared slides (Table 13). Each count averaged together the number of bacteria visible in ten different frames of the same prepared slide.

Table 13. Prepared Slide Direct Count Results (40x magnification)

	Exp 1 Start	*Exp 1 End*	*Exp 2 Start*	*Exp 2 End*	*Exp 3 Start*	*Exp 3 End*
Mean Count per Frame	43.9	166.3	28	63.6	24.7	63.1
Standard Deviation	18.19	46.93	11.96	21.17	12.67	24.85
Cells per mL of initial water sample	$2.27x10^5$	$8.59x10^5$	$1.28x10^5$	$3.26x10^5$	$1.45x10^5$	$3.29x10^5$

Experiment 1B exhibited the highest initial, final bacterial counts, and exhibited the greatest change in abundance from the beginning to the end of the experiment. Experiment 2B and Experiment 3B have very similar initial and final frame counts, however Experiment 3's initial is just lower than Experiment 2's, leading to Experiment 3 having a slightly higher change in concentration and more growth. This tends to inversely correlate with the pH results, where Experiment 1B has the biggest decrease in pH, while Experiment 2B and 3B have smaller and more similar pH drops.

The most abundant bacterial shape observed in all slides were rod-shaped. Sphere-shaped bacteria were also present, but to a much lesser degree. In the initial slide, sphere-shaped bacteria appeared approximately 2-4 times less than the rod-shapes. In the final slides, sphere-shaped bacteria were more abundant, but still overall less than the rod-shaped. Sphere-shaped bacteria had the strongest presence in the final Experiment 1 and Experiment 3 slides. Occasionally, there would be appearances of rod-shaped bacteria stacked end on end, with the longest observed chain being no more than four bacteria in length. These occurred the most often within the final Experiment 1 observations but were present within all the other slides to a lesser degree. These could be observations of filamentous organisms. Solids were included

within the sample solutions. Bacteria appeared more abundantly concentrated around the edges of solids than free-floating within the solution.

3.3.2.5 Precipitates and Biological Differences

Precipitates were collected from the biotic and abiotic reactors and examined using the SEM to see if there were any structural and chemical differences between them. There are notable differences between the observed abiotic and biotic precipitates (Figures 22 and 23). The abiotic precipitates appeared as large aggregates ranging from 100-200 microns across with the occasional pyrite particle suspended within. The suspended pyrite particles ranged from 4-10 microns across, which is about .4-2% of the original sized pyrite grains added to the reactors. To be clear, grains suspended within the precipitate aggregate are not the main pyrite grains used in the reactors. The gram of pyrite grains added to the reactors was used as part of the DNA extractions that were completed post-experimentation. Any mineral particles suspended within precipitate are pieces that were large enough not to be removed by the cleaning process but are smaller still than the desired range. Chemically, the abiotic precipitate was identified to contain primarily iron and oxygen. Aluminum was also occasionally identified throughout the precipitates.

Precipitates collected from the biotic reactors contained filamentous structures running throughout the aggregate. These structures typically had a diameter ranging from 1 to 2 microns and ran continuously throughout the precipitate structure (Figure 22). Suspended mineral particles within the biotic precipitate ranged from 5 to 20 microns were usually larger than the mineral particles suspended in the abiotic aggregate. One precipitate contained a pyrite particle suspended in the filamentous structures that was unusually large at

approximately 50 microns across. Chemically, the biotic precipitate was identified as also being composed primarily of iron and oxygen, with aluminum occasionally identified. This is identical to the abiotic precipitate. Aggregates caught in the mass and the filamentous structures both exhibited this chemical pattern.

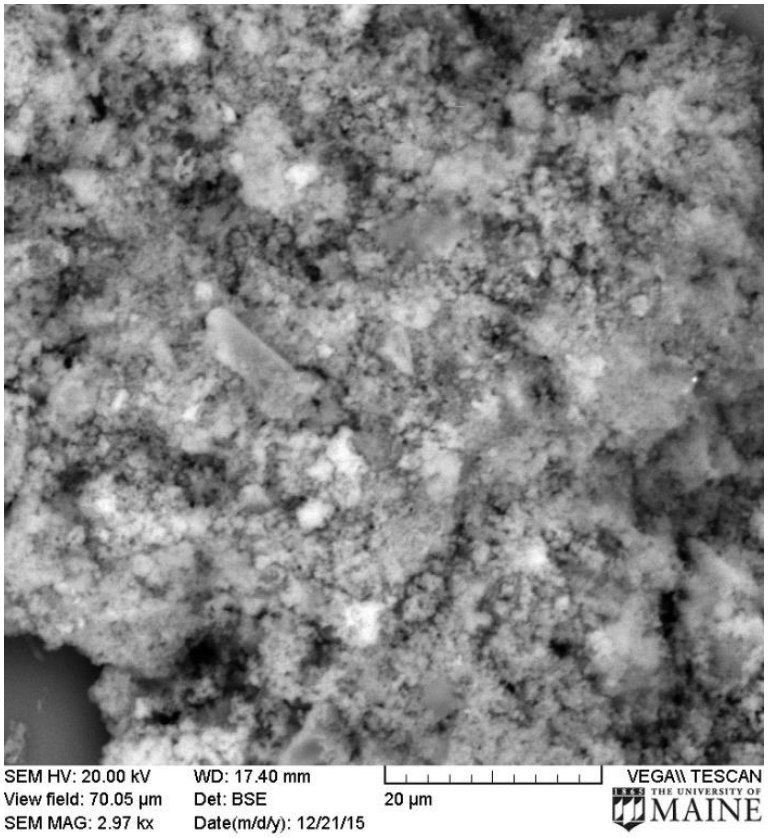

Figure 22. Abiotic Precipitate Body. Photographed in high vacuum conditions. The abiotic precipitate is an amorphous mass.

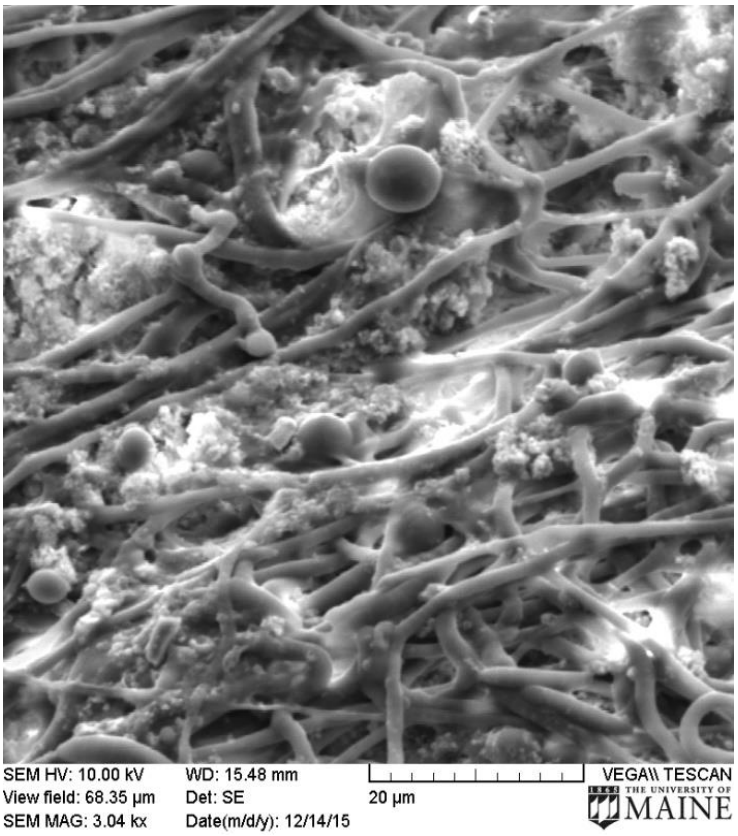

Figure 23. Biotic Precipitate Body. Photograph was taken in high vacuum conditions. Structure is comprised of numerous stalks, 2-5 microns in diameter, with amorphous masses suspended throughout.

3.3.2.6 Statistical Results

3.3.2.6.1 Linear Mixed-Effect Model Results

3.3.2.6.1.1 Treatment Results

Linear mixed-effect models were run to test if there were any significant differences in rates between experimental treatments for sulfate concentration and pH. Two models were run for each experiment for sulfate. As explained within Section 3.3.2.2, sulfate concentration exhibits a trend that is overall not linear when including the initial data point. There is a rapid increase in concentration during the first 24 hours of each experiment. By removing the initial data point, the sulfate trend becomes much more linear and appropriately tested by these

models. These models found that there are no significant differences between abiotic and biotic treatments for sulfate concentration rates for all experiments between 4 and 840 hours (Table 14). There are significant differences between treatments for Experiment 1 when the initial data point is included. Experiments 2 and 3 still do not have significant differences across time for sulfate, even when the initial time point is included. For each of the three experiments, rate of pH change found to be significantly different between biotic and abiotic treatments. Rates of DO and conductivity change were also tested to determine if there were differences between abiotic and biotic treatments for each experiment. The overall rates in DO concentration were not significantly different between treatments in any of the experiments. Conductivity rates were not significantly different between treatments for Experiment 1 but were for Experiments 2 and 3.

Table 14. Mixed-Effect Model Significance Test Results for Rate of Sulfate Concentrations vs. Treatment. A Pr-Value < 0.05 is significant and is starred.

Test Name	Pr-Value with T0	Pr-Value without T0
Exp. 1 Oct. Sulfate	0.02403*	0.62731
Exp. 2 Dec. Sulfate	0.21024	0.69045
Exp. 3. Jan. Sulfate	0.44238	0.770

Table 15. Linear Mixed-Effect Model Significance Test Results for Rate of Other Parameters vs. Treatment. A Pr-Value < 0.05 is significant and is starred.

Tested Parameter	Exp 1: October	Exp 2: December	Exp 3: January
pH	9.16×10^{-10}*	$<2 \times 10^{-16}$*	$<2 \times 10^{-16}$*
Conductivity	0.7199	1.6×10^{-4}*	2.94×10^{-8}*
DO	0.683141	0.1663	0.655

3.3.2.6.1.2 Experimental Differences

Linear mixed-effect regression models were also used to assess if there were significant differences for, pH, DO concentration, and conductivity rates between different experiments. Each experiments rate was compared to others (i. e. 1A vs. 2A, 2A vs. 3A, 1A vs. 3A). This was done for both the abiotic and biotic treatments. This was also done to compare the rate of change of sulfate concentration between experiments but using normal linear regression models. Since the initial values of these parameters are not the same across treatments and experiments, these tests are important since comparing regressions is the best way to determine if there are differences between experiments (Yan and Su 2009). The results of these tests (Table 16) show that the trends across time for pH in the biotic experiments are all significantly different from one another. For abiotic pH, Experiment 1A is significantly different from 2A and 3A, but 2A and 3A are not significantly different from each other.

Table 16. Linear Mixed-Effect Regression Model Results for Chemical Parameters Between Experiments. A Pr-Value < 0.05 is significant and is starred.

Test	Exp. 1 vs. Exp. 2	Exp. 1 vs. Exp. 3	Exp. 2 vs. Exp. 3
Abiotic pH	0.0272*	9.10×10^{-14}*	0.1085
Biotic pH	8.88×10^{-16}*	0.00158*	0.0107*
Abiotic Sulfate	0.1987	0.207	0.09113
Biotic Sulfate	0.9071	0.2158	0.717
Abiotic Conductivity	0.00297*	0.264244	5.05×10^{-8}*
Biotic Conductivity	0.000718*	0.000452*	0.03135*
Abiotic DO	0.000283*	0.5524	0.0924
Biotic DO	1.18×10^{-6}*	0.0805	9.34×10^{-13}*

3.3.2.6.2 Experimental Redundancy Analyses

Multiple RDAs were run for the experimental data. Due to the lack of data for most metal concentrations from Experiment 1, two RDAs were run: one that did not include Experiment 1 (Figure 23) and one that did (Figure 24). The RDA that included Experiment 1 used all data that was measured for all experiments (i.e. sulfate concentration, pH, etc.). Data measured on the ICP-OES was excluded from this RDA. The second RDA excluding Experiment 1 was run while incorporating all chemical data including the ICP-OES collected data for Experiments 2 and 3. Results of the two individual RDAs show that including the ICP data accounts for a much greater amount of variance within the microbial community (Table 17). This makes Figure 24 a better overall model of the variance.

The experimental RDAs reveal the chemical drivers of the experiment along two different axes. In both Figures 24 and 25, one of the primary explanatory axes runs from the upper-left quadrant to the lower-right. Higher DO concentrations and alkalinity concentrations fall in the upper-left quadrant, while increases in hydrogen concentrations, sulfate, conductivity, and various metals are opposite in lower-right quadrant. The initial communities fall towards the upper-left quadrant, while the final communities are pushed towards the lower right. This tells us that as the experiment went on, the communities were driven by the dropping pHs, rising conductivity, and rising sulfate within the reactors. Genera that are present only in the initial experimental reactors (*Sideroxydans, Methylobacter, Polynucleobacter*) are driven toward the upper-left quadrant. Also visible in Figure 24, is a second axis that is perpendicular to the DO/Conductivity axis. This axis is represented by aluminum and magnesium concentrations, with higher value falling in the lower-left quadrant. Moving into

the upper-right quadrant represents decreases in these values. Our initial and final communities are spread similarly along this axis, with Experiment 1 being associated with the highest concentrations of aluminum, Experiment 2 the second highest, and Experiment 3 having the lowest. This shows that aluminum and magnesium were inadvertently selected for within the experiments and may have affected the microbial communities more than originally expected. In Figure 25, the overall communities are spread across a similar secondary axis, but the explanatory vectors are not identified. This is likely also an aluminum driven axis. Genera populous in the final experimental reactors, *Acidisoma* and *Acidocella*, favor higher concentrations along this secondary axis.

Table 17. Experimental RDAs' Explanatory Statistics

Test	Unadjusted R^2	Adjusted R^2	Total Variance % Explained	Axes 1 Variance %	Axes 2 Variance %	Total Axes Variance
Exp. RDA 1 (Figure 24)	0.98778	0.9715	97.15%	59.92%	23.339%	83.262%
Exp. RDA 2 (Figure 25)	0.6945	0.5673	56.73%	37.45%	20.78%	58.23%

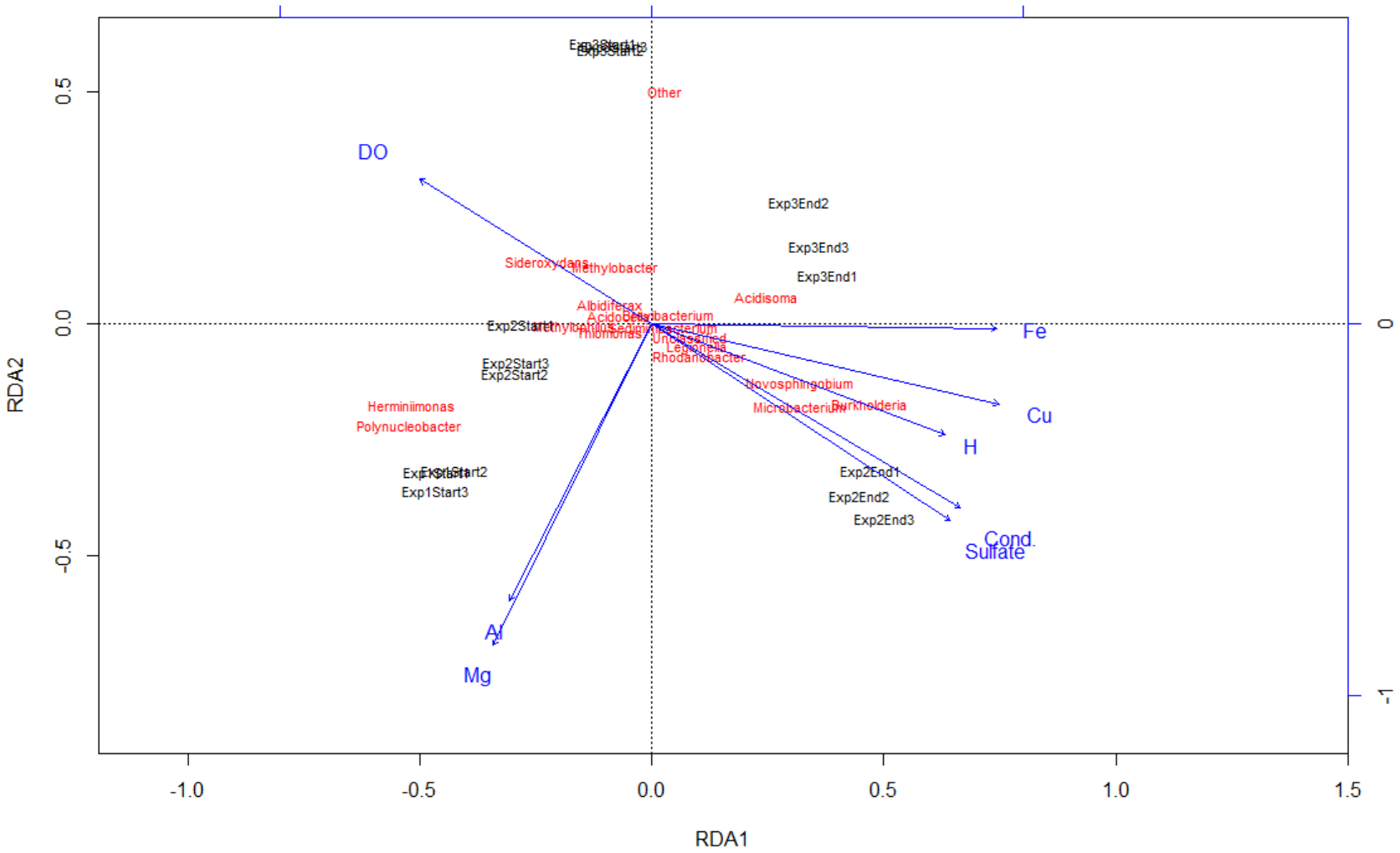

Figure 24. Experimental RDA 1 Results (Excludes Experiment 1, Includes ICP Data) [Scaling 2]. Explanatory vectors are plotted in blue, communities in black, and individual genera in red. Data is spread along two perpendicular axes; upper-left to lower right quadrants, and bottom-left to upper-right quadrants.

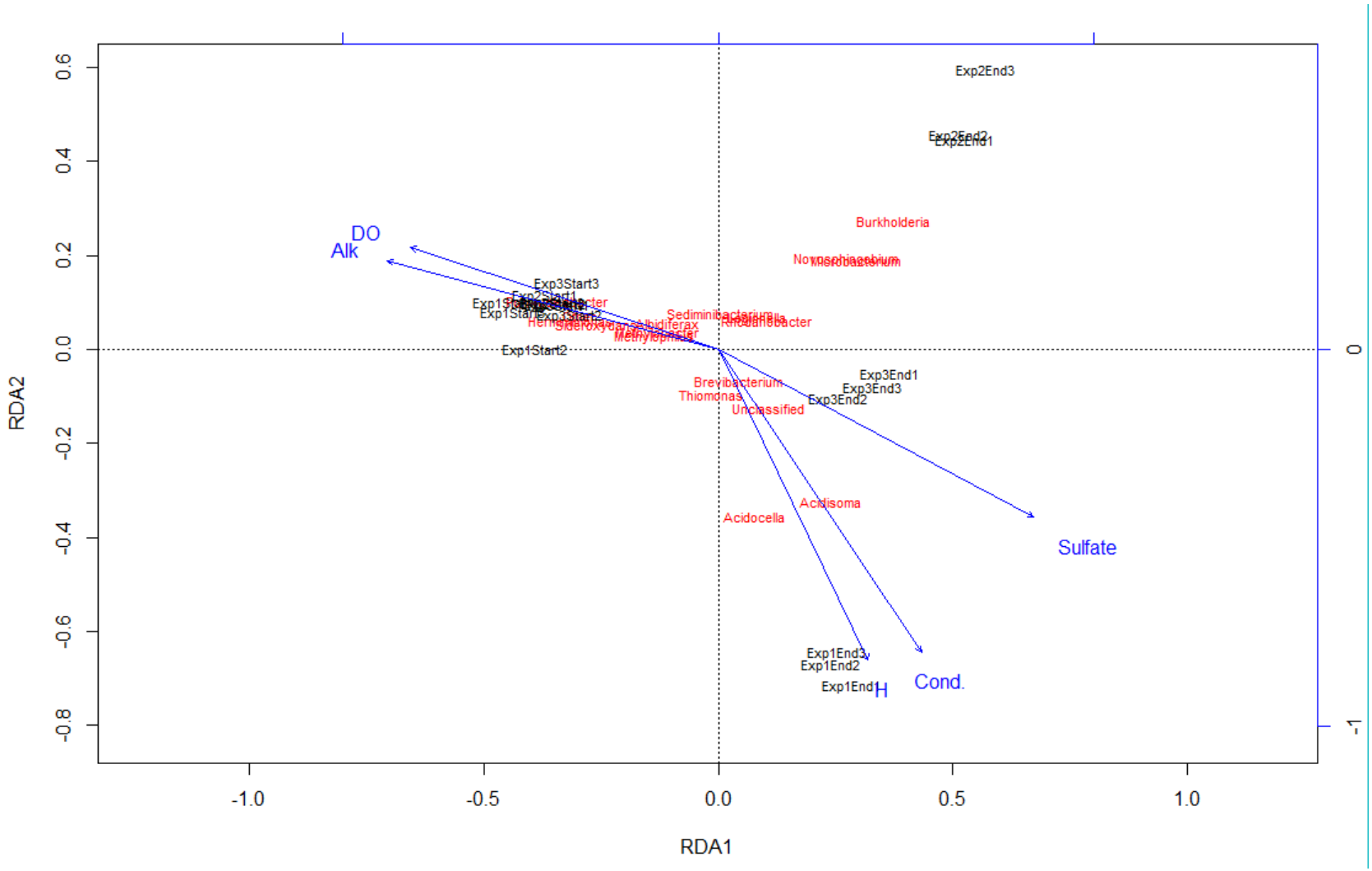

Figure 25. Experimental RDA 2 Results (Includes Experiment 1, Excludes ICP Data) [Scaling 2]. Explanatory vectors are plotted in blue, communities in black, and individual genera in red. Data appears to be spread along two axes like Figure 24, even though the ICP data was not included in this RDA.

3.4 Discussion

3.4.1 Impact of Biota on Pyrite Oxidation

3.4.1.1 Rates of Production

Overall rates of change for hydrogen ion and sulfate concentrations were calculated for the experiments and compared to results of the statistical models. Hydrogen ion production rates were calculated using the following equation:

$$Rate = {([H^+]_i - [H^+]_f)}/{\Delta t}$$ (**Eq. 18**)

840 hours were used as Δt for both the abiotic and biotic treatments (Table 18). Hydrogen concentration trends slightly resemble the logistic function (Figures 28-30 in Appendix A) but can be summarized by finding a linear slope. (Verhulst 1845). Many other chemical reactions can alter pH in an aquatic system (alkalinity, carbon balance, etc.) (Benjamin 2015, Drever 1988, Stumm and Morgan 1981), so changing rates of sulfate production within the reactors must also be investigated.

Table 18. Calculated Rates of Change in Experimental Hydrogen Ion Concentration

	Treatment	Overall Rate (mol/L/s)
Experiment 1 (October)	Abiotic	-1.29×10^{-12}
	Biotic	2.41×10^{-10}
Experiment 2 (December)	Abiotic	-1.52×10^{-12}
	Biotic	4.23×10^{-11}
Experiment 3 (January)	Abiotic	10^{-12}
	Biotic	2.60×10^{-11}

Since pyrite oxidation releases both sulfate and hydrogen ions into the aqueous system (Lowson 1982), we would expect sulfate concentration to increase along with the decreasing pHs. We would expect to see the greatest increase in sulfate be in October, and the least being in January. The experiments begin at different sulfate concentrations, so overall changes in sulfate concentration were evaluated. Each experiment had two distinctly different rates. These are the sharp increase in concentration that occurs within the first 24 hours of each experiment, and then the steadier increase until the end of each. Due to this, rates were calculated for the first 24 hours and then for the remainder of the experiment, as well as an overall rate for the entire length of the experiment (Table 19). The overall rate was calculated slightly differently for 0-24 hours and 24-840 hours. The following equations were used for those calculations respectively:

$$Rate = {([SO_4^{2-}]_i - [SO_4^{2-}]_{t24})}/{\Delta t}$$ **(Eq. 19)**

$$Rate = {([SO_4^{2-}]_{t24} - [SO_4^{2-}]_f)}/{\Delta t}$$ **(Eq. 20)**

There is essentially no difference between the abiotic and biotic rates, and this coincides with the results of the statistical models of sulfate concentration as a function of time. For pH, there are notable differences between the treatments in terms of rates of hydrogen ion production, which also coincides with the results of the statistical models for hydrogen ion concentration as a function of time.

Table 19. Calculated Rates of Change in Experimental Sulfate Oxidation

	Treatment	Overall Rate (mol/L/s)	0-24 hrs Rate (mol/L/s)	24-840 hrs Rate (mol/L/s)
Experiment 1 (October)	Abiotic	1.72×10^{-9}	4.41×10^{-8}	5.75×10^{-10}
	Biotic	1.84×10^{-9}	4.5×10^{-8}	8.17×10^{-10}
Experiment 2 (December)	Abiotic	1.67×10^{-9}	3.01×10^{-8}	8.33×10^{-10}
	Biotic	1.37×10^{-9}	2.61×10^{-8}	6.46×10^{-10}
Experiment 3 (January)	Abiotic	5.39×10^{-10}	1.55×10^{-8}	9.86×10^{-11}
	Biotic	5.2×10^{-10}	1.6×10^{-8}	6.46×10^{-11}

3.4.1.2 Significance of Sulfide Oxidation

The linear mixed-effect models found that the change in sulfate concentration across time between abiotic and biotic treatments for all experiments is not significantly different when excluding the initial data point. This would suggest that the present microbial community is not accelerating the process of pyrite oxidative dissolution. In all cases of oxidative dissolution, sulfide is oxidized to sulfate with ferrous iron being released into solution (Lowson 1982). The ferrous iron is then oxidized to ferric iron, which helps to further oxidize pyrite both abiotically and biotically if not oxidized to iron hydroxide precipitates (Edwards et al. 1999, Glesiner et al. 2005, Lowson 1982).

There are a few ways within the reactors that the oxidation of iron or sulfide in pyrite could be being biotically accelerated without us being able to observe it. The ways include partial oxidation of sulfide to sulfur (Cardoso et al. 2006), solid phase oxidation of Fe (II) to Fe (III) (Aller and Rude 1988), or the presence of sulfate reducing bacteria (Hao et al. 1996). If partial oxidation was occurring, the sulfur produce would have to be in the solid phase. Since only soluble sulfur was measured on the ICP, it is difficult to compare trends between the measured sulfur (Figure 17) and the measured sulfate concentrations (Figure 16). This would also make it difficult to observe sulfur being reduced by sulfate reducing bacteria. These

bacteria would be able to grow within our reactors (Hao et al. 1996), but no classified genera were identified. More information, such as analyzing the amount of solid phase sulfur or the speciation of soluble iron, would have been needed to better assess if these processes were occurring in these reactors. What was observed suggests that the microbial community in the biotic reactors was not increasing the oxidation of the pyrite. This is supported by the classified iron and sulfide oxidizing bacteria that were present in the initial community dying off by the end of the experiments. Even if the microbial population was not accelerating pyrite oxidation, something in the biotic reactors is driving the pH down. To better assess the potential causes of this, we must take a closer look at how the microbial community has changed in our reactors to fit the present chemical conditions.

3.4.2 Experimental Community Evolution

3.4.2.1 Standard Comparison

In each of the three experiments, the microbial community changes distinctively from the initial to the final community. There are remnants of the original community present, but new bacteria that were not initially dominant no comprise most of the final community. The abundant classified genera present at the end of the experiments are acidophiles that thrive in the low pH conditions of the biotic treatment reactors. It's important to relate what is present in this project to what has been observed in both acidified ground and surface waters.

Most of the bacterial genera present in all the starting communities (i.e. *Herminiimonas* and *Polynucleobacter*) have all but vanished by the end of the experiments. These genera are commonly associated with surface water as discussed in Chapters 1 and 2 and are primarily Betaproteobacteria and Actinobacteria (Fierer et al. 2007, Lindstrom et al. 2005, Van der Gucht

et al. 2005). The experimental reactors generate conditions that are not ideal for normal surface water bacteria (Fierer et al. 2007, Lindstrom et al. 2005, Van der Gucht et al. 2005), with pHs that started and ended well below 7. As conditions in the reactors changed, they either became too extreme for these bacteria, or the bacteria ran out of constituent they needed for growth, like organic matter.

It is also important to compare these communities to iron-oxidizing bacterial communities (FeOB) found around more circumneutral pHs, as the experimental reactors spent most of the experiment length in moderately acidic conditions (pH 3.5 - 5.5) rather than extreme acidity (pH < 3). Many of these bacterial species come from Betaproteobacteria which does represent a large proportion of both the initial and final communities (Almaraz et al. 2017, Emerson et al. 2007, Emerson and Moyer 1997, Fleming et al. 2014). Common genera that have been observed and isolated from iron-oxidizing mats include *Leptothrix* and *Sideroxydans*, as well as members of the family Gallionellaceae (Emerson and Moyer 1997, Fleming et al. 2014, Neubauer et al. 2002). *Sideroxydans* and Gallionellaceae are both present in the field and initial experimental communities (Figures 12, 22, 25, 26). Sideroxydans dies off, most likely due to the reactors dropping below its ideal pH (Emerson et al. 2007, Emerson and Moyer 1997). *Leptothrix* and the genus *Gallionella* have also been identified in multiple circumneutral iron-rich groundwater communities. Both genera are known to form stalk like structures (James and Ferris 2004, Krepski et al. 2011). *Thiomonas*, a common Betaproteobacteria genus found in most ARD solutions (Auld et al. 2013, Baker and Banfield 2003, Chen et al 2014, Hallberg 2010), is present in both the initial and final communities of Experiment 1 but does not comprise a significant portion of the community. Even though most of the surface water bacteria die off,

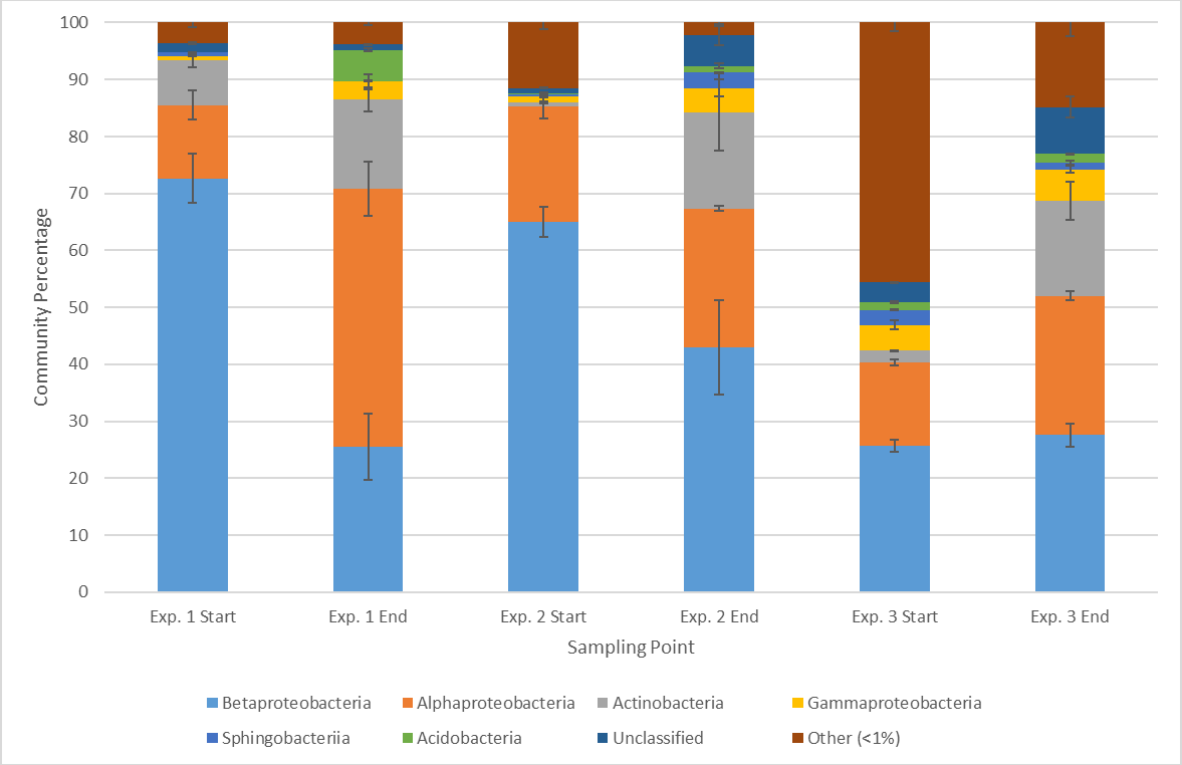

Figure 26. Experimental Microbial Communities Organized by Class (NCBI Accession #: PRJNA430708). The final experimental communities are comprised primarily of Alphaproteobacteria. Betaproteobacteria decreases below the 33% mark that is common in surface water communities (Fierer et al. 2007, Lindstrom et al. 2005, Van der Gucht et al. 2005).

Betaproteobacteria still makes up a large portion of the community (Figure 26). They are at approximately 25-28% of the final community in Experiments 1B and 3B and to 42% in Experiment 2B. This is still around the typical 33% of the community that is usually observed in surface water communities (Fierer et al. 2007, Lindstrom et al. 2005, Van der Gucht et al. 2005). Betaproteobacteria also comprise the majority of circumneutral iron-rich groundwater communities, and *Leptothrix* and *Gallionella* are both part of this class (James and Ferris 2004, Kolbel-Boelke et al. 1988, Krepski et al. 2011).

Alphaproteobacteria is the order that thrives in our reactors. While present in the initial communities, this is not a dominant order in either surface or groundwater communities. This

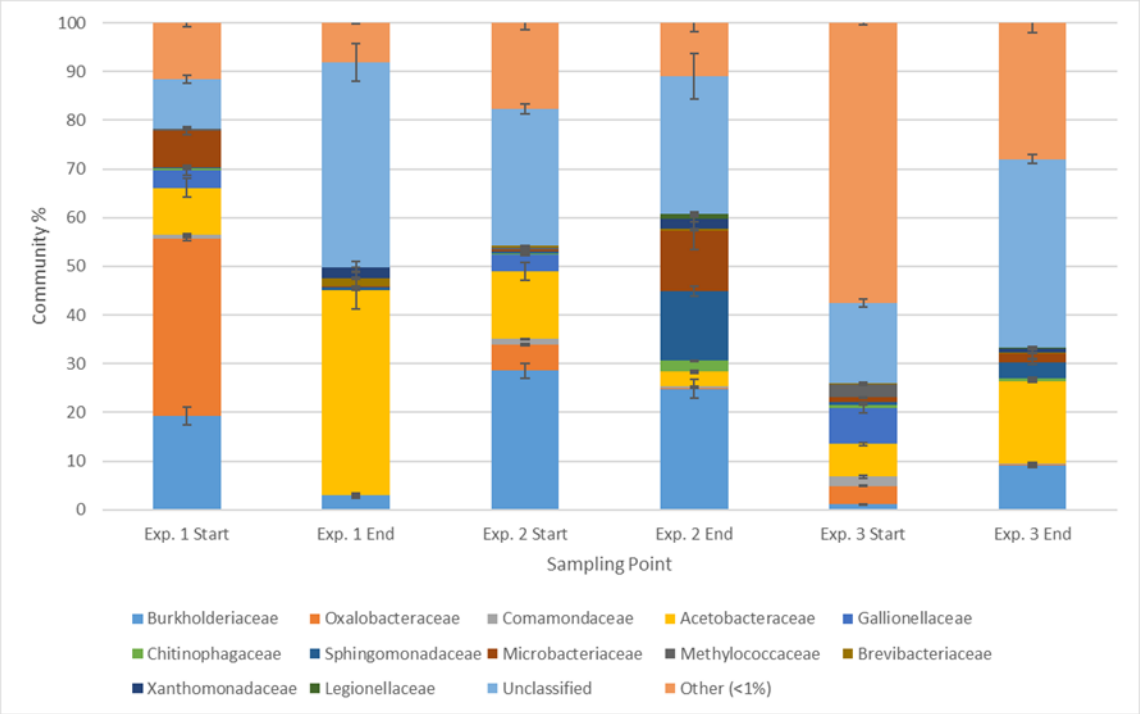

Figure 27. Experimental Microbial Communities Organized by Family (NCBI Accession #: PRJNA430708). A large majority of the communities is comprised of the family Acetobacteriaceae. They have their largest population in Experiment 1, followed by Experiment 3, and finally Experiment 2.

class does not contain any bacteria that are normally the drivers of biotic sulfide oxidation (Hao et al. 2010). The presence of acidophiles *Acidocella* and *Acidisoma* is not unusual due to the acidic nature of the reactors, but they are not acidophiles typically associated with sulfide oxidation environments (Baker and Banfield 2003, Belova et al. 2009, Hallberg 2010, Wakao et al. 2002). Their known isolates do not metabolize any of the common constituents such as sulfate or iron (Belova et al. 2009, Wakao et al. 2002). Many of the unclassified bacteria in these communities are members of the family Acidobacteria. Its role is not well understood in sulfide oxidizing environments (Auld et al. 2013, Baker and Banfield 2003, Hallberg 2010).

The experimental microbial communities have changed throughout the experiments to ones that reflect the reactors' acidifying conditions, but do not constitute what could be

considered a typical an extreme sulfide oxidation community, even in the presence of pyrite. This is due to the reactors not adjusting to their favored conditions within the experimental period. Based on class, the final experimental communities resemble circumneutral iron-rich stream and groundwater communities (Almaraz et al. 2017, Emerson et al. 2007, Emerson and Moyer 1997, James and Ferris 2004, Krepski et al. 2011, Neubaurer et al. 2002).

3.4.2.2 Precipitate Implications

Iron-oxidizing bacteria that tend to grow end on end with each other and surround themselves with an organic sheath have been observed (Emerson and Weiss 2004, Fleming et al. 2014, Rentz et al. 2007). Precipitates collect and deposit on these sheathes, resulting in the structures observed in these experiments (Emerson and Weiss 2004, Fleming et al. 2014, Rentz et al. 2007). Within these precipitates, the filamentous structures chemically identify as Fe and O. It was originally thought that they were potentially formed by the genus *Leptothrix.* This genus is known for its filamentous structures that get coated with precipitates and it typically occurs in standing or slow-flowing water that is neutral to slightly acidic, just like those observed within our reactors (Emerson and Weiss 2004, Fleming et al. 2014, Rentz et al. 2007). It also prefers low concentrations of organic matter. It is possible that the shaking of the reactors may have not been suitable for *Leptothrix*. The structures observed in the biotic experimental reactors strongly resemble structures created by *Leptothrix ochracea* and other organisms from the family Gallionellaceae in SEM images taken by Fleming et al. (2014) in their study of biologic succession of circumneutral iron mats. No *Leptothrix* were identified in our communities through sequencing (Figure 21), but bacteria that have a similar physical structure were observed under the microscope. Gallionellaceae do have a strong presence in the initial

communities but died off by the end of the experiments (Figure 27). It is possible one of the unclassified OTUs produced through the metagenomics assay was *Leptothrix*, as indicated by the observed bacteria, but the physical observed bacteria could also be an unclassified relative. Two unclassified OTUs were a large proportion (%) of the final experimental communities, and their taxonomy was identified up to Betaproteobacteria, which does match *Leptothrix*, but is still very vague for identification. No bacteria other than the stalks were observed to be directly attached to any of the mineral particles that were suspended in the aggregate. This suggests that there is no significant difference in pyrite oxidation between abiotic and biotic treatments in these experiments.

Since most of these precipitates are composed of Fe and O, they represent a portion of the total iron content that was removed from solution. Total iron content recorded by the ICP would increase if the precipitates had not solidified and been filtered out of those samples. The trace amounts of aluminum detected within the precipitates would indicate this is also true aluminum concentrations.

3.4.2.3 Relationship to Solution Chemistry

The experimental RDA results show correlations between the final experimental communities and the chemical parameters, where the experimental communities are response variables, and the stream chemistry is a set of explanatory variables. Multiple RDAs were run for the experiments due to incomplete data results from the ICP-OES readings. The lack of end data for Experiment 1 metal concentrations is discussed in Section 2.3.5.

While pH not only tailors the conditions of the reactors to those that are for acidophiles, the bacteria are clearly what is causing significant changes in the pH. The pH only decreases

within the biotic reactors. Based on the [H+] growth, it appears that whatever is changing the pH has preferences for specific conditions or nutrients. Within the experimental reactors, *Acidisoma*, *Acidocella*, and unclassified bacteria from their family may potentially be facilitating the increase in hydrogen ions through the production of acetic acid, and thus the decrease in pH we observed. Both Experiment 1B and Experiment 2B exhibit slow increases in [H+] before shifting into a faster increase (Figures 28 and 29 respectively). This could be the conditions of the reactor reaching ideal conditions for the responsible bacteria, such as pH decreasing enough for them to increase growth, or by the increased oxidation of organic matter from bacteria that began to die off from the changing conditions. Eventually the sharper increase in [H+] begins to level out again in both experiments, likely caused by the limiting of a certain nutrient or moving outside ideal conditions for [H+] generation again. This observed decrease in rate could be caused by other scenarios, such as the occlusion of a reaction surface by the formation of a biofilm or a film of secondary mineral (Sand et al. 2001). The timing for the initial slow increase in Experiment 2B was about twice the length as that in Experiment 1B, while the following sharp increase lasted about half the time before leveling out again. There was no sharp increase in either sulfur or sulfate concentrations in the Experiment 1B and 2B corresponding with the sharper increase of [H+] (Tables 10 and 11 for sulfur, Table 32 for sulfate), so it cannot be associated with increased dissolution of pyrite. Other options for why this happening must be explored within the microbial community.

One possibility for the decrease in pH may relate to *Acidisoma* and *Acidocella*. These genera are members of the Acetobacteraceae family, known for producing acetic acid through obligate aerobic fermentation (Mamlouk and Gullo 2013, Rao 1957, Raspor and Goranovic

2008). As conditions become more acidic through the abiotic pyrite oxidation, conditions become ideal for these bacteria, which then accelerate the acidification process through production of organic acids (Mamlouk and Gullo 2013, Rao, 1957, Raspor and Goranovic 2008). The acetic acid is primarily produced by the oxidation of sugars, ethanol, or carbohydrates (Rao 1957). Even though *Acidocella* and *Acidisoma* are members of this family, neither of these genera are known to produce acetic acid (Belova et al. 2009, Wakao et al. 2002). However, unclassified Acetobacteraceae strains are present in the reactors. *Acidocella* does have one species known to use ethanol as an electron source to produce energy (Kimoto et al. 2010). This is important, due to the cleaning of the instruments with ethanol between measurements. Experiment 1B exhibits the most extensive pH change, as discussed in Sections 3.3.2 and 3.4.1.1. In this experiment, Acetobacteraceae comprises approximately 9% initially and 42% of the final community population based on the results of replicates (Figure 27). In Experiment 2B and Experiment 3B Acetobacteraceae only comprise 14% and 7% of the community respectively at the experiments start. Experiment 2B has a final Acetobacteraceae proportion of 3% while Experiment 3 has a final proportion of 17%. This corresponds with slower pH decreases in these experiments. Experiment 2B is the only experiment that exhibits a decrease in Acetobacteraceae population. The use of ethanol as a prevention agent for contamination would not have contributed enough carbon for the bacteria to solely produce enough H+ to be responsible for the total pH change. Each probe was rinsed with deionized water following each ethanol wash, and then dried with a sterile lab wipe, meaning that the amount of ethanol added would be extremely small.

It is known that some of the bacteria in the initial communities are dying off throughout the experiments, which could provide a source of organic material for use in acid production. This would be suitable to maintain a stable population, but to see growth increase as was observed through the direct counts, additional organic matter would have to be present (Novick 1955). A source of organic matter that would be present in Blood Brook in October, but not December or January, would leaf matter. Trees would be shedding their leaves, which could fall into Blood Brook, decay, and create higher concentrations of organic carbon. Dissolved organic matter fluxes in streams are driven by shifting hydrologic conditions (Mulholland 1997). Dissolved organic matter concentrations would increase during periods of stormflow, due to shifting flowpaths and water entering the stream interacting more with litter and humic material (Fiebig et al. 1990, Hemond 1990, Mulholland 1997). Per this information, we would expect the January experiment to have the highest amount of dissolved organic matter due to it being stormflow dominated. Decaying leaf litter should be trapped underneath the snow, and material from that would be transported into Blood Brook. The observed bacterial activity does not support this, as the most growth occurred in October.

The pH could be being lowered without accelerating the pyrite oxidation by purple bacteria through oxidizing aqueous ferrous iron to ferric iron while fixing carbon. This occurs through a photoautotrophic redox reaction where an electron is taken from Fe (II) and added to CO_2 to fix carbon (Ehrenreich and Widdel 1994). However, this is also not a likely possibility as this is commonly an anaerobic process and requires light, which was limited while inside the shaker baths (Ehrenreich and Widdel 1994).

3.4.2.4 Aluminum Effects Upon Community Structure

What causes the reactors in Experiment 1B to be the most suitable for *Acidisoma* and *Acidocella*? They are present in the collected field communities, albeit in very small amounts that only have 1 or 2 reads per sample and grew to become the most abundant members of the final experimental communities. What is preventing them from becoming a more dominant part of the community in the second two experiments? Blood Brook's elevated aluminum concentrations may play a role in controlling the development of the microbial community under acidic conditions. Al concentration varied along the same axis as conductivity, sulfate, and most other metal concentrations within the field RDA (Figure 12). This is due Blood Brook's flow source affecting concentrations, which creates a confounding effect on aluminum. This confounding effect, along with the field pH not dropping below 4.8 within the study period (Al^{+3} is not the dominant aqueous species of aluminum until below approximately a pH of 4.5 [Driscoll and Schecher 1990]), would explain why we do not observe any strong distinct effects by the high aluminum in the field.

The final experimental microbial communities appear to be affected by the higher concentrations of aluminum found in the water samples taken from Blood Brook. Many of the genera present exhibit some form of promoted growth or resistance to aluminum toxicity. Wakao et al. (2002) found that *Acidocella* and two other acidophilic genera not present in these experiments were tolerant to concentrations of monomeric aluminum up to 100 µM in acid medium below a pH 3.5. Their growth was also strongly enhanced under these conditions. Other bacteria present in the final communities have also been shown to exhibit strong monomeric aluminum tolerance such as *Acidisoma* and *Burkholderia* (Belova et al. 2009, Woods

and Sokol 2006). The larger proportion of *Acidisoma* in Experiment 3 compared to Experiment 2 makes sense in context with the aluminum and iron concentrations each experiment. Experiment 3 not only has a higher final aluminum, but also has a lower final iron concentration than Experiment 2. These conditions would create a higher aluminum toxicity in Experiment 3, even with a slightly higher final pH than Experiment 2, resulting in the higher proportion of *Acidisoma*. At the low pHs present in the final reactors, the main constituent aluminum would complex with would be sulfate (Driscoll and Schecher 1990). The pH in Experiment 1 is too low even to complex in sulfate. Experiment 3's lower sulfate concentrations would mean less complexed aluminum, even at a slightly higher pH (Driscoll and Schecher 1990), which supports that aluminum toxicity would be higher in Experiment 3 than in 2. Aluminum toxicity succession within our experiments in descending order appears to be Experiment 1, 2, and then 3. This matches with the observed successional order of the final microbial communities and the spread observed in the experimental RDAs (Figures 24 and 25).

3.4.3 Future Work

Discussed below are some ways that the information gained in this project can be expanded upon to answer questions that were not answered here.

3.4.3.1 Changes to Experimental Parameters

The biggest question coming out of this research is how the microbial community results and reactor chemistry would look if the experiments could progress for longer amounts of time? Were our results the community stabilizing, or would the community have evolved further into one that contained more familiar acidophilic bacteria had the pHs continued to drop? The simplest way to assess this would be to run the same experiments again but allow

them to progress for a longer amount of time. Increasing experiment length to 10 weeks would allow pH to continue to drop, and for the microbial community to further develop in response to the chemical changes.

The second change suggested change to the experimental parameters would be to ensure that the reactors are oxygenated. While these experimental reactors were shaken to allow DO to enter the reactor system, DO concentrations varied quite a bit and were not close to the saturation point. Attempting to ensure DO availability for the reactors caused the complicated and limited sampling from the reactors. By finding a better solution to the DO issue, it would both make sampling easier and ensure that anaerobic processes would not be viable within the reactors.

By having larger volumes, it would also allow for increase testing of chemical parameters that were excluded here. These would include dissolved organic carbon and iron speciation. Another alternative could have been having even more replicates for each treatment, and sacrificing them at various times for sampling purposes. Replication would be possible for each time point, but the random factor of using different reactors would still need to be accounted for.

An alternative reactor configuration could be used to confirm the results of this methodology. An unsaturated column reactor where sample water would be recirculated through would be an option (Zhang et al. 2006). The water from Blood Brook would be continuously pumped through the column of packed pyrite. Fluid could be collected periodically out of the column for testing. The circulation would also unsure DO saturation.

3.4.3.2 Other Maine Acidic Streams

Because Blood Brook is only one location near an unmined sulfide deposit in the state of Maine, it would be important to identify other streams located near deposits that could be considered acidic. Since microbial communities can vary spatially (Fierer and Jackson 2006), communities found in another acidic stream are not guaranteed to be structured or behave similarly to Blood Brook. Locating these streams and evaluating them in a similar manner to what we did in this project would allow the comparison of multiple locations across the state which would lead to a more complete knowledge of the naturally acidic stream system in Maine as a whole.

3.4.3.3 Natural Acidity vs. Impacted Site

Another future possibility for this project would be to perform the same experiment again, using water samples collected at identical times throughout the year with both Blood Brook and a site known to have been impacted by mining in the past. The data in Appendix B was beginning to test this using water samples from Callahan mine, located in Harborside, Maine. However, samples could only be accessed by permission. This site has also been heavily remediated causing results that would be helpful in investigating questions we were not asking, like the efficacy of remediation or post-remediation community structure. A better site would be the remnants of Douglass Mine, located in Blue Hill, Maine. Present at this site is a stream that flows directly over the area where the tailings pile used to sit, directly to the south-east of the mining site (LePage et al. 1991). We would expect Douglass Mine's microbial community to be structured differently than that of Blood Brook's. Being a mine waste environment, it is different than Blood Brook both chemically and likely microbially as well. Studying it in the

same way as we did Blood Brook would allow us to understand the differences between seasonal changes in mine waste environments vs. acidic stream environments.

3.5 Conclusions

Based on the observed data, the original hypothesis that Blood Brook's oxidation potential would be diminished due to dilution of the microbial community during sampling points Blood Brook was dominated by stormflow can be rejected. Oxidation potential as exhibited by change in sulfate concentration was shown to have no significant difference between abiotic and biotic treatments and little difference between experiments. The hypothesis that Blood Brook's microbial community would evolve into one comprised of acidophilic iron and sulfide oxidizers can also be rejected. While the community did develop into an acidophilic one in the experimental conditions, there was not a strong presence of classified iron or sulfide oxidizer. The community resembled one of either a circumneutral iron-rich groundwater or surface water community. The community structural evolution was primarily driven by the decreasing pHs and increasing specific conductance, as indicated by the experimental RDAs. Additional insights into Blood Brook's microbial communities' structural evolution were gained through the experimental data. Aluminum may have a stronger influence upon the microbial communities' structural evolution during acidifying conditions than originally expected. Bacterial growth patterns, aluminum concentrations, the presence of bacteria that have been shown to exhibit increased growth in high aluminum concentrations (*Acidisoma* and *Acidocella*), and implications by the RDAs, all lead to this conclusion. This is intriguing because aluminum has not really been considered in the past as a specific driver of

the development of microbial communities in acidified systems (Baker and Banfield 2003, Hallberg, 2010, Johnson and Hallberg 2003, Nordstrom 2010).

REFERENCES

Akcil, A., & Koldas, S. (2005). Acid Mine Drainage (AMD): causes, treatment and case studies. *Journal of Cleaner Production*, *14*, 1139–1145. http://doi.org/10.1016/j.jclepro.2004.09.006

Aller, R. C., & Rude, P. D. (1988). Complete oxidation of solid phase sulfides by manganese and bacteria in anoxic marine sediments. *Geochimica et Cosmochimica Acta*, *52*(3), 751–765.

Almaraz, N., Whitaker, A. H., Andrews, M. Y., & Duckworth, O. W. (2017). Assessing Biomineral Formation by Iron-oxidizing Bacteria in a Circumneutral Creek. *Journal of Contemporary Water Research & Education*, (160), 60–71.

Ancion, P.-Y., Lear, G., Dopheide, A., & Lewis, G. D. (2013). Metal concentrations in stream biofilm and sediments and their potential to explain biofilm microbial community structure. *Environmental Pollution*, *173*, 117–124. http://doi.org/10.1016/j.envpol.2012.10.012

Appanna, V. D., & St. Pierre, M. (1994). Influence of phosphate on aluminum tolerance in Pseudomonas fluorescens. *FEMS Microbiology Letters*, *124*(3), 327–332.

Auld, R. R., Myre, M., Mykytczuk, N. C. S., Leduc, L. G., & Merritt, T. J. S. (2013). Characterization of the microbial acid mine drainage microbial community using culturing and direct sequencing techniques. *Journal of Microbiological Methods*, *93*(2), 108–15. http://doi.org/10.1016/j.mimet.2013.01.023

Baker, B. J., & Banfield, J. F. (2003). Microbial communities in acid mine drainage. *FEMS Microbiology Ecology*, *44*(2), 139–52. http://doi.org/10.1016/S0168-6496(03)00028-X

Baker, M. A., Dahm, C. N., & Valett, H. M. (2000). Anoxia, Anaerobic Metabolism, and Biogeochemistry of the Stream-water-Ground-water Interface. In *Streams and Ground Waters* (pp. 259–283).

Baker-Austin, C., Potrykus, J., Wexler, M., Bond, P. L., & Dopson, M. (2010). Biofilm development in the extremely acidophilic archaeon "Ferroplasma acidarmanus" Fer1. *Extremophiles*, *14*(6), 485–491. http://doi.org/10.1007/s00792-010-0328-1

Banderas, A., & Guiliani, N. (2013). Bioinformatic prediction of gene functions regulated by quorum sensing in the bioleaching bacterium Acidithiobacillus ferrooxidans. *International Journal of Molecular Sciences*, *14*(8), 16901–16. http://doi.org/10.3390/ijms140816901

Bates, D., Maechler, M., Bolker, B., & Walker, S. (2015). Fitting Linear Mixed-Effects Models Using lme4. *Journal of Statistical Software*, *67*(1), 1-48. doi:10.18637/jss.v067.i01.

Beaton, E. D., Stevenson, B. S., King-sharp, K. J., Stamps, B. W., Nunn, H. S., & Stuart, M. (2016). Local and Regional Diversity Reveals Dispersal Limitation and Drift as Drivers for Groundwater Bacterial Communities from a Fractured Granite Formation. *Frontiers in Microbiology*, *7*(12), 1–16. http://doi.org/10.3389/fmicb.2016.01933

Belova, S. E., Pankratov, T. A., Detkova, E. N., Kaparullina, E. N., & Dedysh, S. N. (2009). Acidisoma tundrae gen. nov., sp. nov. and Acidisoma sibiricum sp. nov., two acdiophilic, psychotolerant members of the Alphaproteobacteria from acidic northern wetlands. *International Journal of Systematic and Evolutinary Microbiology*, *59*(9), 2283–2290.

Belzile, N., Chen, Y. W., Cai, M. F., & Li, Y. (2004). A review on pyrrhotite oxidation. *Journal of Geochemical Exploration*, *84*(2), 65–76. http://doi.org/10.1016/j.gexplo.2004.03.003

Benjamin, M. M. (2015). *Water Chemistry* (2nd Edition). Grove, Illinois: Waveland Press, Inc.

Blight, K. R., & Ralph, D. E. (2008). Aluminium sulphate and potassium nitrate effects on batch culture of iron oxidising bacteria. *Hydrometallurgy*, *92*, 130–134. http://doi.org/10.1016/j.hydromet.2008.02.010

Bloom, P. R. (1983). The kinetics of gibbsite dissolution in nitric acid. *Soil Science of America Journal*, *47*(1), 164–168.

Blowes, D. W., Ptacek, C. J., Jambor, J. L., & Weisener, C. G. (2003). The geochemistry of acid mine drainage. *Treatise on Geochemistry*, *9*, 149–204. Retrieved from http://adsabs.harvard.edu/abs/2003TrGeo...9..149B

Bigelow, R. C., & Plumlee, G. S. (1995). The Summitville mine and its downstream effects. *US Geological Survey Open-File Report,* 95-23.

Bohn, H. L., McNeal, B. L., & O'Connor, G. A. (1985). *Soil Chemistry*. Wiley-Interactive, New York.

Borcard, D., Gillet, F., & Legendre, P. (2011). *Numerical Ecology with R*. (R. Gentleman, K. Hornik, & G. G. Parmigiani, Eds.). New York: Springer International Publishing.

Bouley, B., & Hodder, R. (1984). Strata-Bound Massive Sulfide Deposits in Silurian-Devonian. *Economic Geology*, *79*, 1693–1702.

Brantley, S. L., & Olsen, A. A. (2013). *Reaction Kinetics of Primary Rock-Forming Minerals under Ambient Conditions*. *Treatise on Geochemistry: Second Edition* (2nd ed., Vol. 7). Elsevier Ltd. http://doi.org/10.1016/B978-0-08-095975-7.00503-9

Brantner, J. S., Haake, Z. J., Burwick, J. E., Menge, C. M., Hotchkiss, S. T., & Senko, J. M. (2014). Depth-dependent geochemical and microbiological gradients in Fe(III) deposits resulting from coal mine-derived acid mine drainage. *Frontiers in Microbiology*, *5*(May), 215. http://doi.org/10.3389/fmicb.2014.00215

Braun, B., Schroder, J., Knecht, H., & Szewzyk, U. (2016). Unraveling the microbial community of a cold groundwater catchment system. *Water Research*, *107*(10), 113–126. http://doi.org/10.1016/j.watres.2016.10.040

Brielmann, H., Griebler, C., Schmidt, S. I., Michel, R., & Lueders, T. (2009). Effects of thermal energy discharge on shallow groundwater ecosystems. *Federation of European Microbial Science*, *68*, 273–286. http://doi.org/10.1111/j.1574-6941.2009.00674.x

Brino, A. (2016). Controversy over metal mining in Maine rekindled. *Bangor Daily News*, p. Online.

Burgot, J.-L. (2012). Solubility and pH. In *Ionic Equilibria in Analytical Chemistry* (pp. 633–658).

Buttle, J. M. (1994). Isotope hydrograph separations and rapid delivery of pre-event water from drainage basins. *Progress in Physical Geography: Earth and Environment*, *18*(1), 16–41.

Cairn, N. (2013). The battle for Bald Mountain. *Portland Press Herald*, p. Online.

Caissie, D., Pollock, T. L., & Cunjak, R. A. (1996). Variation in stream water chemistry and hydrograph separation in a small drainage basin. *Journal of Hydrology*, *178*(1–4), 137–157.

Cardoso, R. B., Sierra-Alvarez, R., Rowlette, P., Flores, E. R., Gomez, J., & Field, J. A. (2006). Sulfide oxidation under chemolithoautotrophic denitrifying conditions. *Biotechnology and Bioengineering*, *95*(6), 1148–1157.

Chen, Y., Li, J., Chen, L., Hua, Z., Huang, L., Liu, J., … Shu, W. (2014). Biogeochemical processes governing natural pyrite oxidation and release of acid metalliferous drainage. *Environmental Science & Technology*, *48*(10), 5537–45. http://doi.org/10.1021/es500154z

Coleman, R. N., & Gaudet, I. D. (1993). THIOBACILLUS NEPOLITANUS IMPLICATED IN THE DEGRADATION OF CONCRETE TANKS USED FOR POTABLE WATER STORAGE. *Water Research*, *27*(3), 413–418.

Constantz, J., Thomas, C. L., & Zellweger, G. (1994). Influence of diurnal variations in stream temperature on stream flow loss and groundwater recharge. *Water Resources Research*, *30*(12), 3253–3264.

Cousins, C. (2017). Maine lawmakers buck LePage, pass mineral mining rules after years of debate. *Bangor Daily News*, p. Online.

Craw, D. (2000). Water-rock interaction and acid neutralization in a large schist debris dam, Otago, New Zealand. *Chemical Geology*, *171*, 17–32. http://doi.org/10.1016/S0009-2541(00)00231-X

Crump, B. C., Armbrust, E. V., & Baross, J. A. (1999). Phylogenetic Analysis of Particle-Attached and Free-Living Bacterial Communities in the Columbia River, Its Estuary, and the Adjacent Coastal Ocean. *Applied and Environmental Microbiology*, *65*(7), 3192–3204.

Davis, W. B., McCauley, M. J., & Byers, B. R. (1971). Iron requirements and aluminum sensitivity of hydroxamic acid-requiring strain of Bacillus megaterium. *Journal of Bacteriology*, *105*(2), 589–594.

DeNicola, D. M., & Stapleton, M. G. (2002). Impact of acid mine drainage on benthic communities in streams: the relative roles of substratum vs. aqueous effects. *Environmental Pollution*, *119*(3), 303–315.

Docherty, K. M., Young, K. C., Maurice, P. A., & Bridgham, S. D. (2006). Dissolved Organic Matter Concentration and Quality Influences upon Structure and Function of Freshwater Microbial Communities. *Microbial Ecology*, *52*, 378–388. http://doi.org/10.1007/s00248-006-9089-x

Dold, B. (2010). Basic concepts in environmental geochemistry of sulfidic mine-waste management. *Waste Management*, *24*(March), 173–198. Retrieved from http://www.intechopen.com/source/pdfs/9675/InTech-Basic_concepts_in_environmental_geochemistry_of_sulfidic_mine_waste_management.pdf

Dopheide, A., Lear, G., He, Z., Zhou, J., & Lewis, G. D. (2015). Functional Gene Composition, Diversity and Redundancy in Microbial Stream Biofilm Communities. *PLOS One*, *10*(4), 1–21. http://doi.org/10.1371/journal.pone.0123179

Dopson, M., & Holmes, D. S. (2014). Metal resistance in acidophilic microorganisms and its significance for biotechnologies. *Applied Microbiology and Biotechnology*, 8133–8144. http://doi.org/10.1007/s00253-014-5982-2

Dopson, M., Lövgren, L., & Boström, D. (2009). Silicate mineral dissolution in the presence of acidophilic microorganisms: Implications for heap bioleaching. *Hydrometallurgy*, *96*(4), 288–293. http://doi.org/10.1016/j.hydromet.2008.11.004

Drever, J. I. (1988). *The Geochemistry of Natural Waters* (2nd Edition). Englewood Cliffs, NJ: Prentice Hall.

Driscoll Jr., C. T., Baker, J. P., Bisogni Jr., J. J., & Schofield, C. L. (1980). Effect of aluminium speciation on fish in dilute acidified waters. *Nature*, *284*, 161–164.

Driscoll, C. T., & Schecher, W. D. (1990). The chemistry of aluminum in the environment. *Environmental Geochemistry and Health*, *12*(1), 28–49.

Druschel, G. K., Baker, B. J., Gihring, T. M., & Banfield, J. F. (2004). Acid mine drainage biogeochemistry at Iron Mountain, California. *Geochemical Transactions*, *5*(2), 13–32. http://doi.org/10.1063/1.1769131

Duncan, J. M., Groffman, P. M., & Band, L. E. (2013). Towards closing the watershed nitrogen budget : Spatial and temporal scaling of denitrification. *Journal of Geophysical Research: Biogeosciences*, *118*(June), 1105–1119. http://doi.org/10.1002/jgrg.20090

Eaton, A. D., Clesceri, L. S., Rice, E. W., & Greenberg, Arnold, E. (2005). *Standard Methods for the Examination of Water and Wastewater* (21st ed.). Washington, DC: American Public Health Association.

Edwards, K. J., Gihring, T. M., & Banfield, J. F. (1999). Seasonal Variations in Microbial Populations and Environmental Conditions in an Extreme Acid Mine Drainage Environment. *Applied and Environmental Microbiology*, *30*(7), 3627–3632.

Edwards, K. J., Goebel, B. M., Rodgers, T. M., Schrenk, M. O., Gihring, T. M., Cardona, M. M., Mcguire, M. M., Hamer, R. J., Pace, N. R., Banfield, J. F. (1999). Geomicrobiology of Pyrite (FeS2) Dissolution: Case Study at Iron Mountain, California. *Geomicrobiology Journal*, *16*(2), 155–179. http://doi.org/10.1080/014904599270668

Edwards, K. J., Bond, P. L., Druschel, G. K., Mcguire, M. M., Hamers, R. J., & Banfield, J. F. (2000). Geochemical and biological aspects of sulfide mineral dissolution: lessons from Iron Mountain, California. *Chemical Geology*, *169*, 383–397.

Emerson, D., & Moyer, C. (1997). Isolation and Characterization of Novel Iron-Oxidizing Bacteria That Grow at Circumneutral pH. *Applied and Environmental Microbiology*, *63*(12), 4784–4792.

Emerson, D., Rentz, J. A., & Plaia, T. (2007). Sideroxydans lithotrophicus, gen. nov, sp. nov. and Gallionella capsiferriformans sp. nov., oxygen-dependent ferrous iron-oxidizing bacteria that grow at circumneutral pH. *International Journal of Systematic and Evolutionary Microbiology*.

Emerson, D., & Weiss, J. V. (2004). Bacterial Iron Oxidation in Circumneutral Freshwater Habitats: Findings from the Field and the Laboratory. *Geomicrobiology Journal*, *21*(6), 405–414. http://doi.org/10.1080/01490450490485881

Espana, J. S. (2007). *The Behavior of Iron and Aluminum in Acid Mine Drainage*.

Evangelou, V. P. (1998). *Environmental Soil and Water Chemistry: Principles and Applications*.

Fantone, I., Grieco, G., Strini, A., & Cavallo, A. (2014). The effect of Alpine metamorphism on an oceanic Cu-Fe sulfide ore : the Herin deposit , Western Alps , Italy. *Periodico Di Mineralogia*, 345–365. http://doi.org/10.2451/2014PM0019

Fiebig, D. M., Lock, M. A., & Neal, C. (1990). Soil water in the riparian zone as a source of carbon for a headwater stream. *Journal of Hydrology*, *116*(1–4), 217–237.

Fiechter, S., Birkolz, M., Hartmaan, A., Dulski, P., Gliersig, M., Tributsch, H., & Tilley, R. J. D. (1992). The microstructure and stoichiometry of pyrite FeS2-x. *Journal of Materials Research*, *7*(7), 1829–1838.

Fierer, N., & Jackson, R. B. (2006). The diversity and biogeography of soil bacterial communities. *PNAS*, *103*(3), 626–631.

Fierer, N., Morse, J. L., Berthrong, S. T., Bernhardt, E. S., & Jackson, R. B. (2007). Environmental Controls on the Landscape-Scale Biogeography of Stream Bacterial Communities. *Ecology*, *88*(9), 2162–2173.

Findlay, S. (1995). Importance of surface-subsurface exchange in stream ecosystems: The hyporheic zone. *Limnology and Oceanography*, *40*(1), 159–164.

Findlay, S., & Sobczak, W. V. (2000). Microbial Communities in Hyporheic Sediments. In *Streams and Ground Waters* (pp. 287–306).

Fischer, H., Pusch, M., & Schwoerbel, J. (1996). Spatial distribution and respiration of bacteria in stream-bed sediments. *Archiv Fur Hydrobiologie*, *137*(3), 281–300.

Fischer, J., Quentmeier, A., Gansel, S., Sabados, V., & Friedrich, C. G. (2002). Inducible aluminum resistance of Acidiphilium cryptum and aluminum tolerance of other acidophilic bacteria. *Archives of Microbiology*, (178), 554–558. http://doi.org/10.1007/s00203-002-0482-7

Fisher, M. M., & Triplett, E. W. (1999). Automated Approach for Ribosomal Intergenic Spacer Analysis of Microbial Diversity and Its Application to Freshwater Bacterial Communities. *Applied and Environmental Microbiology*, *65*(10), 4630–4636.

Fleming, E. J., Cetinic, I., Chan, C. S., King, D. W., & Emerson, D. (2014). Ecological succession among iron-oxidizing bacteria. *The ISME Journal*, *8*, 804–815. http://doi.org/10.1038/ismej.2013.197

Fobes, C. B. (1946). *Climatic Divisions of Maine*. Orono, ME.

Foley, M. E. (2003). *The Iron Age of Maine - 1800's - Katahdin Iron Works*.

Franken, R. J. M., Storey, R. G., & Williams, D. D. (2001). Biological, chemical and physical characteristics of downwelling and upwelling zones in the hyporheic zone of a north-temperate stream. *Hydrobiologia*, *444*, 183–195.

Frossard, A., Gerull, L., Mutz, M., & Gessner, M. O. (2013). Shifts in microbial community structure and function in stream sediments during experimentally simulated riparian succession. *Federation of European Microbial Science*, *84*(2), 398–410. http://doi.org/10.1111/1574-6941.12072

Galecki, A., & Burzykowski, T. (2012). Linear Mixed-Effects Model. In *Linear Mixed-Effects Models Using R* (pp. 245–273).

Galhardi, J. A., & Bonotto, D. M. (2016). Hydrogeochemical features of surface water and groundwater contaminated with acid mine drainage (AMD) in coal mining areas : a case study in southern Brazil. *Environmental Science and Pollution Research*, (1515). http://doi.org/10.1007/s11356-016-7077-3

Gammons, C., Nimick, D., Parker, S., Snyder, D., Mccleskey, R., Amils, R., & Poulson, S. (2008). Photoreduction fuels biogeochemical cycling of iron in Spain's acid rivers. *Chemical Geology*, *252*(3–4), 202–213. http://doi.org/10.1016/j.chemgeo.2008.03.004

Genty, T., Bussière, B., Potvin, R., Benzaazoua, M., & Zagury, G. J. (2012). Dissolution of calcitic marble and dolomitic rock in high iron concentrated acid mine drainage: Application to anoxic limestone drains. *Environmental Earth Sciences*, *66*(8), 2387–2401. http://doi.org/10.1007/s12665-011-1464-3

Ghoorah, M., Dlugogorski, B. Z., Balucan, R. D., & Kennedy, E. M. (2014). Selection of acid for weak acid processing of wollastonite for mineralization of CO2. *Fuel*, *122*, 277–286. http://doi.org/10.1016/j.fuel.2014.01.015

Ginn, T. R., Wood, B. D., Nelson, K. E., Scheibe, T. D., Murphy, E. M., & Clement, T. P. (2002). Processes in microbial transport in the natural subsurface. *Advances in Water Resources*, *25*(8–12), 1017–1042.

Gleisner, M., & Herbert, R. B. (2002). Sulfide mineral oxidation in freshly processed tailings: Batch experiments. *Journal of Geochemical Exploration*, *76*(3), 139–153. http://doi.org/10.1016/S0375-6742(02)00233-9

Gleisner, M., Herbert, R. B., & Frogner Kockum, P. C. (2006). Pyrite oxidation by Acidithiobacillus ferrooxidans at various concentrations of dissolved oxygen. *Chemical Geology*, *225*(1–2), 16–29. http://doi.org/10.1016/j.chemgeo.2005.07.020

Goldstein, J. I., Newbury, D. E., Michael, J. R., Ritchie, N. W. M., Scott, J. H. J., & Joy, D. C. (2017). *Scanning Electron Microscopy and X-Ray Microanalysis* (4th ed.). Springer.

Golubev, S. V., Pokrovsky, O. S., & Schott, J. (2005). Experimental determination of the effect of dissolved CO2 on the dissolution kinetics of Mg and Ca silicates at 25 degrees C. *Chemical Geology*, *217*, 227–238.

González, A., Bellenberg, S., Mamani, S., Ruiz, L., Echeverría, A., Soulère, L., … Guiliani, N. (2013). AHL signaling molecules with a large acyl chain enhance biofilm formation on sulfur and metal sulfides by the bioleaching bacterium Acidithiobacillus ferrooxidans. *Applied Microbiology and Biotechnology*, *97*(8), 3729–37. http://doi.org/10.1007/s00253-012-4229-3

Grantham, M. C., & Dove, P. M. (1997). Microbially catalyzed dissolution of iron and aluminum oxyhydroxide mineral surface coatings. *Geochimica et Cosmochimica Acta*, *61*(21), 4467–4477.

Gray, J. E., Coolbaugh, M. F., Plumlee, G. S., & Atkinson, W. W. (1994). Environmental geology of the Summitville Mine, Colorado. *Economic Geology*, *89*(8).

Gucht, K. Van Der, Vandekerckhove, T., Vloemans, N., Cousin, S., Muylaert, K., Sabbe, K., … Vyverman, W. (2005). Characterization of bacterial communities in four freshwater lakes differing in nutrient load and food web structure. *FEMS Microbiology Ecology*, *53*, 205–220. http://doi.org/10.1016/j.femsec.2004.12.006

Gupta, R. S. (2017). Estimation of Surface Water Flow: Hydrograph Analysis. In *Hydrology and Hydraulic Systems* (4th Edition, pp. 337–378). Long Grove, IL: Waveland Press, Inc.

Gupta, S. K., Lal, D., & Lal, R. (2009). Novophingobium panipatense sp. nov. and Novophingobium mathurense sp. nov., from oil-contaminated soil. *International Journal of Systematic and Evolutionary Microbiology*, *59*, 156–161.

Haan, S. B. de. (1991). A review of the rate of pyrite oxidation in aqueous systems at low temperature. *Earth-Science Reviews*, *31*, 1–10.

Hallberg, K. B. (2010). New perspectives in acid mine drainage microbiology. *Hydrometallurgy*, *104*(3–4), 448–453. http://doi.org/10.1016/j.hydromet.2009.12.013

Hanson, L. S., & Sauchuk, S. A. (1991). *Field Guide to the Geology and Geomorphology of the Carrabasset Formation and Economic Deposits in Central Maine*.

Hao, C., Wang, L., Gao, Y., Zhang, L., & Dong, H. (2010). Microbial diversity in acid mine drainage of Xiang Mountain sulfide mine , Anhui Province , China. *Extremophiles*, *14*, 465–474. http://doi.org/10.1007/s00792-010-0324-5

Hao, O. J., Chen, J. M., Huang, L., & Buglass, R. L. (1996). Sulfate-reducing bacteria. *Critical Reviews in Envrionmental Science and Technology*, *26*(2), 155–187.

Harvey, J. W., & Wagner, B. J. (2000). Quantifying Hydrologic Interactions between Streams and Their Subsurface Hyporheic Zones. In *Streams and Ground Waters* (pp. 3–44).

Hedin, L. O., von Fischer, J. C., Ostrom, N. E., Kennedy, B. P., Brown, M. G., & Roberston, G. P. (1998). THERMODYNAMIC CONSTRAINTS ON NITROGEN TRANSFORMATIONS AND OTHER BIOGEOCHEMICAL PROCESSES AT SOIL-STREAM INTERFACES. *Ecology*, *79*(2), 684–703.

Hellweger, F. (1997). AGREE - DEM Surface Reconditioning System. *University of Texas, Austin.*

Hemond, H. F. (1990). Acid neutralizing capacity, alkalinity, and acid-base status of natural waters containing organic acids. *Environmental Science & Technology*, *24*(10), 1486–1489.

Hendricks, S. P. (1996). Bacterial biomass, activity, and production within the hyporheic zone of a north-temperate stream. *Archiv Fur Hydrobiologie*, *136*(4), 467–487.

Hill, A. R. (2000). Stream Chemistry and Riparian Zones. In *Streams and Ground Waters* (pp. 83–110).

Holmes, R. M. (2000). The Importance of Ground Water to Stream Ecosystem Function. In *Streams and Ground Waters* (pp. 137–148).

Hu, G., Dam-Johansen, K., Wedel, S., & Hansen, J. P. (2006). Decomposition and oxidation of pyrite. *Progress in Energy and Combustion Science*, *32*(3), 295–314. http://doi.org/10.1016/j.pecs.2005.11.004

Huminicki, D. M. C. (2006). *Effect of Coatings on Mineral Reaction Rates in Acid Mine Drainage*.

Huminicki, D. M. C., & Rimstidt, J. D. (2008). Neutralization of sulfuric acid solutions by calcite dissolution and the application to anoxic limestone drain design. *Applied Geochemistry*, *23*(2), 148–165. http://doi.org/10.1016/j.apgeochem.2007.10.004

Jambor, J. L., Dutrizac, J. E., Raudsepp, M., & Groat, L. A. (2003). Effect of Peroxide on Neutralization-Potential Values of Siderite and Other Carbonate Minerals. *Journal of Environmental Quality*, *32*(November), 2373–2378.

James, R. E., & Ferris, F. G. (2004). Evidence for microbial-mediated iron oxidation at a neutrophilic groundwater spring. *Chemical Geology*, *212*(3–4), 301–311.

Jamieson, H. E. (2011). Geochemistry and Mineralogy of Solid Mine Waste: Essential Knowledge for Predicting Environmental Impact. *Elements*, *7*(6), 381–386. http://doi.org/10.2113/gselements.7.6.381

Janzen, M. P., Nicholson, R. V., & Scharer, J. M. (2000). Pyrrhotite reaction kinetics: Reaction rates for oxidation by oxygen, ferric iron, and for nonoxidative dissolution. *Geochimica et Cosmochimica Acta*, *64*(9), 1511–1522. http://doi.org/10.1016/S0016-7037(99)00421-4

Jenson, S. K., & Domingue, J. O. (1988). Extracting Topographic Structure from Digital Elevation Data for Geographic Information System Analysis. *Photogrammetric Engineering and Remote Sensing*, *54*(11), 1593–1600.

Jerz, J. K., & Rimstidt, J. D. (2004). Pyrite oxidation in moist air. *Geochimica et Cosmochimica Acta*, *68*(4), 701–714. http://doi.org/10.1016/S0016-7037(03)00499-X

Jezberova, J., Jezbera, J., Brandt, U., Lindstrom, E. S., Langenheder, S., & Hahn, M. W. (2010). Ubiquity of Polynucleobacter necessarius ssp. asymbioticus in lentic freshwater habitats of a heterogenous 2000 km2 area. *Environmental Microbiology*, *12*(3), 658–669.

Johnson, D. B. (2014). Recent Developments in Microbiological Approaches for Securing Mine Wastes and for Recovering Metals from Mine Waters. *Minerals*, *4*(2), 279–292. http://doi.org/10.3390/min4020279

Johnson, D. B. (2012). Geomicrobiology of extremely acidic subsurface environments. *Federation of European Microbial Science*, *81*(1), 2–12. http://doi.org/10.1111/j.1574-6941.2011.01293.x

Johnson, D. B. (1998). Biodiversity and ecology of acidophilic microorganisms. *FEMS Microbiology Ecology*, *27*, 307–317.

Johnson, D. B., & Hallberg, K. B. (2005). Acid mine drainage remediation options: a review. *The Science of the Total Environment*, *338*(1–2), 3–14. http://doi.org/10.1016/j.scitotenv.2004.09.002

Johnson, D. B., & Hallberg, K. B. (2003). The microbiology of acidic mine waters. *Research in Microbiology*, *154*(7), 466–473.

Jones, C. F., LeCount, S., Smart, R. S. C., & White, T. J. (1992). Compositional and structural alteration of pyrrhotite surfaces in solution: XPS and XRD studies. *Applied Surface Science*, *55*(1), 65–85.

Jones, D. S., Lapakko, K. A., Wenz, Z. J., Olson, M. C., Roepke, E. W., Sadowsky, M. J., Novak, P. J., Bailey, J. V. (2017). Novel Microbial Assemblages Dominate Weathered Sulfide-Bearing Rock from Copper-Nickel Deposits in the Duluth Complex, Minnesota, USA. *Applied and Environmental Microbiology*, *83*(16), 1–15.

Jones, R. M., & Johnson, D. B. (2015). Acidithrix ferrooxidans gen . nov ., sp . nov .; a filamentous and obligately heterotrophic , acidophilic member of the Actinobacteria that catalyzes dissimilatory oxido-reduction of iron. *Research in Microbiology*, *166*(2), 111–120. http://doi.org/10.1016/j.resmic.2015.01.003

Jurjovec, J., Ptacek, C. J., & Blowes, D. W. (2002). Acid neutralization mechanisms and metal release in mine tailings: A laboratory column experiment. *Geochimica et Cosmochimica Acta*, *66*(9), 1511–1523. http://doi.org/10.1016/S0016-7037(01)00874-2

Kalinowski, B. E., & Schweda, P. (1996). Kinetics of muscovite, phlogopite and biotite dissolution and alteration at pH 1-4, room temperature. *Geochimica et Cosmochimica Acta*, *60*, 367–385.

Kang, H., Kim, H., Lee, B.-I., Joung, Y., & Joh, K. (2014). Sediminibacterium goheungense sp. nov., isolated from a freshwater reservoir. *International Journal of Systematic and Evolutionary Microbiology*, *64*, 1328–1333.

Kemp, P. F., & Aller, J. Y. (2003). Bacterial diversity in aquatic and other environments: what 16S rDNA libraries can tell us. *FEMS Microbiology Ecology*, (47), 161–177. http://doi.org/10.1016/S0168-6496(03)00257-5

Kim, Y.-J., Nguyen, N.-L., Weon, H.-Y., & Yang, D.-C. (2013). Sediminibacterium ginsengisoli sp. nov., isolated from soil of a ginseng field, and emended descriptions of the genus Sediminibacterium and of Sediminibacterium salmoneum. *International Journal of Systematic and Evolutionary Microbiology*, *63*, 905–912.

Kimoto, K., Aizaws, T., Urai, M., Ve, N. B., Suzuki, K., Nakajima, M., & Sunairi, M. (2010). Acidocella aluminiidurans sp. nov., an aluminium-tolerant bacterium isolated from Panicum repens grown in a highly acidic swamp in actual acid sulfate soil area of Vietnam. *International Journal of Systematic and Evolutinary Microbiology*, *60*, 764–768.

King, H. E., Plümper, O., Geisler, T., & Putnis, A. (2011). Experimental investigations into the silicification of olivine: Implications for the reaction mechanism and acid neutralization. *American Mineralogist*, *96*(10), 1503–1511. http://doi.org/10.2138/am.2011.3779

Knauss, K. G., Nguyen, S. N., & Weed, H. C. (1993). Diopside dissolution kinetics as a function of pH, C02, temperature, and time. *Geochimica et Cosmochimica Acta*, *57*, 285–294.

Kolbel-Boelke, J., Anders, E.-M., & Nehrkorn, A. (1988). Microbial communities in the saturated groundwater environment II: Diversity of bacterial communities in a Pleistocene sand aquifer and their in vitro activities. *Microbial Ecology*, *16*(1), 31–48.

Korehi, H., Blothe, M., & Schippers, A. (2014). Microbial diversity at the moderate acidic stage in three different sulfidic mine tailings dumps generating acid mine drainage. *Research in Microbiology*, *165*(9), 713–718.

Krepski, S. T., Hanson, T. E., & Chan, C. S. (2011). Isolation and characterization of a novel biomineral stalk-forming iron-oxidizing bacterium from a circumneutral groundwater seep. *Environmental Microbiology*, *14*(7).

Kuznetsova, A., Brockhoff, P. B., & Christensen, R. H. B. (2017). lmerTest Package: Tests in Linear Mixed-Effect Models. *Journal of Statistical Software*, *82*(13), 1-26. doi: 10.18637/jss.v082.i13 (URL: http://doi.org/10.18637/jss.v082.i13).

Lang, E., Swiderski, J., Stackebrandt, E., Schumann, P., Sproer, C., & Sahin, N. (2007). Herminiimonas saxobsidens sp. nov., isolated from a lichen-colonized rock. *International Journal of Systematic and Evolutionary Microbiology*, *57*(11), 2618–2622.

Larsson, L., Olsson, G., Holst, O., & Karlsson, H. T. (1990). Pyrite oxidation by thermophilic archaebacteria. *Applied and Environmental Microbiology*, *56*(3), 697–701.

Legendre, P., & Gallagher, E. D. (2001). Ecologically meaningful transformations for ordination of species data. *Oceologia*, *2001*(September 2000), 271–280. http://doi.org/10.1007/s004420100716

Lepage, C. A., Foley, M. E., & Thompson, W. B. (1991). *Mining in Maine: past, present, and future*.

Lindsay, M. B. J., Condon, P. D., Jambor, J. L., Lear, K. G., Blowes, D. W., & Ptacek, C. J. (2009). Mineralogical, geochemical, and microbial investigation of a sulfide-rich tailings deposit characterized by neutral drainage. *Applied Geochemistry*, *24*(12), 2212–2221.

Lindstrom, E. S., Agterveld, M. P. K., & Zwart, G. (2005). Distribution of Typical Freshwater Bacterial Groups Is Associated with pH, Temperature, and Lake Water Retention Time. *Applied and Environmental Microbiology*, *71*(12), 8201–8206. http://doi.org/10.1128/AEM.71.12.8201

Liu, J., Hua, Z.-S., Chen, L.-X., Kuang, J.-L., Li, S.-J., Shu, W.-S., & Huang, L.-N. (2014). Correlating microbial diversity patterns with geochemistry in an extreme and heterogeneous environment of mine tailings. *Applied and Environmental Microbiology*, *80*(12), 3677–86. http://doi.org/10.1128/AEM.00294-14

Liu, W., & Zhang, X. (2014). Experimental Study of Microbial Pyrite Oxidation: A Suggestion for Geologically Useful Biosignatures. *Geomicrobiology Journal*, *32*(5), 466–471. http://doi.org/10.1080/01490451.2014.942446

Liu, Z.-P., Wang, B.-J., Liu, Y.-H., & Liu, S.-J. (2005). Novosphingobium tehuense sp. nov., a novel aromatic-compound-degrading bacterium isolated from Taihu Lake, China. *International Journal of Systematic and Evolutionary Microbiology*, *55*, 1229–1232.

Londry, K. L., & Sherriff, B. L. (2005). Comparison of Microbial Biomass, Biodiversity, and Biogeochemistry in Three Contrasting Gold Mine Tailings Deposits. *Geomicrobiology Journal*, *22*(5), 237–247. http://doi.org/10.1080/01490450590947797

Loveland-Curtze, J., Miteva, V. I., & Brenchley, J. E. (2009). Herminiimonas glaciei sp. nov., a novel ultramicrobacterium from 3042 m deep Greenland glacial ice. *International Journal of Systematic and Evolutionary Microbiology*, *59*(6), 1272–1277.

Lowson, R. T. (1982). Aqueous oxidation of pyrite by molecular oxygen. *Chemical Reviews*, *82*, 461–497.

Maamar, S. Ben, Aquilina, L., Quaiser, A., Pauwels, H., Michon-Coudouel, S., Vergnaud-Ayraud, V., … Dufresne, A. (2015). Groundwater Isolation Governs Chemistry and Microbial Community Structure Along Hydrologic Flowpaths. *Frontiers in Microbiology*, *6*(December), 1–13. http://doi.org/10.3389/fmicb.2015.01457

Mamlouk, D., & Gullo, M. (2013). Acetic Acid Bacteria: Physiology and Carbon Sources Oxidation. *Indian Journal of Microbiology*, *53*(4), 377–384. http://doi.org/10.1007/s12088-013-0414-z

Marvinney, R. G. (2015). *Overview of Maine Metallic Mineral Deposits and Mining*.

Marvinney, R. G., & Berry IV, H. N. (2015). *Maine Geological Survey CIRCULAR NO. 15-10: Legacy Mines in Maine*.

May, H. M., Helmke, P. A., & Jackson, M. L. (1979). Gibbsite solubility and thermodynamic properties of hydroxyaluminum ions in aqueous solutions at 25˚ C. *Geochimica et Cosmochimica Acta*, *43*(6), 861–868.

MacDonald, T. L., & Martin, R. B. (1988). Aluminum Ions in Biological Systems. *Trends in Biochemical Science*, *13*(1), 15–19.

Maine Geological Survey. (2005). History of Metal Mining in Maine.

McClenaghan, S. H., Lentz, D. R., Martin, J., & Diegor, W. G. (2009). Gold in the Brunswick No. 12 volcanogenic massive sulfide deposit, Bathurst Mining Camp, Canada: Evidence from bulk ore analysis and laser ablation ICP-MS data on sulfide phases. *Mineralium Deposita*, *44*(5), 523–557. http://doi.org/10.1007/s00126-009-0233-7

McDonnell, J. J., Bonell, M., Stewart, M. K., & Pearce, A. J. (1990). Deuterium variations in storm rainfall: Implications for stream hydrograph separation. *Water Resources Research*, *26*(3), 455–458.

Mendez, M. O., Neilson, J. W., & Maier, R. M. (2008). Characterization of a Bacterial Community in an Abandoned Semiarid Lead-Zinc Mine Tailing Site. *Applied and Environmental Microbiology*, *74*(12), 3899–3907.

Meruane, G., & Vargas, T. (2003). Bacterial oxidation of ferrous iron by Acidithiobacillus ferrooxidans in the pH range 2.5-7.0. *Hydrometallurgy*, *71*, 149–158. http://doi.org/10.1016/S0304-386X(03)00151-8

Merwade, V. (2012). *Watershed and Stream Network Delineation using ArcHydro Tools*.

Mlejnkova, H., & Sovova, K. (2010). Impact of pollution and seasonal changes on microbial community structure in surface water. *Water Science & Technology*, *61*(11), 2787–2795. http://doi.org/10.2166/wst.2010.080

Monthly Climate Data - Maine. (2018). *US Climate Data.* https://www.usclimatedata.com/climate/maine/united-states/3189

Moshchanetskiy, P. V, Pivovarova, T. A., Belyi, A. V, & Kondrat, T. F. (2014). Effect of Temperature on the Rate of Oxidation of Pyrrhotite Rich Sulfide Ore Flotation Concentrate and the Structure of the Acidophilic Chemolithotrophic Microbial Community. *Microbiology*, *83*(3), 255–261. http://doi.org/10.1134/S0026261714030138

Moshchanetskiy, P. V., Pivovarova, T. a., Belyi, a. V., Bulaev, a. G., Melamud, V. S., & Kondrat'eva, T. F. (2014). Effect of the aeration mode and yeast extract on the oxidation of high-pyrrhotite sulfide ore flotation concentrate and on the composition of the acidophilic chemolithotrophic microbial community. *Microbiology*, *83*(5), 558–567. http://doi.org/10.1134/S0026261714050191

Mulholland, P. J. (1997). Dissolved Organic Matter Concentration and Flux in Streams. *Journal of the North American Benthological Society*, *16*(1), 131–141.

Muller, D., Simeonova, D. D., Riegel, P., Mangenot, S., Lievremont, D., Bertin, P. N., & Lent, M. C. (2006). Herminiimonas arsenicoxydans sp. nov., a metalloresistant bacterium. *International Journal of Systematic and Evolutionary Microbiology*, *56*(8), 1765–1769.

Naiman, R. J., & Decamps, H. (1997). The Ecology of Interfaces: Riparian Zones. *Annual Review of Ecology and Systematics*, *28*(1), 621–658.

National Oceanic and Atmospheric Administration (2015-2016). Local Climatological Data Online.

Navratil, T., Rohovec, J., Amirbahman, A., Norton, S. A., & Fernandez, I. J. (2008). Amorphous Aluminum Hydroxide Control on Sulfate and Phosphate in Sediment-Solution Systems. *Water, Air, and Soil Pollution*, *201*(1–4), 87–98. http://doi.org/10.1007/s11270-008-9929-z

Neubauer, S. C., Emerson, D., & Megonigal, J. P. (2002). Life at the Energetic Edge: Kinetics of Circumneutral Iron Oxidation by Lithotrophic Iron-Oxidizing Bacteria Isolated from the Wetland-Plant Rhizosphere. *Applied and Environmental Microbiology*, *68*(8), 3988–3995. http://doi.org/10.1128/AEM.68.8.3988

Ni, Z. Y., Gu, G. H., Yang, H. S., & Qiu, G. Z. (2014). Bioleaching of pyrrhotite by Sulfobacillus thermosulfidooxidans. *Journal of Central South University*, *21*(7), 2638–2644. http://doi.org/10.1007/s11771-014-2224-9

Nordstrom, D. K. (2010). Advances in the Hydrogeochemistry and Microbiology of Acid Mine Waters. *International Geology Review*, *42*(6), 499–515. http://doi.org/10.1080/00206810009465095

Nordstrom, D. K. (1982). Aqueous pyrite oxidation and the consequent formation of secondary iron minerals. In J. A. Kittrick, D. F. Fanning, & L. R. Hossner (Eds.), *Acid Sulfate Weathering* (pp. 37–56). Soil Science Society of America Special Publication.

Nordstrom, D. K., Plummer, L. N., Langmuir, D., Busenberg, E., May, H. M., Jones, B. F., & Parkhurst, D. L. (1990). Revised chemical equilibrium data for major water-mineral reactions and their limitations. In D. C. Melchior & R. L. Bassett (Eds.), *Chemical Modeling of Aqueous Systems II* (vol. 416, pp. 398–413). Washington, DC: Am. Chem. Soc. Symp. Ser.

Nordstrom, D. K., & Southam, G. (1997). Geomicrobiology of sulfide mineral oxidation. In J. F. Banfield & K. H. Nealson (Eds.), *Geomicrobiology: Interactions between Microbes and Minerals* (pp. 361–385). Washington, DC: Mineralogical Society of America.

Novick, A. (1955). Growth of Bacteria. *Annual Review of Microbiology*, *9*, 97–110.

Oberholster, P. J., Cheng, P.-H., Botha, A.-M., & Genthe, B. (2014). The potential of selected macroalgal species for treatment of AMD at different pH ranges in temperate regions. *Water Research*, *60*(21), 82–92. http://doi.org/10.1016/j.watres.2014.04.031

Orandi, S., & Lewis, D. M. (2013). Synthesising acid mine drainage to maintain and exploit indigenous mining micro-algae and microbial assemblies for biotreatment investigations. *Environmental Science and Pollution Research*, *20*(2), 950–956. http://doi.org/10.1007/s11356-012-1006-x

Oksanen, J., Blanchet, F. G., Friendly, M., Kindt, R., Legendre, P., McGlinn, D., Minchin, P. R., O'Hara, R. B., Simpson, G. L., Solymos, P., Stevens, M. H. H., Szoecs, E., & Wagner, H. (2018). Vegan: Community Ecology Package. R package version 2.4-6. https://CRAN.R-project.org/package=vegan

Packman, A. I., & Bencala, K. E. (2000). Modeling Surface-Subsurface Hydrological Interactions. In *Streams and Ground Waters* (pp. 45–80).

Paktunc, A. D. (1999). Mineralogical constraints on the determination of neutralization potential and prediction of acid. *Environmental Geology*, *39*(December), 103–112.

Park, J., Jagasia, R., Kaufmann, G. F., Mathison, J. C., Ruiz, D. I., Moss, J. a, … Janda, K. D. (2007). Infection control by antibody disruption of bacterial quorum sensing signaling. *Chemistry & Biology*, *14*(10), 1119–27. http://doi.org/10.1016/j.chembiol.2007.08.013

Peres-Neto, P. R., Legendre, P., Dray, S., & Borcard, D. (2006). VARIATION PARTITIONING OF SPECIES DATA MATRICES: ESTIMATION AND COMPARISON OF FRACTIONS. *Ecology*, *87*(10), 2614–2625.

Peter, J. M., Leybourne, M. I., Scott, S. D., & Gorton, M. P. (2014). Geochemical constraints on the tectonic setting of basaltic host rocks to the Windy Craggy Cu-Co-Au massive sulphide deposit, northwestern British Columbia. *International Geology Review*, *56*(12), 1484–1503. http://doi.org/10.1080/00206814.2014.947335

Peters, D. L., Buttle, J. M., Taylor, C. H., & LaZerte, B. D. (1995). Runoff Production in a Forested, Shallow Soil, Canadian Shield Basin. *Water Resources Research*, *31*(5), 1291–1304.

Pierre Louis, A.-M., Yu, H., Shumlas, S. L., Van Aken, B., Schoonen, M. a. a., & Strongin, D. R. (2015). Effect of Phospholipid on Pyrite Oxidation and Microbial Communities under Simulated Acid Mine Drainage (AMD) Conditions. *Environmental Science & Technology*, (2), 150612093517008. http://doi.org/10.1021/es505374g

Pina, R. G., & Cervantes, C. (1996). Microbial interactions with aluminum. *Biometals*, *9*(August 1996), 311–316. http://doi.org/10.1007/BF00817932

Planchon, O., & Darboux, F. (2002). A fast, simple, and versatile algorithm to fill the depressions of digital elevation models. *Catena*, *46*(2), 159–176.

Plante, B., Benzaazoua, M., & Bussière, B. (2011). Predicting Geochemical Behaviour of Waste Rock with Low Acid Generating Potential Using Laboratory Kinetic Tests. *Mine Water and the Environment*, *30*(1), 2–21. http://doi.org/10.1007/s10230-010-0127-z

Plumlee, G. S. (1999). The environmental geology of mineral deposits. In *Reviews in Economic Geology* (pp. 71–116). Littleton, CO: Society of Economic Geologists.

Porcal, P., Amirbahman, A., Kopacek, J., & Norton, S. A. (2010). Experimental photochemical release of organically bound aluminum and iron in three streams in Maine, USA. *Environmental Monitoring Assessment*, *171*(1–4), 71–81. http://doi.org/10.1007/s10661-010-1529-x

Qu, J. H., & Yuan, H. L. (2008). Sediminibacterium salmoneum gen. nov., sp. nov., a member of the phylum Bacteriodetes isolated from sediment of a eutrophic reservoir. *International Journal of Systematic and Evolutionary Microbiology*, *58*(9), 2191–2194.

R Core Team (2017). R: A language and environment for statistical computing. R Foundation for Statistical Computing, Vienna, Austria. https://www.R-project.org/.

Rao, M. R. R. (1957). Acetic Acid Bacteria. *Annual Review of Microbiology*, *11*, 317–338.

Raspor, P., & Goranovic, D. (2008). Biotechnological Applications of Acetic Acid Bacteria. *Critical Reviews in Biotechnology*, *28*(2), 101–124.

Rentz, J. A., Kraiya, C., Luther III, G. W., & Emerson, D. (2007). Control of Ferrous Iron Oxidation within Circumneutral Microbial Iron Mats by Cellular Activity and Autocatalysis. *Environmental Science & Technology*, *41*(17), 6084–6089. http://doi.org/10.1021/es062203e

Rieder, J. P., Redente, E. F., Richard, C. E., & Paschke, M. W. (2013). An Approach to Restoration of Acidic Waste Rock at a High-Elevation Gold Mine in Colorado, USA. *Ecological Restoration*, *31*(3), 283–294.

Rimstidt, J. D., Chermak, J. A., & Gagen, P. M. (1994). Rates of reaction of galena, sphalerite, chalcopyrite, and arsenopyrite. In *Environmental Geochemistry of Sulfide Oxdiation* (pp. 2–13).

Robinson, D. G., Ehlers, U., Herken, R., Herrmann, B., Mayer, F., & Schurmann, F. W. (1987). Methods for SEM. In *Methods of Preparation for Electron Microscopy* (pp. 145–171). Springer.

Rojas-Chapana, J. A., & Tributsch, H. (2001). Biochemistry of sulfur extraction in bio-corrosion of pyrite by Thiobacillus ferrooxidans. *Hydrometallurgy*, *59*, 291–300.

Salek, S. S., Kleerebezem, R., Jonkers, H. M., Voncken, J. H. L., & Van Loosdrecht, M. C. M. (2013). Determining the impacts of fermentative bacteria on wollastonite dissolution kinetics. *Applied Microbiology and Biotechnology*, *97*(6), 2743–2752. http://doi.org/10.1007/s00253-012-4590-2

SanClements, M. D., Fernandez, I. J., & Norton, S. A. (2010). Phosphorus in Soils of Temperate Forests: Linkages to Acidity and Aluminum. *Soil Science of America Journal*, *74*(6), 2175–2186. http://doi.org/10.2136/sssaj2009.0267

Sand, W., Gehrke, T., Jozsa, P.-G., & Schippers, A. (2001). (Bio)chemistry of bacterial leaching - direct vs. indirect bioleaching. *Hydrometallurgy*, *59*, 159–175.

Santelli, C. M., Welch, S. a., Westrich, H. R., & Banfield, J. F. (2001). The effect of Fe-oxidizing bacteria on Fe-silicate mineral dissolution. *Chemical Geology*, *180*(1–4), 99–115. http://doi.org/10.1016/S0009-2541(01)00308-4

Schloss, P. D. (2009). Introducing mothur: Open-source, platform-independent, community-supported software for describing and comparing microbial communities. *Applied and Environmental Microbiology*, *75*(23), 7537–7541.

Schoonen, M., Elsetinow, A., Borda, M., & Strongin, D. (2000). Effect of temperature and illumination on pyrite oxidation between pH 2 and 6. *Geochemical Transactions*, *4*, 1–11. http://doi.org/10.1039/b004044o

Schrenk, M. O., Edwards, K. J., Goodman, R. M., Hamers, R. J., & Banfield, J. F. (1998). Distribution of Thiobacillus ferrooxidans and Leptospirillum ferrooxidans: Implications for Generation of Acid Mine Drainage. *Science*, *279*(5356), 1519–1522. http://doi.org/10.1126/science.279.5356.1519

Sibrell, P. L., Watten, B. J., Haines, T. A., & Spaulding, B. W. (2006). Limestone fluidized bed treatment of acid-impacted water at the Craig Brook National Fish Hatchery, Maine, USA. *Aquacultural Engineering*, *34*(2), 61–71. http://doi.org/10.1016/j.aquaeng.2005.05.003

Sickel, W., Grafe, T. U., Meuche, I., & Steffan-Dewenter, I. (2016). Bacterial Diversity and Community Structure in Two Bornean Nepenthes Species with Differences in Nitrogen Acquisition Strategies. *Microbial Ecology*, (71), 938–953. http://doi.org/10.1007/s00248-015-0723-3

Simpson, E. H. (1949). Measurement of diversity. *Nature*, *163*, 688.

Singer, P. C., & Stumm, W. (1970). Acid mine drainage-rate determining step. *Science*, *167*, 1121–1123.

Singer, P. C., & Stumm, W. (1968). Kinetics of the oxidation of ferrous iron. In *2nd Symp. Coal Mine Drainage Research* (pp. 12–34). National Coal Association/Bituminous Coal Research.

Solomon, M. (2008). Brine-pool deposition for the Zn-Pb-Cu massive sulphide deposits of the Bathurst mining camp, New Brunswick, Canada. II. Ocean anoxia during mineralisation. *Ore Geology Reviews*, *33*(3–4), 352–360. http://doi.org/10.1016/j.oregeorev.2007.04.002

Stevenson, R. J. (1997). Scale-dependent causal frameworks and the consequences of benthic algal hetrogeneity. *Journal of North American Benthological Society*, *16*, 248–262.

Stromberg, B., & Banwart, S. (1994). Kinetic modelling of geochemical processes at the Aitik mining waste rock site in northern Sweden. *Applied Geochemistry*, *9*(5), 583–595.

Stumm, W., & Morgan, J. J. (1981). *Aquatic Chemistry* (2nd Edition). New York: Wiley-Interscience.

Stuyfzand, P. J. (1999). Patterns in groundwater chemistry resulting from groundwater flow. *Hydrogeology Journal*, *7*(1), 15–27.

Sverdrup, H. U. (1990). *The Kinetics of Base Cation Release Due to Chemical Weathering*. Lund, Sweden: Lund University Press.

Szabó, K. É., Itor, P. O. B., Bertilsson, S., Tranvik, L., & Eiler, A. (2007). Importance of rare and abundant populations for the structure and functional potential of freshwater bacterial communities. *Aquatic Microbial Ecology*, *47*(1), 1–10.

Takabe, Y., Kameda, I., Suzuki, R., Nishimura, F., & Itoh, S. (2014). Changes of microbial substrate metabolic patterns through a wastewater reuse process, including WWTP and SAT concerning depth. *Water Research*, *60*, 105–17. http://doi.org/10.1016/j.watres.2014.04.036

Talling, J. F. (2010). Potassium - a non-limiting nutrient in fresh waters? *Freshwater Reviews*, *3*, 97–104.

Tan, G.-L., Shu, W.-S., Zhou, W.-H., Li, X.-L., Lan, C.-Y., & Huang, L.-N. (2009). Seasonal and spatial variations in microbial community structure and diversity in the acid stream draining across an ongoing surface mining site. *FEMS Microbiology Ecology*, *70*(2), 277–285. http://doi.org/10.1111/j.1574-6941.2009.00744.x

Temple, K. L., & Colmer, A. R. (1951). The Autotrophic Oxidation of Iron by a New Bacterium: Thiobaccilus Ferrooxidans. *Journal of Bacteriology*, *62*(5), 605–611.

Thomas, J. E., Skinner, W. M., & Smart, R. S. C. (2001). A mechanism to explain sudden changes in rates and products for pyrrhotitie dissolution in acid solution. *Geochimica et Cosmochimica Acta*, *65*(1), 1–12.

Tremblay, A., & Ransijn, J. (2015). LMERConvenienceFunctions: Model Selection and Post-hoc Analysis for (G)LMER Models. R package version 2.10. Https://CRAN.R-project.org/package=LMERConvenienceFunctions

Tributsch, H. (2001). Direct versus indirect bioleaching. *Hydrometallurgy*, *59*, 177–185.

Tu, B., Wang, F., Li, J., Sha, J., Lu, X., & Han, X. (2013). Analysis of Genes and Proteins in Acidithiobacillus ferrooxidans During Growth and Attachment on Pyrite Under Different Conditions. *Geomicrobiology Journal*, *30*(3), 255–267. http://doi.org/10.1080/01490451.2012.668608

Tyson, G. W., Lo, I., Baker, B. J., Allen, E. E., Hugenholtz, P., & Banfield, J. F. (2005). Genome-directed isolation of the key nitrogen fixer Leptospirillum ferrodiazotrophum sp. nov. from an acidophilic microbial community. *Applied and Environmental Microbiology*, *71*(10), 6319–6324. http://doi.org/10.1128/AEM.71.10.6319-6324.2005

Ullman, W. J., Kirchman, D. L., Welch, S. a., & Vandevivere, P. (1996). Laboratory evidence for microbially mediated silicate mineral dissolution in nature. *Chemical Geology*, *132*(1–4), 11–17. http://doi.org/10.1016/S0009-2541(96)00036-8

United States Geological Survey. (2018). USGS Current Water Conditions for the Nation.

Underwood, J. C., Harvey, R. W., Metge, D. W., Repert, D. A., Baumgartner, L. K., Smith, R. L., … Barber, L. B. (2011). Effects of the Antimicrobial Sulfamethoxazole on Groundwater Bacterial Enrichment. *Environmental Science & Technology*, *45*(3), 3096–3101.

Vargas, E., Gutierrez, S., Ambriz, M. E., & Cervantes, C. (1995). Chromosome-encoded inducible copper resistance in Pseudomonas strains. *Antonie van Leeuwenhoek*, *68*(3), 225–229.

Verhulst, Pierre-François. (1845). Recherches mathématiques sur la loi d'accroissement de la population [Mathematical Researches into the Law of Population Growth Increase]. *Nouveaux Mémoires de l'Académie Royale des Sciences et Belles-Lettres de Bruxelles*. 18, 1–42.

Viollier, E., Inglett, P. W., Hunter, K., Roychoudhury, a. N., & Van Cappellen, P. (2000). The ferrozine method revisited: Fe(II)/Fe(III) determination in natural waters. *Applied Geochemistry*, *15*(6), 785–790. http://doi.org/10.1016/S0883-2927(99)00097-9

Voisin, J., Cournoyer, B., & Mermillod-Blondin, F. (2016). Assessment of artificial substrates for evaluating groundwater microbial quality. *Ecological Indicators*, *71*(8), 577–586. http://doi.org/10.1016/j.ecolind.2016.07.035

Wakao, N., Yasuda, T., Jojima, Y., Yamanka, S., & Hiraishi, A. (2002). Enhanced Growth of Acidocella facilis and Related Acidophilic Bacteria at High Concentrations of Aluminum. *Microbes and Environment*, *17*(2), 98–104.

Walsh, F., & Mitchell, R. (1972). A pH-Dependent Succession of Iron Bacteria. *Environmental Science & Technology*, *6*(9), 809–812.

Weber, P. A., Thomas, J. E., Skinner, W. M., & Smart, R. S. C. (2005). A methodology to determine the acid-neutralization capacity of rock samples. *Canadian Mineralogist*, *43*, 1183–1192. http://doi.org/10.2113/gscanmin.43.4.1183

Weisener, C. G. (2002). *The reactivity of iron and zinc sulfide mineral surfaces: adsorption and dissolution mechanisms.* University of South Australia.

Weiss, J. V., Rentz, J. A., Plaia, T., Neubauer, S. C., Merrill-Floyd, M., Lilburn, T., … Emerson, D. (2007). Characterization of neutrophilic Fe (II)-oxidizing bacteria isolated from the rhizosphere of wetland plants and description of Ferritophicum radicicola gen. nov. sp. nov., and Sideroxydans paludicola sp. nov. *Geomicrobiology Journal*, *24*(7–8), 559–570.

Welch, S. A., & Banfield, J. F. (2002). Modification of olivine surface morphology and reactivity by microbial activity during chemical weathering. *Geochimica et Cosmochimica Acta*, *66*(2), 213–221. http://doi.org/10.1016/S0016-7037(01)00771-2

Whiting, M. (2011). Katahdin Iron Works and its Effect On the Water Quality of the West Branch of the Pleasant River. *Maine Department of Environmental Protection*, 1–23.

Williams, A. J., Alpers, C. N., Sumner, D. Y., & Campbell, K. M. (2016). Filamentous Hydrous Ferric Oxide Biosignatures in a Pipeline Carrying Acid Mine Drainage at Iron Mountain Mine, California. *Geomicrobiology Journal*, *34*(3), 193–206. http://doi.org/10.1080/01490451.2016.1155679

Williams, R. A. D., & Hoare, D. S. (1972). Physiology of a New Facultatively Autotrophic Thermophilic Thiobacillus. *Journal of General Microbiology*, *70*(May), 555–566.

Williamson, M. A., Kirby, C. S., & Rimstidt, J. D. (2006). Iron Dynamics in Acid Mine Drainage. *Industrial & Engineering Chemistry*, 2411–2423. Retrieved from http://pubs.acs.org/doi/abs/10.1021/ie50449a020

Winter, T. C., Harvey, J. W., Franke, O. L., & Alley, W. M. (1998). *Ground Water and Surface Water: A Single Resource*.

Winterbourn, M. J., Mcdiffett, W. F., & Eppley, S. J. (2000). Aluminium and iron burdens of aquatic biota in New Zealand streams contaminated by acid mine drainage : effects of trophic level. *The Science of the Total Environment*, *254*, 45–54.

Woods, D. E., & Sokol, P. A. (2006). The genus Burkholderia. In M. Dworkin, S. Falkow, E. Rosenberg, K. H. Schliefer, & E. Stackebrandt (Eds.), *The Prokaryotes - A Handbook on the Biology of Bacteria* (3rd Edition, pp. 848–860). New York, NY: Springer-Verlag.

Yan, X., & Su, X. G. (2009). *Linear Regression Analysis: Theory and Computing*. World Scientific Publishing.

Zhang, H., & Bloom, P. R. (1999). The pH Dependence of Hornblende Dissolution. *Soil Science*, *164*(9), 624–632. http://doi.org/10.1097/00010694-199909000-00002

Zhang, H., Bruns, M. A., & Logan, B. E. (2006). Biological hydrogen production by Clostridium acetobutylicum in an unsaturated flow reactor. *Water Research*, *40*(4), 728–734.

Zhang, P., Van Nostrand, J. D., He, Z., Chakraborty, R., Deng, Y., Curtis, D., Fields, M. W., Hazen, T. C., Arkin, A. P., & Zhou, J. (2015). A Slow-Release Substrate Stimulates Groundwater Microbial Communities for Long-Term in Situ Cr(VI) Reduction. *Environmental Science & Technology*, *49*, 12922–12931. http://doi.org/10.1021/acs.est.5b00024

APPENDIX A. ADDITIONAL EXPERIMENTAL DATA

Located in this appendix are complete additional chemical and biologic data sets for the experimental data. While most of the chemical data used in this thesis is mean data, the complete data for all experimental replicates can be found here. All biological data can be found online. The original metagenomic results within the NCBI database can be located using BioProject accession number PRJNA430708.

Experimental Data and Figures

Table 20. Experiment 1: October pH

Time (hrs)	0	4	24	48	72	96	120	144	168	192	216	240	264	288	312	336
Abiotic-1	4.24	4.22	4.42	4.53	4.84	4.92	5.08	5.2	5.34	5.54	5.91	6.38	6.82	6.69	6.74	6.53
AB-2	4.24	4.16	4.29	4.32	4.5	4.43	4.6	4.68	4.66	4.72	4.74	4.79	4.76	4.75	4.7	4.73
AB-3	4.24	4.21	4.31	4.41	4.51	4.61	4.66	4.71	4.77	4.82	4.88	4.91	4.88	4.88	4.87	4.89
AB-4	4.24	4.18	4.33	4.39	4.51	4.74	4.78	4.81	4.8	4.85	4.85	4.85	4.84	4.78	7.17	6.73
AB-5	4.24	4.13	4.21	4.25	4.55	4.56	4.59	4.6	4.6	4.68	4.71	4.27	4	3.53	3.39	3.28
AB-6	4.24	4.18	4.28	4.27	4.34	4.42	4.43	4.44	4.45	4.47	4.13	3.72	3.35	3.21	3.44	3.14
AB Mean	4.24	4.18	4.31	4.36	4.54	4.61	4.69	4.74	4.77	4.85	4.87	4.82	4.78	4.64	5.05	4.88
AB Std. Dev.	0	0.03	0.06	0.09	0.15	0.17	0.2	0.23	0.28	0.33	0.53	0.81	1.07	1.12	1.46	1.4
Biotic-1	4.79	4.69	4.58	4.54	4.42	4.57	4.49	4.48	4.54	4.63	4.66	4.62	4.56	4.54	4.54	4.46
B-2	4.79	4.75	4.73	4.49	4.44	4.48	4.45	4.24	3.76	3.46	3.36	3.27	3.21	3.14	3.13	3.09
B-3	4.79	4.77	4.68	4.43	4.34	4.39	4.26	3.88	3.48	3.28	3.21	3.11	3.06	3.01	2.98	2.99
B-4	4.79	4.74	4.66	4.41	4.31	4.34	4.22	4.02	3.63	3.36	3.13	2.95	2.85	2.78	2.74	2.68
B-5	4.79	4.65	4.59	4.42	4.29	4.34	4.25	4.16	3.92	3.68	3.37	3.19	3.09	3.02	2.99	3.03
B-6	4.79	4.74	4.7	4.52	4.4	4.46	4.35	4.08	3.64	3.49	3.4	3.28	3.22	3.18	3.18	3.19
B Mean	4.79	4.72	4.66	4.47	4.37	4.43	4.34	4.14	3.83	3.65	3.52	3.4	3.33	3.28	3.26	3.24
B Std. Dev.	0	0.04	0.05	0.05	0.06	0.08	0.1	0.19	0.34	0.45	0.52	0.55	0.56	0.58	0.59	0.57

Table 20 cont.

Time (hrs)	384	432	480	504	528	552	576	600	624	648	816	840
Abiotic-1	6.78	5.54	6.13	6.88	7.11	6.98	6.99	7.09	6.74	6.84	7.39	7.41
AB-2	4.46	4.43	4.49	4.53	4.68	4.91	4.94	5.02	5.01	5.05	4.81	4.91
AB-3	4.59	4.51	4.42	4.43	4.46	4.47	4.5	4.54	4.47	4.43	4.14	4.27
AB-4	6.57	6.69	6.23	6.42	6.26	6.39	6.28	6.25	6.16	6.1	6.1	6.07
AB-5	3.12	3.04	3	3.02	2.99	2.99	2.97	3	2.98	2.97	3.02	3.02
AB-6	2.9	2.81	2.79	2.78	2.77	2.77	2.76	2.76	2.75	2.77	2.72	2.73
AB Mean	4.74	4.5	4.51	4.68	4.71	4.75	4.74	4.78	4.68	4.69	4.7	4.73
AB Std. Dev.	1.51	1.35	1.34	1.54	1.58	1.57	1.56	1.57	1.48	1.5	1.65	1.64
Biotic-1	4.31	4.14	4.08	4.01	3.94	3.87	3.8	3.79	3.74	3.66	3.67	3.57
B-2	2.96	2.95	2.95	2.92	2.93	2.9	2.89	2.9	2.89	2.88	2.81	2.83
B-3	6.47	6.18	5.82	6.04	6.02	5.94	5.99	5.88	5.79	5.46	4.86	4.46
B-4	2.55	2.52	2.53	2.53	2.52	2.5	2.51	2.52	2.5	2.51	2.46	2.46
B-5	2.82	2.77	2.77	2.76	2.73	2.73	2.7	2.72	2.69	2.68	2.63	2.63
B-6	3.02	2.98	2.98	2.93	2.91	2.88	2.88	2.88	2.85	2.84	2.78	2.82
B Mean	3.69	3.59	3.52	3.53	3.51	3.47	3.46	3.45	3.41	3.34	3.2	3.13
B Std. Dev.	1.36	1.27	1.14	1.21	1.21	1.18	1.2	1.16	1.13	1.01	0.83	0.69

Table 21. Experiment 1: October Specific Conductance (µS/cm)

Time (hrs)	0	4	24	48	72	96	120	144	168	192	216	240	264	288	312	336	384	432	480
Abiotic-1	237	289	336	352	371	408	445	720	759	768	827	842	1928	1951	1931	1949	2030	2210	2200
AB-2	237	278	315	328	334	334	356	349	364	375	405	410	432	448	472	481	518	504	581
AB-3	237	269	311	328	334	333	338	345	347	350	355	354	372	383	397	423	429	441	456
AB-4	237	271	307	318	322	319	327	331	333	335	338	340	345	349	396	399	409	414	414
AB-5	237	269	312	325	323	323	327	328	331	332	335	347	370	447	501	560	607	612	656
AB-6	237	269	303	308	314	312	316	324	326	328	341	370	498	569	588	653	793	904	935
AB Mean	237	274	314	326	333	338	351	399	410	415	433	444	657	691	714	744	798	847	874
AB Std. Dev.	0	7.4	11	13	18	32	44	144	157	159	178	180	570	568	548	545	566	631	617
Biotic-1	213	247	292	311	320	1431	1441	1440	1436	1430	1436	1410	1428	1425	1435	1429	1444	1460	1447
B-2	213	253	298	321	332	352	395	415	463	549	598	665	700	752	816	862	916	979	993
B-3	213	250	298	314	319	333	340	369	440	509	523	652	701	745	779	816	256	268	272
B-4	213	260	309	326	337	339	347	365	407	477	582	740	922	1029	1142	1252	1393	1478	1532
B-5	213	244	288	306	316	339	328	334	352	393	471	566	615	675	724	773	852	921	969
B-6	213	252	299	315	327	328	336	353	405	446	471	529	557	577	610	630	671	733	754
B Mean	213	251	297	315	325	520	530	546	584	634	680	760	820	867	918	960	922	973	994
B Std. Dev.	0	5	6.5	6.5	7.5	407	408	401	383	359	341	298	294	285	283	283	409	418	423

Table 21 cont.

Time (hrs)	504	528	552	576	600	624	648	816	840
Abiotic-1	2190	2230	2310	2300	2300	2310	2290	2350	2310
AB-2	608	662	663	696	733	774	792	808	856
AB-3	460	468	475	480	487	496	507	526	536
AB-4	419	423	421	426	426	434	434	447	451
AB-5	716	763	759	796	806	804	818	852	842
AB-6	978	1024	1042	1053	1070	1075	1080	1136	1130
AB Mean	895	928	945	958	970	982	987	1020	1021
AB Std. Dev.	607	615	643	635	631	630	620	636	618
Biotic-1	1449	1453	1437	1448	1449	1447	1446	1445	1458
B-2	1007	1028	1048	1065	1083	1110	1119	1232	1208
B-3	291	326	328	332	339	346	356	377	379
B-4	1538	1172	1587	1600	1619	1629	1623	1700	1696
B-5	985	1015	1025	1042	1062	1086	1108	1215	1220
B-6	770	788	804	817	833	847	859	932	931
B Mean	1007	964	1038	1051	1064	1077	1085	1150	1149
B Std. Dev.	418	348	412	415	415	414	409	417	417

Table 22. Experiment 1: October Dissolved Oxygen Concentration (mg/L)

Time (hrs)	0	4	24	48	72	96	120	144	168	192	216	240	264	288	312	336	384	432	480
Abiotic-1	6.94	6.57	4.17	4.4	3.73	4.97	5	5.27	5.86	5.67	5.88	5.48	5.79	5.44	6.62	4.26	4.76	4.4	0.41
AB-2	6.94	5.4	4.39	5.62	5.46	5.06	3.47	5.68	3.58	5	5.79	5.2	5.29	4.05	6.68	5.28	4.94	4.94	4.4
AB-3	6.94	5.22	4.39	5.75	5.31	3.16	3.78	5.75	3.7	5.74	5.73	4.74	3.85	5.15	5.64	5.01	4.5	4.03	4.28
AB-4	6.94	5.64	4.22	5.62	4.26	4.66	4.92	4.07	5.19	5.46	5.72	4.11	3.21	3.76	4.58	4.98	5.06	4.75	5.1
AB-5	6.94	5.08	4.3	5.82	4.8	3.58	4.44	4.66	4.97	5.6	5.42	3.36	3.55	5.4	4.52	2.54	5.26	4.7	4.92
AB-6	6.94	5.26	4.33	5.64	5	4.19	4.47	4.97	5.08	5.55	4.77	1.92	0.2	4.86	4.6	4.85	4.65	5.06	5.13
AB Mean	6.94	5.53	4.3	5.47	4.76	4.27	4.35	5.07	4.73	5.5	5.55	4.14	3.65	4.78	5.44	4.49	4.86	4.65	4.04
AB Std. Dev.	0	0.5	0.08	0.49	0.6	0.7	0.56	0.58	0.82	0.24	0.38	1.21	1.8	0.65	0.94	0.92	0.25	0.34	1.66
Biotic-1	7.98	4.81	4.55	5.33	5.71	4.56	4.95	4.88	5.95	5.77	5.29	3.35	4.67	6.24	5.1	5.03	4.65	4.66	5.54
B-2	7.98	5.19	4.4	5.38	5.35	2.91	4.74	4.31	5.63	5.2	4.49	2.95	3.93	5.53	4.91	5.08	5.09	4.95	5.49
B-3	7.98	5.72	4.41	4.88	5.2	4.28	4.95	5.2	5.16	5.49	3.79	4.8	5.29	5.09	5.45	5.42	5.23	4.7	5.4
B-4	7.98	5.04	4.42	5.43	4.64	4.96	3.86	4.1	3.91	4.89	5.07	0.14	5.04	0.26	4.66	5.02	5.27	4.76	4.4
B-5	7.98	5.36	4.28	5.42	5.88	4.92	4.95	5.36	4.82	5.16	5.02	3.82	4.86	4.96	4.04	5.26	4.86	4.72	5.18
B-6	7.98	5.22	4.45	3.48	3.68	4.71	3.75	2.88	2.46	4.96	4.42	4.82	5.07	4.86	5.03	5.76	5.27	5.2	3.93
B Mean	7.98	5.22	4.42	4.99	5.08	4.39	4.53	4.45	4.65	5.24	4.68	3.31	4.81	4.49	4.86	5.26	5.06	4.83	4.98
B Std. Dev.	0	0.28	0.08	0.7	0.74	0.7	0.52	0.83	1.17	0.3	0.51	1.58	0.44	1.95	0.44	0.26	0.23	0.19	0.62

Table 22 cont.

Time (hrs)	504	528	552	576	600	624	648	816	840
Abiotic-1	4.86	5.79	6.19	5.75	6.36	5.78	5.38	5.41	5.83
AB-2	4.93	5.76	6.3	6.29	5.99	5.91	5.77	5.76	5.51
AB-3	5.2	6.78	6.5	5.87	5.72	6.1	6.01	6.19	5.98
AB-4	5.18	6.74	6.18	6.01	5.97	6.02	6.09	5.4	5.38
AB-5	5.75	6.36	6.34	6.32	5.38	5.99	6.31	6.19	4.9
AB-6	5.46	6.71	6.23	6.49	5.01	5.74	6.27	6.17	6.23
AB Mean	5.23	6.36	6.29	6.12	5.74	5.92	5.97	5.85	5.64
AB Std. Dev.	0.3	0.43	0.11	0.26	0.44	0.13	0.32	0.35	0.43
Biotic-1	4.83	6.67	6.05	5.93	4.8	5.36	6.03	4.99	6.52
B-2	5.62	6.62	6	6.31	5.33	5.79	5.5	6.15	6.35
B-3	5.25	6.39	5.98	6.65	5.6	5.84	6.17	6.19	6.45
B-4	4.41	6.07	6.23	6.48	4.75	5.75	6.99	5.47	6.41
B-5	5.48	6.84	6.07	6.46	6.04	5.36	6.08	6.21	6.33
B-6	5.43	6.82	5.05	6.44	6.24	6	5.67	5.15	5.79
B Mean	5.17	6.57	5.9	6.38	5.46	5.68	6.07	5.69	6.31
B Std. Dev.	0.42	0.27	0.39	0.22	0.57	0.24	0.47	0.51	0.24

Table 23. Experiment 2: December pH

Time (hrs)	0	4	24	48	72	96	120	144	168	192	216	240	264	288	312	336	360	384
Abiotic-1	4.96	4.9	5.19	5.3	5.79	6.03	5.48	5.88	5.73	5.88	5.84	4.48	4.61	4.54	4.64	4.88	5.04	5.11
AB-2	4.96	4.76	4.86	4.97	5.31	5.8	5.42	5.38	5.71	5.87	5.84	4.65	4.71	4.7	4.74	4.84	4.97	5.09
AB-3	4.96	4.75	4.82	4.78	5.29	5.31	5.36	5.26	5.24	5.29	5.2	4.79	4.88	4.88	4.85	4.79	4.81	4.83
AB-4	4.96	4.55	4.67	4.8	4.67	5.18	5.16	5.17	5.12	5.15	5.12	4.8	4.78	4.8	4.82	4.85	5.09	5.05
AB-5	4.96	5.36	5.3	5.29	5.52	5.64	5.56	5.46	5.45	5.49	5.46	4.75	4.64	4.62	4.64	4.47	4.64	4.7
AB-6	4.96	4.53	4.76	4.66	4.74	5.07	5	4.87	5.06	5.14	5.27	5.36	4.51	4.5	4.57	4.53	4.65	4.6
AB Mean	4.96	4.81	4.93	4.97	5.22	5.5	5.33	5.34	5.38	5.47	5.45	4.64	4.69	4.67	4.71	4.73	4.87	4.9
AB Std. Dev.	0	0.28	0.23	0.25	0.4	0.34	0.19	0.31	0.27	0.31	0.29	0.17	0.12	0.14	0.1	0.16	0.18	0.2
Biotic-1	5.52	5.61	5.41	5.19	5.17	5.33	5.24	5.13	5.2	5.14	4.96	4.38	4.32	4.37	4.38	3.94	4.31	4.38
B-2	5.52	5.62	5.3	5.05	4.89	5.07	5.06	4.89	4.83	4.81	4.71	4.35	4.34	4.3	4.29	3.85	4.18	4.19
B-3	5.52	5.61	5.32	4.91	4.79	4.93	4.92	4.85	4.76	4.72	4.65	4.38	4.26	4.3	4.26	3.78	4.14	4.2
B-4	5.52	5.6	5.15	5.65	4.59	4.67	4.68	4.7	4.53	4.55	4.45	4.23	4.14	4.16	4.13	3.67	4.03	4.06
B-5	5.52	5.51	5.09	4.75	4.86	4.75	4.69	4.58	4.46	4.43	4.33	4.14	4.06	4.08	4.07	3.61	3.94	3.99
B-6	5.52	5.6	5.2	4.81	4.67	4.85	4.87	4.79	4.73	4.72	4.61	4.38	4.28	4.29	4.27	3.8	4.14	4.15
B Mean	5.52	5.59	5.24	5.06	4.83	4.93	4.91	4.82	4.75	4.73	4.62	4.31	4.23	4.25	4.23	3.77	4.12	4.16
B Std. Dev.	0	0.04	0.11	0.3	0.18	0.22	0.2	0.17	0.24	0.22	0.2	0.09	0.1	0.1	0.1	0.11	0.12	0.12

Table 23 cont.

Time (hrs)	408	432	456	480	504	792	816	840
Abiotic-1	4.94	4.45	4.45	4.41	4.59	6.32	6.3	6.49
AB-2	5.36	5.25	5.27	5.12	5.14	5.77	5.91	5.96
AB-3	4.88	4.64	4.76	4.75	4.76	4.61	4.61	4.77
AB-4	5.02	4.82	4.91	4.9	486	4.59	4.54	4.61
AB-5	4.58	4.41	4.56	4.56	4.52	4.65	4.64	4.72
AB-6	4.52	4.3	4.43	4.42	4.42	4.65	4.61	4.63
AB Mean	4.88	4.64	4.73	4.69	4.71	5.1	5.1	5.2
AB Std. Dev.	0.28	0.32	0.29	0.26	0.24	0.69	0.72	0.74
Biotic-1	4.31	4.15	4.32	4.33	4.29	4.03	3.95	4
B-2	4.15	3.98	4.13	4.13	4.08	3.82	3.74	3.82
B-3	4.13	3.93	4.11	4.1	4.03	3.94	3.85	3.94
B-4	4.03	3.83	3.98	3.98	3.94	3.88	3.8	3.89
B-5	3.95	3.75	3.91	3.95	3.86	3.81	3.7	3.78
B-6	4.1	3.92	4.07	4.07	4.01	3.91	3.8	3.87
B Mean	4.11	3.93	4.09	4.09	4.03	3.9	3.81	3.88
B Std. Dev.	0.11	0.12	0.13	0.12	0.13	0.07	0.08	0.07

Table 24. Experiment 2: December Specific Conductance (µS/cm)

Time (hrs)	0	4	24	48	72	96	120	144	168	192	216	240	264	288	312	336	360	384
Abiotic-1	202	251	307	346	367	386	420	439	463	469	468	509	514	522	535	540	539	540
AB-2	202	242	290	308	342	364	372	361	383	387	390	405	411	416	419	420	424	430
AB-3	202	246	302	319	323	334	339	344	346	353	357	363	370	372	378	384	387	387
AB-4	202	237	274	294	293	293	296	297	302	304	306	308	324	316	318	318	389	391
AB-5	202	225	262	286	294	299	304	308	311	315	318	324	329	33	335	338	340	343
AB-6	202	240	273	282	283	286	288	290	293	309	313	324	325	325	327	327	328	331
AB Mean	202	240	285	306	317	327	336	340	350	356	359	372	379	381	385	388	401	404
AB Std. Dev.	0	8.1	16.3	22	30.1	37.7	47.1	51	59.1	58.2	56.9	69.1	68	71.7	75.3	76.7	69.5	69.1
Biotic-1	191.3	222	282	300	306	312	318	317	326	329	330	342	349	353	357	363	364	364
B-2	191.3	224	272	289	297	303	308	309	313	319	324	329	323	332	347	353	355	353
B-3	191.3	223	256	266	271	275	278	278	283	286	291	297	303	308	311	315	318	321
B-4	191.3	226	264	280	286	289	294	296	299	302	306	311	318	322	328	332	335	336
B-5	191.3	229	264	276	280	287	291	296	302	306	311	318	324	330	335	341	343	346
B-6	191.3	221	265	277	285	288	290	293	295	299	302	306	312	316	320	325	328	331
B Mean	191.3	224	267	281	287	292	296	298	303	307	311	317	321	327	333	338	340	342
B Std. Dev.	0	2.7	8.1	10.7	11.3	12	13	12.3	13.6	13.9	13.1	14.9	14.2	14.2	15.6	16.3	15.6	14.3

Table 24 cont.

Time (hrs)	408	432	456	480	504	792	816	840
Abiotic-1	567	583	592	627	615	628	642	643
AB-2	436	438	446	453	462	469	476	494
AB-3	394	400	404	406	408	429	432	438
AB-4	394	396	399	401	404	417	419	424
AB-5	346	349	353	356	358	365	366	372
AB-6	333	336	339	339	341	341	342	345
AB Mean	412	417	422	430	431	441	446	453
AB Std. Dev.	77.3	81.6	43.6	95.3	90.8	93.3	97.9	97.5
Biotic-1	368	371	372	373	377	404	411	418
B-2	361	365	367	370	373	404	410	414
B-3	325	327	330	332	335	352	355	362
B-4	339	342	344	347	347	364	366	372
B-5	348	351	354	355	358	381	384	388
B-6	332	335	338	339	342	361	365	371
B Mean	345	348	351	353	355	378	382	387
B Std. Dev.	15.3	15.7	15.1	15.1	15.5	20.5	22	2.16

Table 25. Experiment 2: December Dissolved Oxygen Concentration (mg/L)

Time (hrs)	0	4	24	48	72	96	120	144	168	192	216	240	264	288	312	360	384	408
Abiotic-1	8.85	6.29	6.42	6.61	6.42	7.04	6.5	6.47	6.19	6.1	6.49	6.11	6.32	6.22	6.18	6.76	7.3	6.62
AB-2	8.85	5.81	6.73	6.9	6.24	6.44	6.08	6.65	6.37	6.19	6.18	5.95	6.68	6.33	6.47	6.36	7.23	6.7
AB-3	8.85	5.69	6.73	6.84	6.19	7.45	6.44	6.27	6.43	6.25	6.03	6.05	6.7	4.81	6.25	6.74	6.84	5.06
AB-4	8.85	5.67	6.95	6.16	6.44	7.23	6.63	6.44	6.97	6.37	6.38	4.69	7.07	6.27	4.63	6.67	7.15	6.68
AB-5	8.85	5.61	6.71	6.36	6.2	7.01	5.92	6.32	6.04	5.75	6.75	6.07	6.69	6.05	5.75	6.73	6.12	6.61
AB-6	8.85	5.5	6.33	6.77	6.29	6.95	6.63	6.74	6.31	6.08	6.24	6.09	6.44	5.17	5.97	6.83	6.58	6.56
AB Mean	8.85	5.76	6.64	6.61	6.3	7.02	6.37	6.48	6.38	6.12	6.34	5.83	6.65	5.81	5.87	6.68	6.87	6.37
AB Std. Dev.	0	0.25	0.21	0.27	0.1	0.31	0.27	0.17	0.29	0.19	0.23	0.51	0.24	0.59	0.6	0.15	0.42	0.59
Biotic-1	11.34	5.3	6.73	6.94	6.48	6.65	6.42	6.61	6.11	6.63	5.96	5.66	7.21	5.85	4.98	6.92	5.58	6.47
B-2	11.34	5.43	6.73	6.46	6.83	6.78	6.69	6.42	5.89	6.45	6.53	6.07	4.87	6.08	4.55	7.17	6.32	6.54
B-3	11.34	6.17	7.2	6.49	6.81	7.09	7.05	6.62	6.19	6.49	6.64	6.09	7.75	6.58	5.38	4.91	6.6	6.36
B-4	11.34	6.1	7.64	5.99	6.64	6.08	6.74	6.57	6.07	4.41	6.76	6.43	7.22	5.49	6.41	6.37	6.45	6.62
B-5	11.34	6.47	6.54	6.28	6.65	6.89	7.09	6.69	6.27	6.23	6.47	6.41	6.93	6.35	6.27	6.93	6.85	6.49
B-6	11.34	6.61	7.21	6.22	6.01	6.78	6.65	6.48	5.99	6.62	6.1	5.11	7.02	6.39	6.21	6.46	6.75	6.38
B Mean	11.34	6.01	7.01	6.4	6.57	6.71	6.77	6.56	6.09	6.14	6.41	5.96	6.83	6.12	5.63	6.46	6.42	6.48
B Std. Dev.	0	0.49	0.38	0.29	0.28	0.31	0.23	0.09	0.12	0.78	0.29	0.46	0.92	0.37	0.71	0.75	0.42	0.09

Table 25 cont.

Time (hrs)	432	456	480	504	792	816	840
Abiotic-1	7.49	6.86	6.72	6.72	6.64	6.12	6.81
AB-2	7.26	6.88	6.36	6.42	6.12	6.15	6.16
AB-3	7.27	6.56	6.06	6.57	6.41	6.01	6.25
AB-4	7.19	6.61	5.95	6.83	6.45	6.61	6.56
AB-5	6.81	6.51	4.59	6.44	6.03	6.16	6.05
AB-6	7.16	6.44	6.49	6.3	6.39	6.79	6.02
AB Mean	7.2	6.64	6.03	6.55	6.34	6.31	6.31
AB Std. Dev.	0.2	0.17	0.69	0.18	0.21	0.29	0.29
Biotic-1	6.75	6.11	6.48	6.25	6.01	6.76	6.08
B-2	6.84	6.1	6.57	4.81	6.13	7.14	4.71
B-3	6.97	6.38	6.69	6.56	6.42	7.17	6.16
B-4	6.52	6.41	5.17	6.56	6.64	6.93	6.73
B-5	7.08	6.73	4.64	5.26	6.62	6.49	6.74
B-6	7.15	6.59	6.98	6.66	6.74	7.01	6.66
B Mean	6.88	6.39	6.09	6.02	6.43	6.92	6.18
B Std. Dev.	0.21	0.23	0.86	0.72	0.27	0.23	0.71

Table 26. Experiment 3: January pH

Time (hrs)	0	4	24	48	72	96	120	144	192	216	240	288	312	336	360	384	408
Abiotic-1	5.41	4.76	4.78	4.92	5.1	5.59	5.7	5.86	5.26	5.2	5.19	4.88	4.97	4.98	4.92	5.56	5.58
AB-2	5.41	5.18	5	5.13	5.23	5.53	5.55	5.84	5.34	5.09	4.88	4.8	4.81	4.8	4.79	4.88	5.13
AB-3	5.41	4.69	4.72	4.89	5.11	5.29	5.42	5.53	5.31	5.07	4.81	4.78	4.87	4.89	4.93	5.06	5.69
AB-4	5.41	5.63	6.14	5.95	5.84	5.9	5.97	6.13	5.83	5.61	5.6	5.56	5.41	5.46	5.41	5.47	5.79
AB-5	5.41	4.79	4.71	4.84	5.13	5.24	5.53	5.16	5.33	5.13	4.93	4.9	4.89	4.99	4.91	4.91	5
AB-6	5.41	4.72	4.6	4.67	5.05	5	5.05	5.06	5	5.07	4.77	4.68	4.72	4.62	4.61	4.72	4.79
AB Mean	5.41	4.96	4.99	5.07	5.24	5.42	5.37	5.6	5.34	5.19	5.03	4.93	4.94	4.96	4.93	5.1	5.33
AB Std. Dev.	0	0.34	0.53	0.42	0.27	0.29	0.28	0.39	0.25	0.19	0.29	0.29	0.22	0.26	0.24	0.31	0.38
Biotic-1	5.45	5.39	5.63	5.7	5.65	5.61	5.56	5.5	5.51	5.31	5.13	5.12	5.06	5.07	4.91	4.95	4.91
B-2	5.45	4.82	4.76	4.85	4.84	4.82	4.87	4.74	4.62	4.6	4.5	4.45	4.45	4.36	4.39	4.4	4.41
B-3	5.45	5.69	6.07	6.08	5.8	5.76	5.48	5.45	5.42	5.36	5.27	5.25	5.28	5.35	5.27	5.24	5.33
B-4	5.45	4.83	4.76	4.79	4.72	4.67	4.67	4.53	4.4	4.4	4.24	4.22	4.21	4.13	4.17	4.19	4.18
B-5	5.45	5.26	4.89	4.91	4.89	4.88	4.79	4.64	4.45	4.47	4.29	4.36	4.25	4.15	4.19	4.17	4.18
B-6	5.45	5..16	4.88	4.94	4.87	4.79	4.76	4.56	4.48	4.51	4.27	4.29	4.26	4.16	4.16	4.17	4.17
B Mean	5.45	5.19	5.16	5.21	5.13	5.09	5.02	4.9	4.81	4.77	4.62	4.61	4.58	4.54	4.51	4.52	4.53
B Std. Dev.	0	0.31	0.5	0.49	0.43	0.43	0.36	0.41	0.47	0.4	0.42	0.41	0.43	0.49	0.43	0.42	0.44

Table 26 cont.

Time (hrs)	432	456	480	504	576	624	672	720	768	792	816	840
Abiotic-1	5.43	5.54	5.45	5.55	5.38	5.55	5.39	5.37	5.42	5.35	5.24	5.33
AB-2	5.25	5.3	5.04	5.02	5.08	5.29	5.29	5.26	5.32	5.21	5.2	5.24
AB-3	5.62	5.52	5.16	5.09	5.16	5.33	5.36	5.1	5.33	5.2	5.19	5.24
AB-4	5.74	5.63	5.45	5.35	5.38	5.41	5.46	5.42	5.49	5.43	5.39	5.45
AB-5	5.01	5.12	5.18	5.15	4.82	4.96	5	4.98	5.01	4.99	4.94	4.99
AB-6	4.82	4.81	4.7	4.78	4.72	4.73	4.68	4.73	4.8	4.81	4.76	4.71
AB Mean	5.31	5.32	5.16	5.16	5.09	5.21	5.2	5.14	5.23	5.16	5.12	5.16
AB Std. Dev.	0.32	0.28	0.26	0.24	0.25	0.28	0.27	0.24	0.24	0.21	0.21	0.24
Biotic-1	4.86	4.91	4.88	4.83	4.75	4.78	4.65	4.74	4.64	4.75	4.53	4.66
B-2	4.41	4.38	4.34	4.35	4.26	4.29	4.26	4.19	4.11	4.16	4.05	4.05
B-3	5.18	5.04	5.04	5.04	5.18	5.19	5.02	4.85	4.86	4.79	4.75	4.77
B-4	4.17	4.12	4.1	4.09	3.97	4.02	3.94	3.87	3.77	3.8	3.74	3.65
B-5	4.18	4.14	4.09	4.1	3.97	3.96	3.87	3.85	3.79	3.75	3.68	3.59
B-6	4.16	4.12	4.08	4.09	3.96	3.98	3.93	3.89	3.79	3.82	3.75	3.69
B Mean	4.49	4.45	4.42	4.42	4.35	4.37	4.28	4.23	4.16	4.18	4.08	4.07
B Std. Dev.	0.39	0.38	0.39	0.38	0.47	0.46	0.43	0.42	0.44	0.44	0.42	0.48

Table 27. Experiment 3: January Specific Conductance (µS/cm)

Time (hrs)	0	4	24	48	72	96	120	144	192	216	240	288	312	336	360	384	408
Abiotic-1	163	203	297	330	359	425	448	481	502	717	745	769	781	785	776	789	798
AB-2	163	194.7	246	270	283	290	296	303	313	330	341	355	365	378	385	390	394
AB-3	163	199	243	258	270	274	279	281	287	302	309	322	326	330	332	336	336
AB-4	163	193.8	237	255	263	269	273	278	281	293	299	305	307	311	313	317	319
AB-5	163	196.2	235	247	253	257	262	264	269	272	278	287	294	296	299	302	304
AB-6	163	197.2	239	251	257	261	263	266	269	275	280	283	285	287	289	290	293
AB Mean	163	197.3	249	268	281	296	303	312	320	365	375	387	393	398	399	404	407
AB Std. Dev.	0	3	21.6	28.4	36.3	58.6	65.6	76.6	82.6	158.7	166.6	172.6	175.4	175.6	171.4	175.1	177.7
Biotic-1	139.2	174.3	220	236	245	250	254	257	261	267	270	280	280	287	290	291	295
B-2	139.2	178.2	231	249	261	268	274	278	283	290	294	300	303	306	309	312	315
B-3	139.2	167.3	218	234	246	253	257	261	265	272	275	278	280	282	283	286	288
B-4	139.2	178.3	218	233	239	244	248	251	255	261	263	271	274	276	279	283	285
B-5	139.2	177.7	225	241	249	254	259	262	266	273	275	283	285	288	290	293	296
B-6	139.2	174.6	219	234	242	248	253	257	261	267	271	276	278	282	285	294	296
B Mean	139.2	175.1	222	238	247	253	257	261	265	272	275	281	283	287	289	293	296
B Std. Dev.	0	3.8	4.7	5.6	7	7.5	8.1	8.4	8.7	9.1	9.5	9.1	9.4	9.4	9.6	9.3	9.5

Table 27 cont.

Time (hrs)	432	456	480	504	576	624	672	720	768	792	816	840
Abiotic-1	793	809	820	811	787	827	874	873	835	859	907	1077
AB-2	407	415	429	443	455	464	475	486	496	503	513	532
AB-3	342	345	355	361	365	368	373	378	384	388	393	401
AB-4	322	324	327	329	332	335	337	339	341	342	345	347
AB-5	308	311	314	317	320	325	327	331	333	335	336	338
AB-6	296	298	301	303	306	309	312	315	318	319	321	323
AB Mean	411	417	424	427	427	438	450	454	451	458	469	503
AB Std. Dev.	174.4	179.3	181.8	177.6	168	181.2	197.2	195.8	181.5	189.6	206	266
Biotic-1	297	301	304	305	310	314	314	317	320	330	331	335
B-2	318	320	322	325	332	336	338	342	347	351	354	357
B-3	290	294	294	297	303	303	305	307	310	313	313	316
B-4	288	291	293	296	304	310	318	323	332	336	343	347
B-5	298	300	303	305	314	321	329	336	341	346	353	361
B-6	299	301	304	307	315	319	325	329	336	338	342	344
B Mean	298	301	303	306	313	317	321	326	331	336	339	343
B Std. Dev.	9.7	9.2	9.5	9.5	9.6	10.3	10.7	11.7	12.5	12.2	14.1	14.9

Table 28. Experiment 3: January Dissolved Oxygen Concentration (mg/L)

Time (hrs)	0	4	24	48	72	96	120	144	192	216	240	288	312	336	360	384	408
Abiotic-1	8.1	7.44	7.73	7	7.62	8.72	7.18	6.69	7.48	6.9	6.81	6.46	6.88	7.29	6.21	6.71	7.27
AB-2	8.1	7.23	7.44	7.92	6.77	8.45	6.56	8.16	7.75	6.84	6.84	7.02	6.96	7.14	6.86	7.15	5.73
AB-3	8.1	6.97	7.44	7.55	6.95	8.07	7.05	7.04	7.65	6.74	6.71	7.24	7.23	7.29	7.43	7.24	7.27
AB-4	8.1	6.19	6	6.91	7..16	7.69	6.96	7.21	7.42	6.59	6.74	7.15	7.19	7.04	7.26	7.48	5.57
AB-5	8.1	7.09	7.06	6.87	7.14	7.62	6.87	7.57	7.35	6.8	6.99	6.96	7.29	6.99	7.05	7.18	7.14
AB-6	8.1	5.69	6.71	6.76	6.66	7.34	6.72	7.55	7.56	7.16	6.6	7.17	7	6.45	7.68	7.11	7.1
AB Mean	8.1	6.77	7.06	7.17	7.05	7.98	6.89	7.37	7.53	6.84	6.78	7	7.09	7.03	7.08	7.14	6.68
AB Std. Dev.	0	0.62	0.57	0.42	0.31	0.48	0.21	0.46	0.14	0.17	0.12	0.26	0.15	0.28	0.47	0.23	0.73
Biotic-1	9.57	7.19	6.86	7.26	6.76	6.64	6.92	7.81	5.92	6.51	6.95	7.61	6.51	7.08	7.04	7.72	5.46
B-2	9.57	6.41	7.49	6.8	5.79	7.05	6.72	7.3	7.31	6.8	6.56	7.22	6.43	6.97	7.05	7.67	5.94
B-3	9.57	7.85	7.37	7.33	7.07	7.34	6.94	7.24	7.85	7.2	6.71	7.98	6.57	7.45	7.72	7.59	7.35
B-4	9.57	7.13	7.41	6.69	7.23	7.75	6.91	7.47	7.8	6.93	6.45	7.75	6.64	7.09	7.62	7.44	7.5
B-5	9.57	7.21	7.8	8.27	7.46	7.89	7.11	7.4	7.55	7.19	6.53	7.84	6.17	7.27	7.67	7.27	7.33
B-6	9.57	7.37	7.4	8.16	5.95	8.11	7.12	7.19	7.93	6.88	4.85	7.4	7.09	6.96	7.83	7.4	7.42
B Mean	9.57	7.19	7.39	7.42	6.71	7.46	6.95	7.4	7.39	6.92	6.34	7.63	6.57	7.14	7.49	7.51	6.83
B Std. Dev.	0	0.42	0.28	0.61	0.63	0.51	0.14	0.21	0.69	0.24	0.69	0.26	0.28	0.17	0.32	0.16	0.82

Table 28 cont.

Time (hrs)	432	456	480	504	576	624	672	720	768	792	816	840
Abiotic-1	7.79	6.95	6.99	8.41	8.2	7.53	6.57	8.36	6.63	7.44	6.2	6.1
AB-2	7.53	7.28	7.28	7.21	7.93	8.46	6.78	8.21	6.65	8	6.88	6.4
AB-3	7.67	7.41	7.28	7.67	8.15	7.65	6.97	8.34	6.87	8.11	6.76	6.68
AB-4	7.35	7.52	7.34	6.64	7.86	7.59	6.97	8.39	6.94	7.45	6.9	6.78
AB-5	7.46	7.71	6.35	7.63	8.15	8.34	6.84	8.35	7.16	5.74	7.06	7.17
AB-6	6.97	7.56	6.38	6.96	8.04	8.08	6.93	8.41	6.68	6.35	7.18	7.48
AB Mean	7.46	7.4	6.94	7.42	8.05	7.94	6.84	8.34	6.82	7.18	6.83	6.77
AB Std. Dev.	0.26	0.24	0.42	0.57	0.12	0.37	0.14	0.06	0.19	0.86	0.31	0.46
Biotic-1	7.39	8.01	7.35	7.05	6.8	7.88	6.11	7.83	6.86	7.73	7.09	7.78
B-2	6.28	7.78	5.86	6.94	7.89	8.4	7.27	7.82	7.13	7.3	6.85	7.56
B-3	7.31	8	7.61	6.1	7.81	8.11	7.67	8.64	7.19	7.6	7.27	7.98
B-4	7.04	7.37	6.78	6.37	7.39	8.05	7.9	8.63	7.11	7.78	6.56	7.73
B-5	7.05	7.99	6.66	7.18	7.9	8.1	7.42	7.83	7.52	7.85	7.48	7.71
B-6	6.58	7.37	7.59	6.93	7.65	7.98	7.42	8.63	7.53	7.28	7.7	7.52
B Mean	6.94	7.75	6.97	6.76	7.57	8.09	7.3	8.23	8.22	7.59	7.16	7.71
B Std. Dev.	0.39	0.28	0.62	0.39	0.39	0.16	0.57	0.4	0.24	0.22	0.38	0.15

Table 29. Experiment 1: October Metal Concentrations (mg/L)

Time (hrs)	Ca	K	Mg	P	Al	B	Cu	Fe	Mn	Na	S	Zn
Abiotic 0	16.2	1.51	16.2	<0.100	2.78	<0.03	0.023	<0.1	0.597	2.91	27.6	0.085
AB 336	44.3	4.09	15.8	0.427	2.34	0.068	0.144	3.12	0.678	5.26	55.2	0.293
AB 840	44.1	15.7	16.3	0.113	2.27	0.349	0.894	40.5	0.76	4.09	106	0.331
Biotic 0	16.2	1.51	16.2	<0.100	2.78	<0.03	0.023	<0.1	0.597	2.91	27.6	0.085
B 4	27.2	5.02	18.4	0.446	2.89	0.043	0.091	3.78	0.676	7.71	46.2	0.286
B 24	33.8	1.77	14.4	0.579	1.72	<0.03	0.103	3.93	0.599	6.76	46.1	0.216

Table 30. Experiment 2: December Metal Concentrations (mg/L)

Time (hrs)	Ca	K	Mg	P	Al	B	Cu	Fe	Mn	Na	S	Zn
Abiotic 0	14.2	1.23	12.3	<0.100	2.08	<0.03	<0.020	3.90	0.554	2.57	26.3	0.104
AB 4	22.2	4.23	14.2	0.472	0.589	<0.03	0.07	0.74	0.65	7.66	36.4	0.228
AB 24	33.8	8.59	13.4	0.172	0.875	<0.03	0.064	2.76	0.66	6.43	41.4	0.251
AB 168	45.7	10.2	14	0.134	1.11	<0.03	0.075	2.66	0.69	6.73	51.3	0.422
AB 336	39.7	31	14.6	0.432	1.31	0.061	0.091	9.33	0.661	5.42	48.9	0.164
AB 504	43	8.68	14.4	0.846	0.387	<0.03	0.105	1.78	0.653	8.35	51.3	0.151
AB 840	38.5	13.4	13.8	0.199	0.724	<0.03	0.098	2.92	0.636	6.28	46.6	0.159
Biotic 0	14.2	1.23	12.3	<0.100	2.08	<0.03	<0.02	3.90	0.554	2.57	26.3	0.104
B 4	19.5	<1	13.3	0.557	0.664	<0.03	0.034	2.06	0.61	6.71	32.9	0.175
B 24	30.4	1.09	12.7	0.693	1.25	<0.03	0.069	3.22	0.579	5.45	39.1	0.189
B 168	33.9	3.08	12.9	0.351	1.42	<0.03	0.089	1.96	0.586	6.23	41.5	0.111
B 336	38.3	2	13.7	0.186	1.53	<0.03	0.151	3.03	0.68	4.19	47.4	0.151
B 504	40.5	5.39	13.9	<0.1	1.58	<0.03	0.191	3.34	1.132	3.83	50.9	0.737
B 840	40.8	2.92	13.4	0.412	1.8	<0.03	0.218	7.06	0.842	3.44	50.6	0.334

Table 31. Experiment 3: January Metal Concentrations (mg/L)

Time (hrs)	Ca	K		Mg	P	Al	B	Cu	Fe	Mn	Na	S	Zn
Abiotic 0	9.58	1.33		8.71	<0.1	1.09	<0.03	<0.020	2.79	0.409	2.52	19.4	0.05
AB 4	18.3	6.48		9.13	0.119	0.812	0.076	0.051	4.21	0.424	4.65	26.3	0.122
AB 24	30.3	6.51		8.81	<0.1	0.526	0.037	0.04	3.62	0.47	3.54	34.1	0.151
AB 168	39.1	9		9.33	<0.1	1.08	0.044	0.054	5.33	0.52	3.4	40.6	0.136
AB 336	42.1	15.2		9.11	<0.1	0.293	0.035	0.025	2.94	0.672	3.38	40.6	0.092
AB 504	36.9	16		8.91	0.11	0.528	0.037	0.05	3.92	0.507	3.75	38.8	0.149
AB 840	37.9	13.7		9.09	<0.1	1.37	0.041	0.093	5.56	0.498	3.41	40.8	0.179
Biotic 0	9.58	1.33		8.71	<0.1	1.09	<0.03	<0.020	2.79	0.409	2.52	19.4	0.05
B 4	19.1	<1		8.51	<0.1	0.957	<0.03	<0.02	3.4	0.427	2.31	25	0.074
B 24	31.1	<1		8.63	<0.1	1.16	<0.03	0.038	4.62	0.44	1.85	34.3	0.116
B 168	41.5	1.86		8.6	0.153	2.1	<0.03	0.05	10.8	0.194	2.2	37.3	0.063
B 336	37.2	3.14		8.9	0.044	1.11	<0.03	0.076	3.8	0.452	2.16	39.5	0.129
B 504	38.6	4.67		8.73	0.114	2.01	<0.03	0.131	2.77	0.464	2.66	41.5	0.127
B 840	38	7.12		8.61	0.184	2.04	<0.03	0.227	6.81	0.491	2.55	43.5	0.171

Table 32. Experimental Mean Sulfate Concentrations (mmol/L)

	Time (hrs)	0	4	24	168	336	504	840
Abiotic	Exp. 1: Oct. '15	1.193	4.518	5.003	4.823	7.986	6.42	6.395
	Exp. 2: Dec. '15	1.226	3.033	3.834	5.177	5.892	5.308	6.277
	Exp. 3: Jan. '16	0.789	1.566	2.132	2.318	2.716	2.797	2.424
Biotic	Exp. 1: Oct. '15	1.193	4.239	5.078	5.615	8.838	7.029	7.477
	Exp. 2: Dec. '15	1.226	2.977	3.48	4.481	5.034	5.27	5.382
	Exp. 3: Jan. '16	0.789	1.411	2.175	2.094	2.194	2.144	2.356

Table 33. Complete Frame Count Data

	Exp 1 Start	*Exp 1 End*	*Exp 2 Start*	*Exp 2 End*	*Exp 3 Start*	*Exp 3 End*
Frame Counts	36	112	15	57	10	19
	42	97	35	64	37	56
	87	189	48	28	6	63
	54	215	5	49	49	69
	25	178	39	85	26	86
	41	254	35	100	26	48
	47	133	28	67	10	39
	32	126	26	54	23	62
	19	164	31	43	27	115
	56	195	18	89	33	74
Mean Count per Frame	43.9	166.3	28	63.6	24.7	63.1
Standard Deviation	18.19	46.93	11.96	21.17	12.67	24.85
Cells per mL of initial water sample	$2.27x10^5$	$8.59x10^5$	$1.28x10^5$	$3.26x10^5$	$1.45x10^5$	$3.29x10^5$

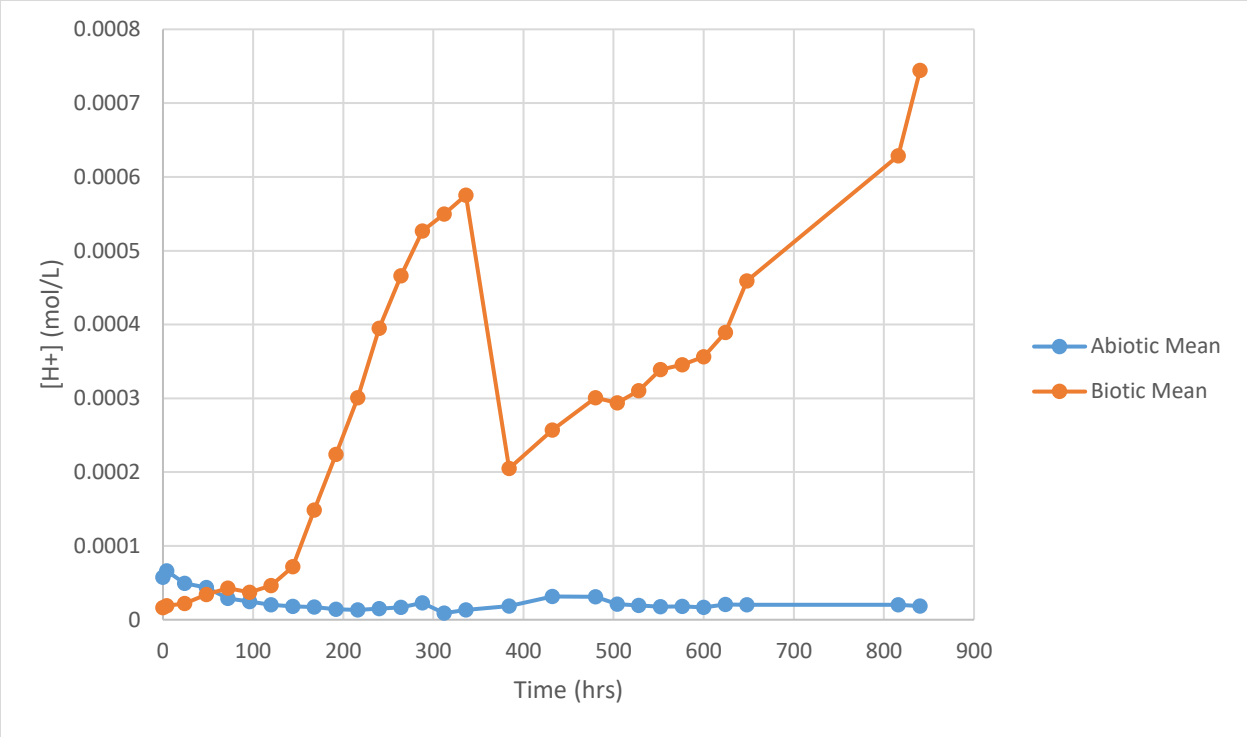

Figure 28. Experiment 1 Mean [H+] (mol/L). There is a clear disparity between the abiotic and biotic treatments. The jump down at 400 hours is due to one replicate that was unlike the others.

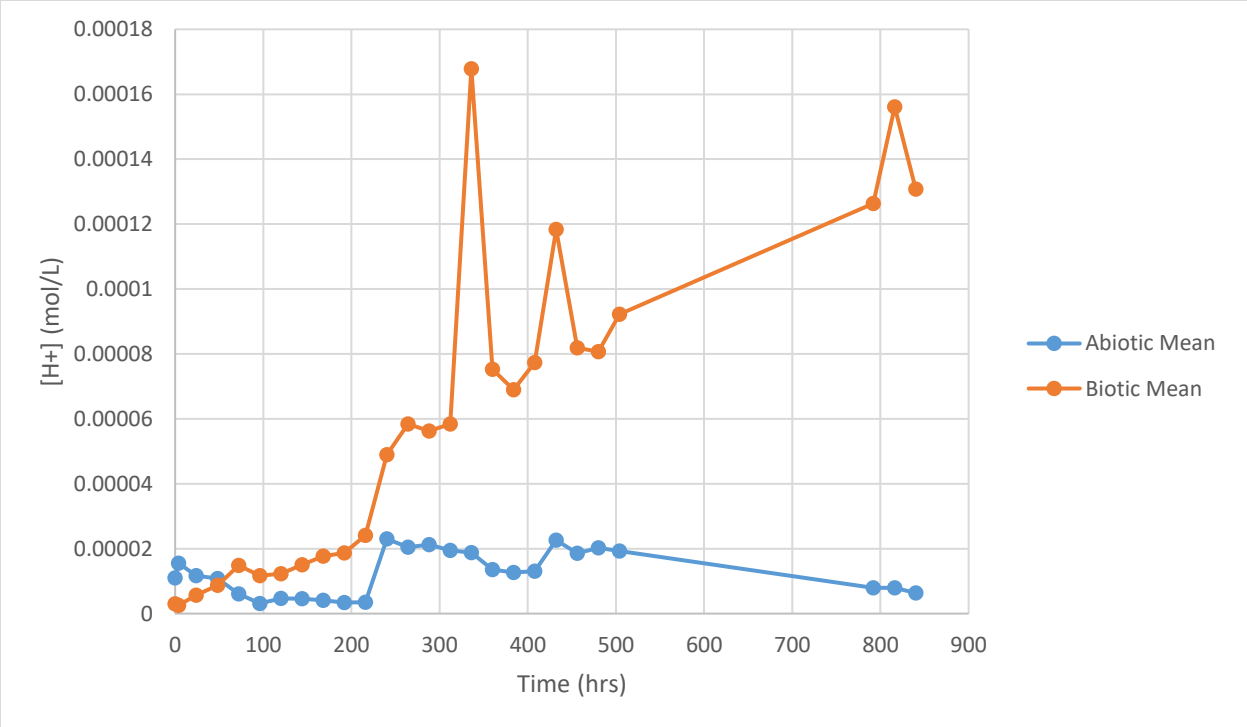

Figure 29. Experiment 2 Mean [H+] (mol/L). There is a clear disparity between the trends in the abiotic and biotic treatments. Single abnormal measurements account for the random biotic spikes.

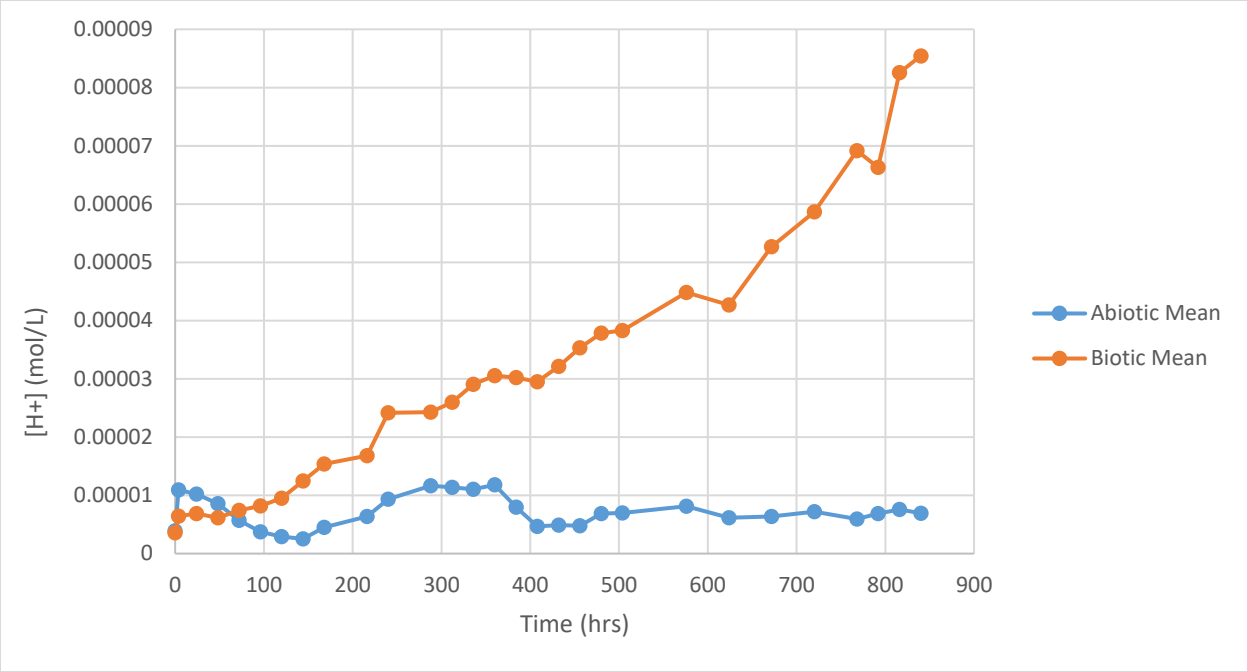

Figure 30. Experiment 3 Mean [H+] (mol/L). There is a clear disparity between abiotic and biotic trends. This biotic trend increases more steadily and linearly than Experiments 1 and 2.

Additional SEM Photos

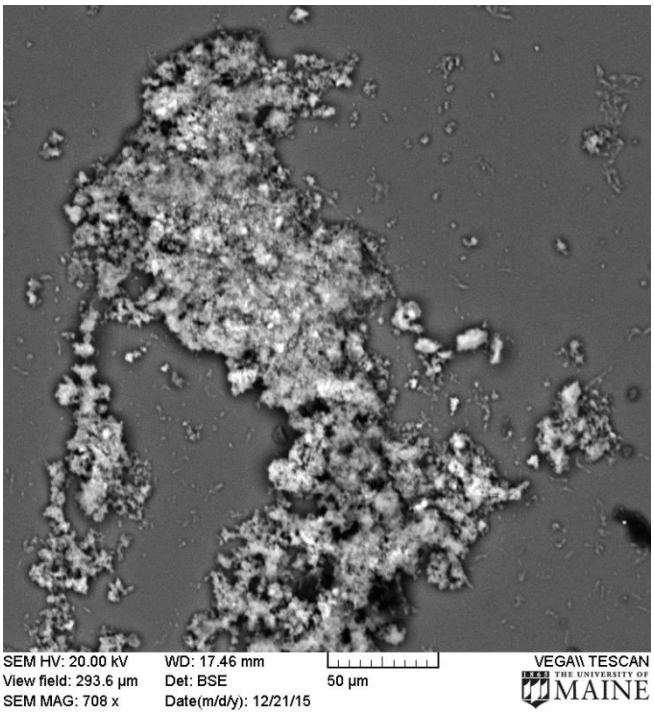

Figure 31. Abiotic Precipitate. Photographed in high vacuum conditions. Body structure is an amorphous mass.

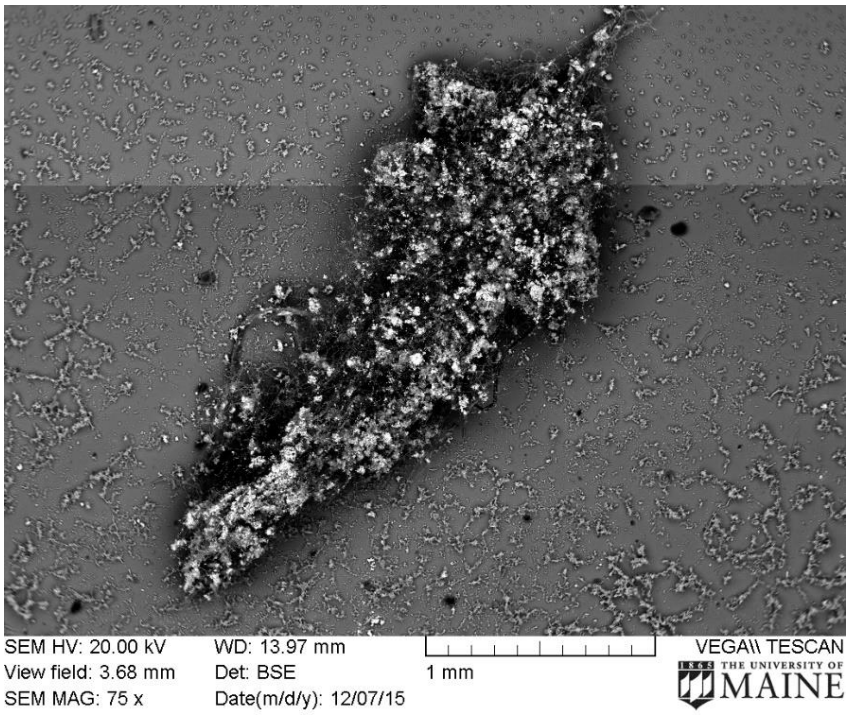

Figure 32. First Biotic Precipitate. Photographed in high vacuum conditions. This precipitate is approximately 3.5 mm in length.

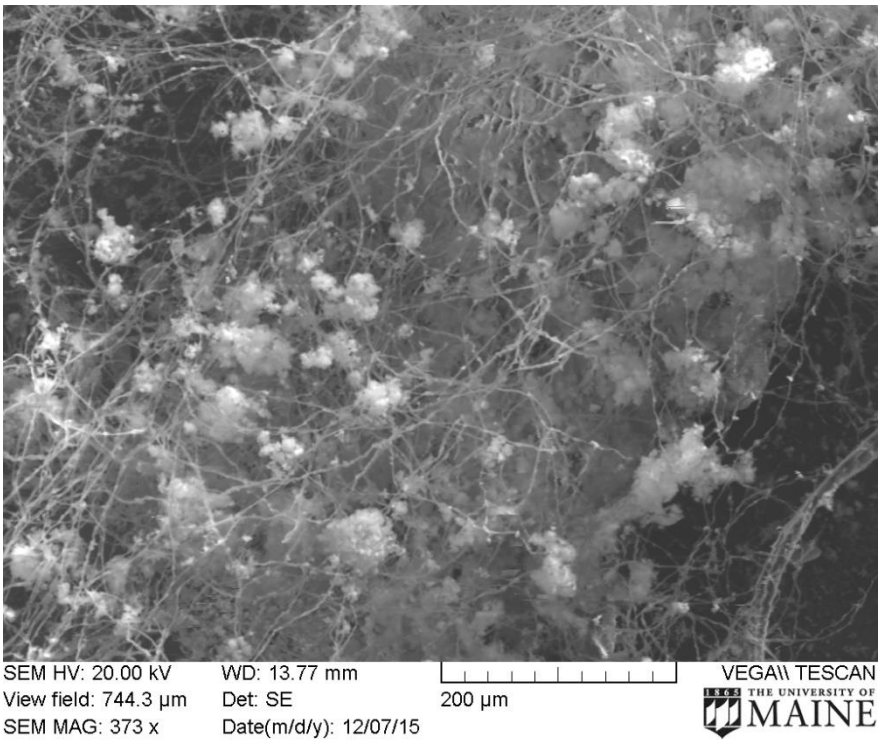

Figure 33. Filamentous Structure (First Biotic Precipitate). Photographed in high vacuum conditions. The body of this precipitate is composed of filaments suspending amorphous masses.

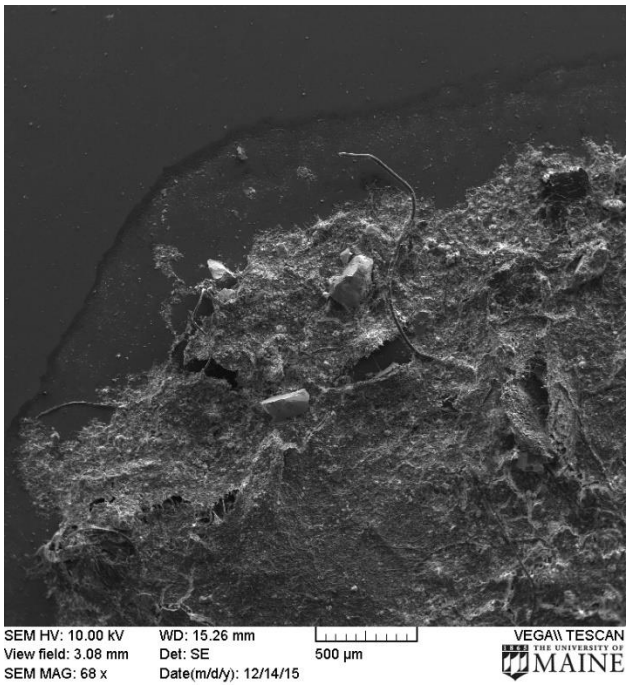

Figure 34. Second Biotic Precipitate. Photographed in high vacuum conditions. This precipitate is also a fibrous mass. Filaments and stalks were denser than the other biotic precipitate.

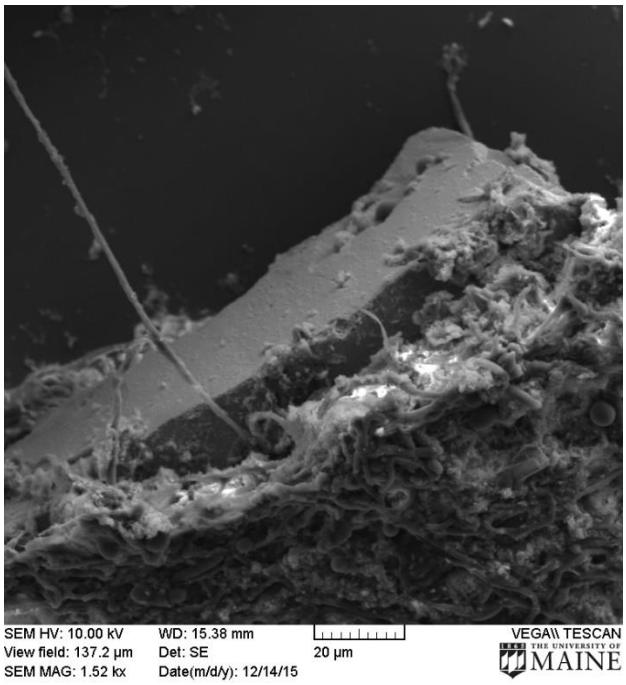

Figure 35. Pyrite Grain (Second Biotic Precipitate). Photographed in high vacuum conditions. The grain was suspended in a mass of filaments and was approximately 100 microns across.

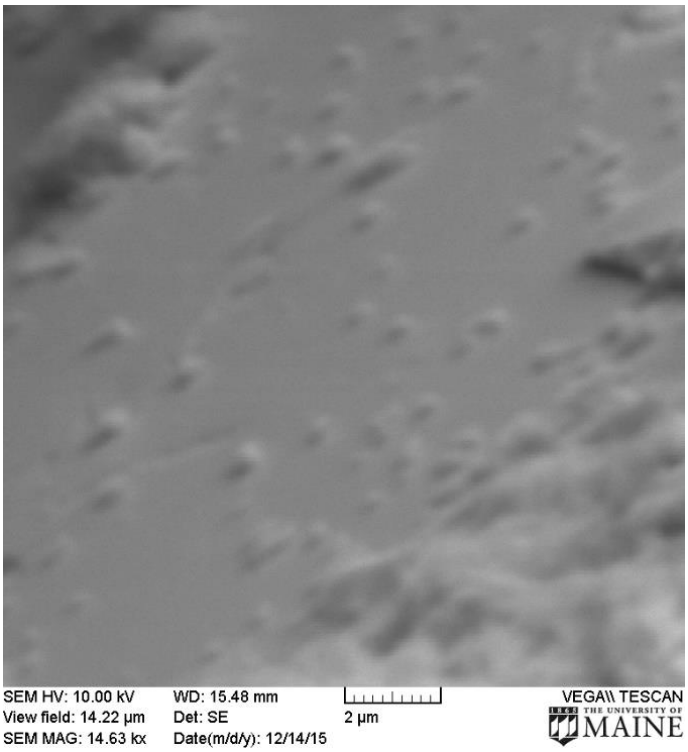

Figure 36. Pyrite Grain Surface. Photographed in high vacuum conditions. No bacteria appear to be attached to the pyrite surface.

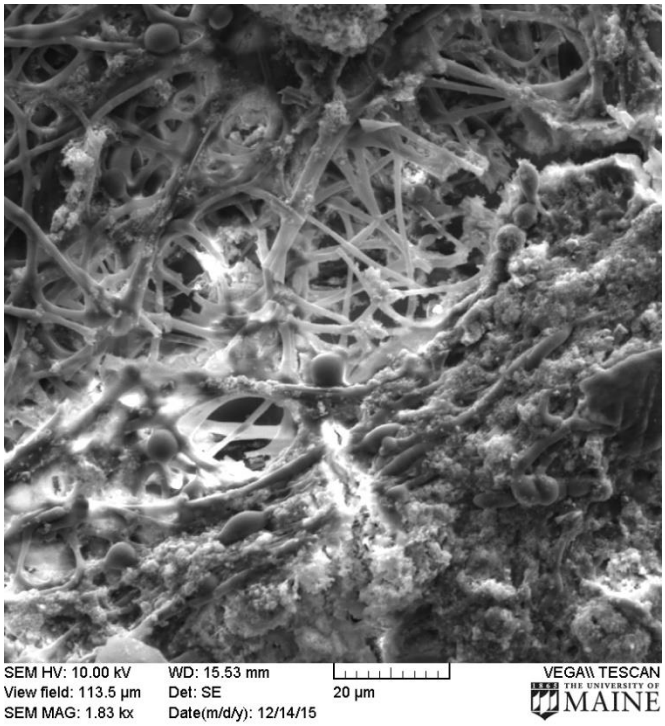

Figure 37. Fibrous Precipitate Body (Second Biotic Precipitate). Photographed in high vacuum conditions. Stalks ranged 2-5 microns in diameter.

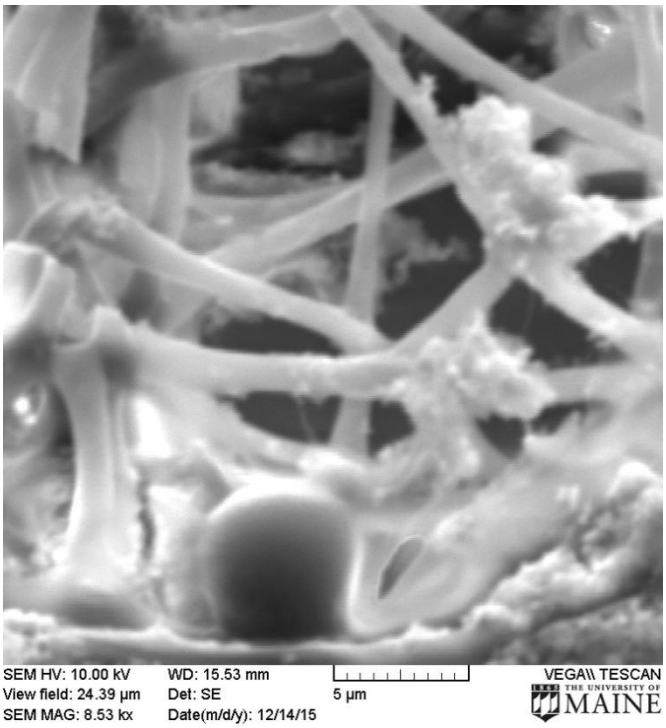

Figure 38. Magnified Precipitate Fiber Structures. Photographed in high vacuum conditions. Amorphous masses can be seen attached to stalks even at this small a scale.

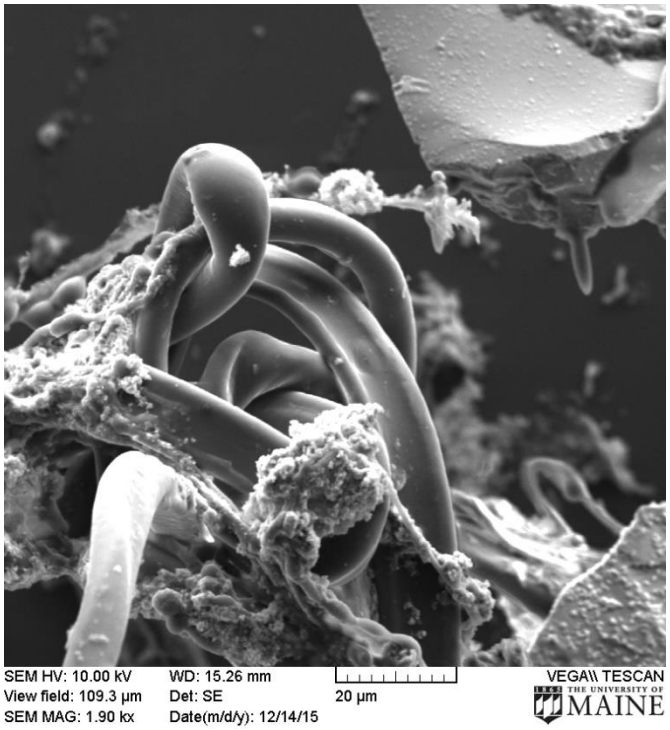

Figure 39. Unknown Structure (Second Biotic Precipitate). Photographed at high vacuum conditions. The structure was abnormal compared to the rest of the precipitate.

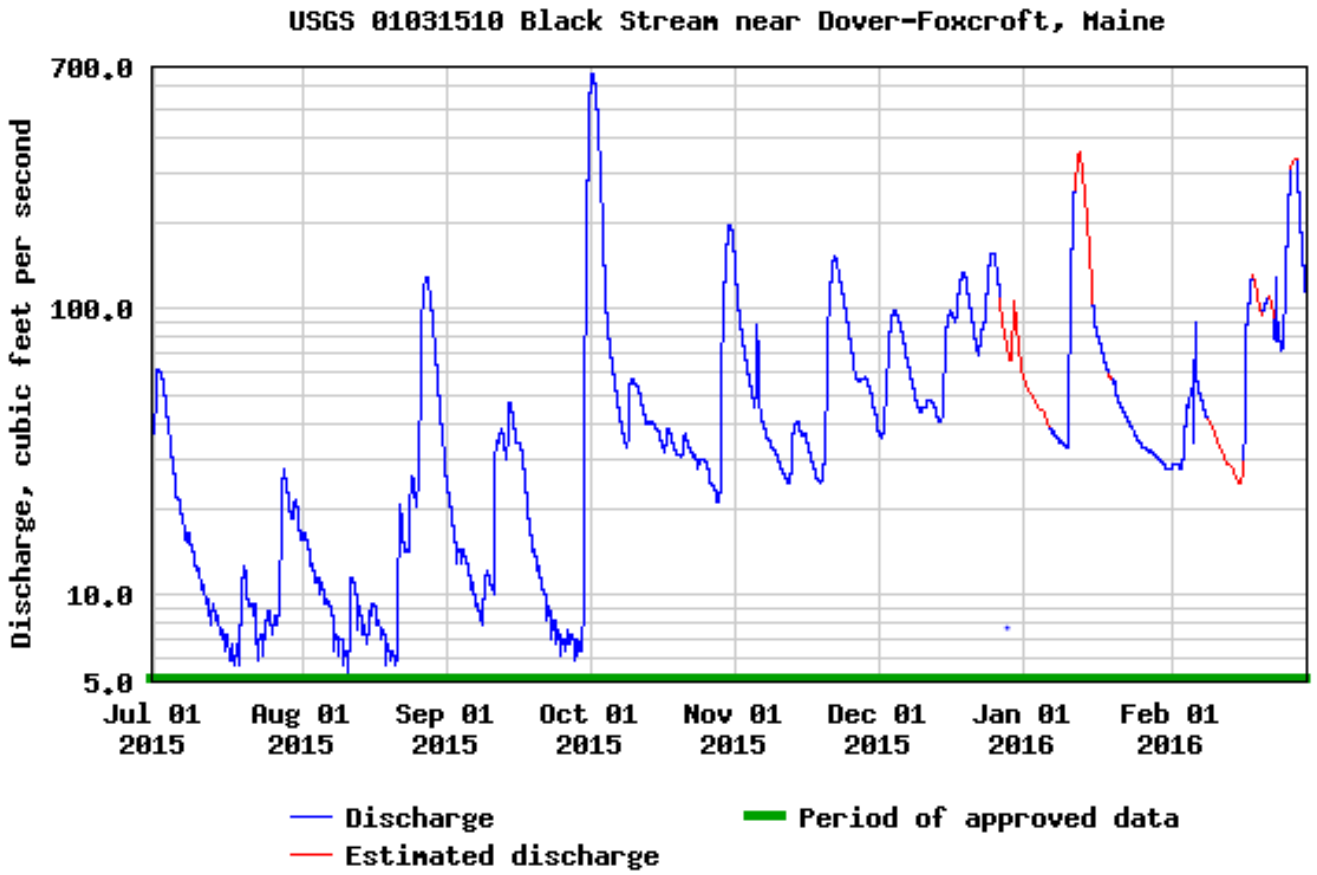

Figure 40. Black Stream Discharge (ft^3/s) (USGS). Hydrograph from Black Stream used to assist in hydrologic flow analyses for Blood Brook. This hydrograph spans the entire study period (July '15 – February '16).

APPENDIX B. CALLAHAN MINE DATA

In this appendix, one can find data pertaining to a water sample collected from Callahan Mine, located in Harborside, Maine. Similar tests were run on this water sample as described in the methods of Chapters 2 and 3, and it was also used in an experiment with the same methods as described as Chapter 3. The original intention was to perform a series of experiments like those conducted for Blood Brook, however, due to Callahan being a Superfund site, access was by permission only. Ultimately, I was only allowed to be given one sample collected from a well that gave access to groundwater beneath the tailings pile of the mine. This water was partially remediated through the addition of organic calcium carbonate shells, such as those of lobsters, clams, and oysters. Data collected from this experiment is presented here as reference for anyone looking to continue work with Callahan water.

Experimental Data

Table 34. Callahan Experiment pH

Time (hrs)	0	4	24	48	72	96	120	144	168	192	216	240	264	288	312	336
Abiotic-1	8.21	8.19	8.28	8.18	8.18	8.23	8.28	8.34	8.3	8.39	8.32	8.44	8.32	8.34	8.45	8.36
AB-2	8.21	8.16	8.32	8.22	8.15	8.29	8.33	8.38	8.31	8.4	8.43	7.73	8.37	8.31	8.44	8.42
AB-3	8.21	8.31	8.4	8.23	8.2	8.3	8.35	8.39	8.36	8.36	8.46	8.31	8.31	8.62	8.64	8.58
AB-4	8.21	8.24	8.41	8.23	8.17	8.32	8.37	8.43	8.35	8.41	8.32	8.36	8.32	8.41	8.49	8.43
AB-5	8.21	8.25	8.4	8.24	8.15	8.26	8.27	8.4	8.35	8.42	8.41	7.76	8.57	8.6	8.61	8.73
AB-6	8.21	8.27	8.44	8.21	8.17	8.31	8.34	8.4	8.38	8.4	8.45	8.34	8.18	8.41	8.5	8.54
AB Mean	8.21	8.24	8.37	8.22	8.17	8.28	8.32	8.39	8.34	8.4	8.4	8.16	8.34	8.45	8.52	8.51
AB Std. Dev.	0	0.05	0.06	0.02	0.02	0.03	0.04	0.03	0.03	0.02	0.06	0.29	0.12	0.12	0.08	0.12
Biotic-1	7.02	7.85	8.34	8.42	8.31	8.33	8.31	8	8.02	8.34	8.38	8.35	8.37	8.37	8.4	8.38
B-2	7.02	7.91	8.41	8.47	8.14	8.2	8.42	8.34	8.38	8.51	8.54	8.53	8.52	8.53	8.57	8.55
B-3	7.02	7.92	8.34	8.46	8.47	8.32	8.1	8.19	8.32	8.29	8.38	8.35	8.37	8.34	8.45	8.5
B-4	7.02	7.88	8.44	8.43	7.85	8.31	8.33	8.2	8.39	8.51	8.58	8.56	8.51	8.43	8.57	8.63
B-5	7.02	7.82	8.36	8.41	8.43	8.41	7.95	8.25	8.19	8.33	8.38	8.46	8.43	8.47	8.54	8.61
B-6	7.02	7.84	8.4	8.44	8.47	8.24	8.34	8.26	8.19	8.34	8.43	8.52	8.49	8.5	8.59	8.62
B Mean	7.02	7.87	8.38	8.44	8.28	8.3	8.24	8.23	8.25	8.39	8.45	8.46	8.45	8.44	8.52	8.55
B Std. Dev.	0	0.04	0.04	0.02	0.22	0.07	0.16	0.11	0.13	0.09	0.08	0.08	0.06	0.07	0.07	0.09

Table 34 cont.

Time (hrs)	384	432	480	504	528	552	576	600	624	648	816	840	864	888	912	936	960
Abiotic-1	8.12	8.29	8.29	8.27	8.16	8.24	8.17	8.22	8.21	8.09	8.21	8.2	8.19	7.99	8.12	8.2	8.12
AB-2	8.37	8.39	8.39	8.31	8.3	8.32	8.27	8.34	8.31	8.22	8.31	8.24	8.26	8.1	8.08	8.16	8.21
AB-3	8.71	8.72	8.7	8.67	8.65	8.66	8.64	8.69	8.67	8.59	8.69	8.66	8.65	8.46	8.58	8.62	8.56
AB-4	8.52	8.5	8.44	8.41	8.43	8.42	8.43	8.52	8.42	8.4	8.47	8.43	8.45	8.34	8.39	8.46	8.49
AB-5	8.74	8.74	8.72	8.66	8.69	8.67	8.66	8.69	8.69	8.6	8.7	8.66	8.68	8.48	8.6	8.62	8.63
AB-6	8.5	8.53	8.48	8.5	8.51	8.48	8.46	8.52	8.53	8.41	8.58	8.48	8.52	8.35	8.42	8.53	8.55
AB Mean	8.49	8.53	8.5	8.47	8.46	8.46	8.44	8.5	8.47	8.38	8.49	8.44	8.46	8.29	8.36	8.43	8.43
AB Std. Dev.	0.21	0.16	0.16	0.16	0.19	0.16	0.18	0.17	0.18	0.18	0.18	0.18	0.18	0.18	0.2	0.19	0.19
Biotic-1	8.52	8.45	8.44	8.42	8.43	8.44	8.44	8.47	8.48	8.41	8.48	8.49	8.48	8.31	8.41	8.47	8.48
B-2	8.59	8.67	8.61	8.51	8.57	8.58	8.55	8.58	8.59	8.54	8.63	8.59	8.58	8.4	8.51	8.55	8.57
B-3	8.51	8.51	8.46	8.44	8.43	8.44	8.43	8.44	8.46	8.42	8.45	8.54	8.6	8.3	8.42	8.61	8.53
B-4	8.64	8.7	8.64	8.58	8.59	8.6	8.57	8.6	8.55	8.53	8.65	8.56	8.49	8.4	8.46	8.59	8.52
B-5	8.55	8.65	8.66	8.54	8.57	8.56	8..53	8.58	8.59	8.52	8.44	8.53	8.56	8.29	8.49	8.61	8.56
B-6	8.65	8.66	8.62	8.58	8.59	8.59	8.58	8.61	8.62	8.54	8.62	8.49	8.59	8.26	8.48	8.55	8.49
B Mean	8.58	8.61	8.57	8.51	8.53	8.53	8.52	8.55	8.55	8.49	8.54	8.53	8.55	8.33	8.46	8.56	8.52
B Std. Dev.	0.05	0.09	0.09	0.06	0.07	0.07	0.06	0.07	0.06	0.06	0.09	0.04	0.05	0.05	0.04	0.05	0.03

Table 34 cont.

Time (hrs)	984	1032	1056	1104	1200	1296	1344
Abiotic-1	8.26	8.13	8.18	8.22	8.2	8.09	8.08
AB-2	8.24	8.23	8.19	8.2	8.2	8.24	8.1
AB-3	8.6	8.63	8.62	8.5	8.52	8.31	8.24
AB-4	8.49	8.51	8.54	8.41	8.42	8.38	8.43
AB-5	8.64	8.64	8.59	8.56	8.58	8.36	8.35
AB-6	8.53	8.58	8.55	8.47	8.51	8.47	8.41
AB Mean	8.46	8.45	8.44	8.39	8.4	8.31	8.27
AB Std. Dev.	0.16	0.2	0.19	0.14	0.15	0.12	0.14
Biotic-1	8.51	8.51	8.51	8.48	8.49	8.48	8.46
B-2	8.58	8.6	8.56	8.56	8.58	8.58	8.55
B-3	8.58	8.59	8.5	8.51	8.52	8.52	8.53
B-4	8.57	8.53	8.51	8.58	8.59	8.6	8.58
B-5	8.58	8.52	8.47	8.53	8.52	8.53	8.5
B-6	8.54	8.55	8.55	8.42	8.58	8.58	8.56
B Mean	8.56	8.55	8.52	8.51	8.55	8.55	8.53
B Std. Dev.	0.03	0.03	0.03	0.05	0.04	0.04	0.04

Table 35. Callahan Experiment Specific Conductance (µS/cm)

Time (hrs)	0	4	24	48	72	96	120	144	168	192	216	240	264	288	312	336
Abiotic-1	2410	2440	2430	2450	2440	2410	2420	2380	2380	2380	2360	2370	2320	2270	2190	2210
AB-2	2410	2400	2410	2410	2420	2390	2390	2390	2390	2380	2370	2390	2330	2290	2250	2230
AB-3	2410	2440	2440	2450	2450	2420	2430	2420	2430	2420	2420	2440	2430	2440	2400	2390
AB-4	2410	2430	2430	2430	2460	2430	2440	2430	2440	2430	2430	2430	2340	2330	2260	2270
AB-5	2410	3030	3030	3020	3040	2990	2990	2980	2970	2960	2950	2980	2940	2940	2910	2900
AB-6	2410	2440	2440	2450	2460	2420	2430	2430	2430	2440	2440	2440	2450	2390	2320	2310
AB Mean	2410	2530	2530	2535	2545	2510	2517	2505	2507	2502	2495	2508	2468	2443	2388	2385
AB Std. Dev.	0	224	224	217	222	215	212	213	208	206	206	213	217	229	242	238
Biotic-1	2440	2450	2470	2460	2480	2410	2390	2400	2400	2350	2270	2280	2260	2230	2220	2210
B-2	2440	2450	2430	2430	2490	2460	2390	2310	2260	2250	2260	2260	2260	2270	2240	2240
B-3	2440	2450	2440	2440	2470	2420	2430	2430	2330	461	481	510	534	568	574	585
B-4	2440	2450	2440	2440	2480	2440	2400	2290	2260	2270	2240	2220	2220	2200	2170	2160
B-5	2440	2470	2460	2470	2480	2420	2420	2410	2370	2320	2270	2260	2260	2270	2250	2240
B-6	2440	2440	2430	2430	2460	2430	2410	2370	2350	2260	2240	2240	2230	2240	2220	2220
B Mean	2440	2452	2445	2445	2477	2430	2407	2368	2328	1985	1960	1962	1961	1963	1946	1942
B Std. Dev.	0	9	15	15	9.4	16.3	14.9	51.8	52.7	683	662	649	638	624	614	608

Table 35 cont.

Time (hrs)	384	432	480	504	528	552	576	600	624	648	816	840	864	888	912	936	960
Abiotic-1	2210	2200	2170	2170	2160	2140	2090	2110	2120	2080	2120	2090	2090	2040	2050	2050	1996
AB-2	2240	2230	2220	2220	2220	2210	2200	2210	2210	2210	2240	2220	2220	2130	2210	2200	2210
AB-3	2410	2410	2410	2380	2380	2350	2390	2380	2390	2370	2390	2380	2380	2380	2370	2370	2370
AB-4	2280	2280	2250	2250	2260	2260	2270	2270	2280	2280	2300	2300	2290	2290	2300	2300	2300
AB-5	2920	2900	2900	2880	2870	2870	2860	2860	2860	2830	2850	2850	2820	2810	2810	2800	2810
AB-6	2310	2310	2300	2310	2320	2320	2320	2320	2330	2330	2350	2350	2350	2360	2360	2370	2370
AB Mean	2395	2388	2375	2368	2368	2358	2355	2358	2365	2350	2375	2365	2358	2335	2350	2348	2343
AB Std. Dev.	243	238	246	238	235	239	245	240	238	234	229	237	227	245	232	230	245
Biotic-1	2250	2250	2270	2290	2300	2310	2300	2340	2320	2320	2350	2360	2350	2350	2370	2380	2380
B-2	2270	2270	2280	2290	2290	2290	2300	2300	2310	2310	2340	2340	2340	2350	2360	2360	2370
B-3	615	639	663	676	680	692	712	731	740	761	791	800	825	849	874	891	906
B-4	2180	2160	2150	2160	2160	2130	2120	2100	2110	2090	2100	2100	2090	2080	2070	2080	2070
B-5	2260	2250	2300	2280	2310	2320	2290	2280	2330	2320	1876	227	261	284	305	325	369
B-6	2240	2260	2260	2240	2260	2270	2270	2270	2280	2280	2290	2290	2270	2250	2250	2220	2210
B Mean	1969	1971	1987	1989	2000	2002	1999	2003	2015	2013	1958	1686	1689	1694	1705	1709	1717
B Std. Dev.	606	597	594	589	592	589	579	574	575	566	548	850	831	819	812	802	786

Table 35 cont.

Time (hrs)	984	1032	1056	1104	1200	1296	1344
Abiotic-1	1952	1891	1895	1922	1842	2910	2940
AB-2	2200	2210	2200	2220	2220	2250	2280
AB-3	2370	2370	2370	2370	2370	2280	2310
AB-4	2290	2300	2310	2310	2320	2370	2360
AB-5	2740	2790	2780	2790	2780	2720	2720
AB-6	2370	2390	2390	2400	2410	2420	2420
AB Mean	2320	2325	2324	2335	2324	2491	2505
AB Std. Dev.	235	266	263	257	277	242	242
Biotic-1	2390	2400	2400	2460	2470	2500	2520
B-2	2370	2380	2380	2420	2450	2490	2510
B-3	926	941	956	979	1004	1030	1044
B-4	2050	2060	2060	2060	2080	2090	2090
B-5	378	410	437	457	506	531	555
B-6	2190	2190	2170	2160	2160	2180	2180
B Mean	1717	1730	1734	1756	1778	1803	1816
B Std. Dev.	778	770	758	762	751	753	750

Table 36. Callahan Experiment Dissolve Oxygen Concentration (mg/L)

Time (hrs)	0	4	24	48	72	96	120	144	168	192	216	240	264	288	312	336
Abiotic-1	4.91	5.3	4.66	4.87	4.43	5.41	5.1	4.52	5.01	5.49	3.25	3.19	4.89	4.36	4.53	5.22
AB-2	4.91	5.16	4.84	4.94	4.56	4.98	4.83	5.05	4.83	5.31	4.71	1.18	4.82	3.42	5.15	5.98
AB-3	4.91	4.98	3.46	5.21	4.69	4.95	5.11	5	5.08	5.3	5.11	4.15	5.19	5.07	4.68	5.23
AB-4	4.91	4.16	4.57	4.92	4.89	4.95	4.71	3.83	5.15	2.94	4.41	2.87	5.05	5.53	3.67	5.05
AB-5	4.91	4.24	4.48	5.22	4.64	4.79	4.71	4.72	4.65	4.57	4.78	0.65	4	5.27	4.88	4.86
AB-6	4.91	4.55	4.52	4.61	5.44	4.86	5.07	3.9	5.56	5.18	4.88	0.55	5.61	5.52	5.09	4.95
AB Mean	4.91	4.73	4.42	4.96	4.77	4.99	4.92	4.5	5.05	4.8	4.52	2.1	4.93	4.86	4.67	5.21
AB Std. Dev.	0	0.44	0.45	0.21	0.33	0.2	0.18	0.48	0.28	0.88	0.61	1.37	0.49	0.75	0.5	0.37
Biotic-1	2.43	4.85	4.78	5.34	5.96	5.33	3.34	4.3	1.04	3.91	4.85	4.65	3.64	5.58	4.84	5.13
B-2	2.43	4.85	4.55	4.53	3.01	2.14	4.64	4.74	4.74	5.08	5.19	4.99	4.81	5.22	5.22	5.24
B-3	2.43	4.27	4.26	5.29	5.31	3.6	2.77	4.15	5.32	5.48	5.22	5.95	3.62	4.53	5.06	4.99
B-4	2.43	4.86	4.59	4.63	0.59	0.17	3.76	5.06	5.42	5.46	4.89	4.7	4.98	5.17	5.26	5.24
B-5	2.43	4.32	4.59	5.05	4.34	4.35	0.29	4.35	3.62	5.33	4.54	3.47	5.86	5.11	5.48	5.06
B-6	2.43	4.86	4.44	4.76	4.08	3.084	3.68	4.1	4.33	5.14	3.18	5.3	4.66	5.22	5.06	5.14
B Mean	2.43	4.67	4.53	4.93	3.88	3.24	3.08	4.45	4.08	5.07	4.64	4.84	4.43	5.14	5.15	5.13
B Std. Dev.	0	0.26	0.16	0.31	1.74	1.67	1.37	0.34	1.49	0.54	0.69	0.75	0.57	0.31	0.2	0.09

Table 36 cont.

Time (hrs)	384	432	480	504	528	552	576	600	624	648	816	840	864	888	912	936	960
Abiotic-1	5.19	4.75	5.35	5.74	7.14	6.1	6.49	6.05	5.45	6.35	6.39	6.74	7.37	6.72	6.83	6.24	6.76
AB-2	5.01	5.62	5.36	5.998	7.25	6.1	5.72	6.07	6.23	6.68	4.72	6.91	7.41	7.23	7.06	7.03	7.04
AB-3	5.45	4.52	5.43	6.05	7.2	4.15	6.62	5.37	5.85	6.34	6.05	6.07	6.93	6.81	7.23	6.37	6.85
AB-4	5.17	4.72	5.3	5.87	7.35	5.4	6.75	6.05	6.47	4.27	6.17	5.99	7	6.4	6.78	6.81	6.73
AB-5	5.24	4.72	5.27	5.87	7.07	5.83	5.77	5.41	5.92	6.06	6.26	6.56	7.41	6.61	6.58	7.07	6.55
AB-6	5.26	4.8	5.11	5.79	6.55	6.11	6.31	6.06	6.19	6.85	6.34	6.61	7.66	6.51	6.57	6.84	6.66
AB Mean	5.22	4.85	5.3	5.88	7.09	5.61	6.28	5.83	6.02	6.09	5.99	6.48	7.3	6.71	6.84	6.73	6.76
AB Std. Dev.	0.13	0.35	0.1	0.11	0.26	0.7	0.4	0.31	0.33	0.85	0.58	0.34	0.25	0.27	0.24	0.31	0.15
Biotic-1	5.24	5.14	5.97	5.39	6.41	6.14	6.59	5.81	6.15	4.76	6.67	6.29	6.62	6.4	7.2	7.31	6.88
B-2	5.32	4.73	5.22	5.48	6.75	4.81	5.95	5.87	6.06	6.05	6.52	6.38	7.17	6.6	6.76	6.92	6.83
B-3	5.21	4.82	5.48	5.65	6.91	5.26	6.42	5.8	6.24	6.5	6.56	6.49	7.18	6.76	7.11	7.11	6.42
B-4	5.29	5.27	5.14	5.63	6.17	5.26	5.95	5.64	5.69	5.88	6.02	6.72	6.61	6.16	6.65	6.23	6.7
B-5	5.27	4.93	5.01	5.77	6.3	6.01	5.91	5.45	5.74	5.91	5.88	6.68	6.03	6.98	6.47	6.81	6.66
B-6	5.11	5.42	4.83	5.58	6.48	5.87	6.65	5.26	5.84	6.21	6.01	6.12	6.33	6.31	6.46	6.43	6.84
B Mean	5.24	5.05	5.27	5.58	6.5	5.56	6.24	5.64	5.95	5.88	6.28	6.45	6.66	6.53	6.77	6.8	6.72
B Std. Dev.	0.07	0.25	0.37	0.12	0.25	0.48	0.32	0.22	0.2	0.54	0.31	0.21	0.42	0.28	0.29	0.37	0.16

Table 36 cont.

Time (hrs)	984	1032	1056	1104	1200	1296	1344
Abiotic-1	7.23	5.97	7.26	6.88	6.86	6.98	6.39
AB-2	7.25	6.42	6.69	7.37	6.59	6.81	6.71
AB-3	6.41	5.06	6.64	7.85	6.16	5.51	6.51
AB-4	6.02	5.35	6.67	7.29	6.43	6.56	6.81
AB-5	6.52	5.91	6.67	6.19	6.16	6.08	5.99
AB-6	6.84	6.04	6.5	7.19	6.7	6.64	6.92
AB Mean	6.71	5.79	6.74	7.13	6.48	6.43	6.55
AB Std. Dev.	0.44	0.45	0.24	0.51	0.26	0.5	0.31
Biotic-1	6.95	5.46	6.41	6.96	6.04	6.83	6.54
B-2	6.7	6.09	5.88	6.99	6.8	6.62	6.67
B-3	6.57	5.64	5.85	7.11	7.01	6.94	6.85
B-4	5.84	6.12	6.23	5.94	6.83	6.36	5.96
B-5	6.77	5.61	6.34	7.02	7.09	7.07	6.48
B-6	6.54	5.53	5.61	6.81	6.67	7.09	5.79
B Mean	6.56	5.74	6.05	6.8	6.74	6.82	6.38
B Std. Dev.	0.35	0.26	0.29	0.4	0.34	0.26	0.38

Table 37. Callahan ICP Measured Metal Concentrations (mg/L)

Time (hrs)	Ca	K	Mg	P	Al	B	Cu	Fe	Mn	Na	S	Zn
Field Samp. 1	313.8	14.9	163.1	0.2894	<0.1	1.678	0.0442	17.38	3.328	17.69	378.9	1.514
Field Samp. 2	277.2	60.5	150.2	0.4424	<0.1	1.489	0.02	12.32	2.424	90.62	343.5	1.048
Field Samp. 3	46.66	12.26	14.73	0.5811	2.21	0.2849	0.7792	42.69	0.75	7.174	94.73	0.2811
Abiotic 0	212.6	29.22	109.3	0.4376	0.8	1.151	0.2811	24.13	2.167	38.49	272.4	0.9477
AB 4	285.4	86.09	162.2	1.475	<0.1	1.69	0.117	11.47	2.13	103.7	402.5	1.378
AB 24	306.9	72.97	165.9	0.3576	<0.1	1.733	0.0987	8.775	2.339	104.6	407.7	1.346
AB 168	295.8	58.38	165.9	1.285	<0.1	1.732	0.0665	4.635	1.215	72.54	410.6	0.702
AB 336	214.3	86.13	158.5	0.5201	<0.1	1.626	0.0326	2.513	0.4503	99.8	388.6	0.3324
AB 1344	287.4	129.3	158.4	1.113	<0.1	1.632	0.1026	7.25	2.106	96.5	392.1	0.8834
Biotic 0	212.6	29.22	109.3	0.4376	0.8	1.151	0.2811	24.13	2.167	38.49	272.4	0.9477
B 4	316.9	87.33	173.8	0.802	<0.1	1.851	0.0697	7.859	1.966	109.4	430.9	1.145
B 24	307.1	75.96	164.5	0.823	<0.1	1.661	0.0713	4.615	2.537	100.6	397	1.458
B 336	229.8	65.61	153.1	0.6165	<0.1	1.518	0.0437	2.125	0.7515	90.19	371.3	0.3454
B 1344	264.5	69.46	151.5	0.5869	6.583	1.506	0.0673	4.907	2.028	86.51	362.9	0.7478

Table 38. Callahan ICP Measured Metal Concentrations (mmol/L)

Time (hrs)	Ca	K	Mg	P	Al	B	Cu	Fe	Mn	Na	S	Zn
Abiotic 0	5.303	0.747	4.498	0.0141	0.0298	0.106	0.00442	0.432	0.0394	1.674	8.493	0.0145
AB 4	7.121	2.202	6.672	0.476	<0.00371	0.156	0.00184	0.205	0.0388	4.511	12.551	0.0211
AB 24	7.658	1.866	6.824	0.0115	<0.00371	0.16	0.00155	0.157	0.0426	4.55	12.713	0.0206
AB 168	7.381	1.493	6.824	0.415	<0.00371	0.16	0.00105	0.083	0.0221	3.155	12.803	0.0107
AB 336	5.347	2.203	6.52	0.0168	<0.00371	0.15	0.00051	0.045	0.0082	4.341	12.117	0.0051
AB 1344	7.171	3.307	6.516	0.0359	<0.00371	0.151	0.00161	0.13	0.0383	4.197	12.226	0.0135
Biotic 0	5.303	0.747	4.498	0.0141	0.0298	0.106	0.00442	0.432	0.0394	1.674	8.493	0.0145
B 4	7.907	2.234	7.149	0.0259	<0.00371	0.171	0.0011	0.141	0.0358	4.759	13.436	0.0175
B 24	7.663	1.943	6.767	0.0266	<0.00371	0.154	0.00112	0.083	0.0462	4.376	12.379	0.0223
B 336	5.734	1.678	6.298	0.0199	<0.00371	0.14	0.00069	0.038	0.0137	3.923	11.578	0.0053
B 1344	6.6	1.776	6.232	0.019	0.244	0.139	0.00106	0.088	0.0369	3.763	11.316	0.0114

APPENDIX C: STATISTICAL CODE AND SOFTWARE PROCEDURES

Statistics in R Code Transcript

```
#sulfate Treatment Comparisons
#Must run lme4 for the lmer function and lmerTest for the lmer function to also test for significance
library(lme4)
library(lmerTest)
bbexp1sulf<-lmer(Exp1~Treatment*Time+(1|Sample), data = bbexpsulf)
summary(bbexp1sulf)
bbexp2sulf<-lmer(Exp2~Treatment*Time+(1|Sample), data = bbexpsulf)
summary(bbexp2sulf)
bbexp3sulf<-lmer(Exp3~Treatment*Time+(1|Sample), data = bbexpsulf)
summary(bbexp3sulf)
#pH Treatment Comparisons
bbexp1pH<-lmer(pH~Treatment*Time+(1|Sample), data = bbexp1)
summary(bbexp1pH)
bbexp2pH<-lmer(pH~Treatment*Time+(1|Sample), data = bbexp2)
summary(bbexp2pH)
bbexp3pH<-lmer(pH~Treatment*Time+(1|Sample), data = bbexp3)
summary(bbexp3pH)
#Conductivity treatment tests
bbexp1cond<-lmer(Cond~Treatment*Time+(1|Sample), data = bbexp1)
summary(bbexp1cond)
bbexp2cond<-lmer(Cond~Treatment*Time+(1|Sample), data = bbexp2)
summary(bbexp2cond)
bbexp3cond<-lmer(Cond~Treatment*Time+(1|Sample), data = bbexp3)
summary(bbexp3cond)
#DO treatment tests
bbexp1DO<-lmer(DO~Treatment*Time+(1|Sample), data = bbexp1)
summary(bbexp1DO)
bbexp2DO<-lmer(DO~Treatment*Time+(1|Sample), data = bbexp2)
summary(bbexp2DO)
bbexp3DO<-lmer(DO~Treatment*Time+(1|Sample), data = bbexp3)
summary(bbexp3DO)
#Can repeat pH tests for conductivity and DO using same dataframes and formula structure
#Comparing sulfate across experiments
#Must first seperate treatments from table and organize into their own tables
#Must rescale time by dividing by 24 to turn into days
#Comparing abiotic sulfate across experiments
```

```
Exp1v2sulfA<-lm(Exp2~Exp1*I(Time/24), data=bbexpsulfA)
summary(Exp1v2sulfA)
Exp1v3sulfA<-lm(Exp3~Exp1*I(Time/24), data=bbexpsulfA)
summary(Exp1v3sulfA)
Exp2v3sulfA<-lm(Exp3~Exp2*I(Time/24), data=bbexpsulfA)
summary(Exp2v3sulfA)
#Comparing biotic sulfate across experiments
Exp1v2sulfB<-lm(Exp1~Exp2*I(Time/24), data=bbexpsulfB)
summary(Exp1v2sulfB)
Exp1v3sulfB<-lm(Exp3~Exp1*I(Time/24), data=bbexpsulfB)
summary(Exp1v3sulfB)
Exp2v3sulfB<-lm(Exp3~Exp2*I(Time/24), data=bbexpsulfB)
summary(Exp2v3sulfB)
#pH, DO, and Conductivity also compared across experiments. New tables were used containing individual chemical parameters for each treatment
#Time scale is very large so must include an adjustment within formulas to change it to days for pH and DO
#Abiotic pH
Exp1v2pHA<-lmer(Exp1~Exp2*I(Time/24)+(1|Sample), data=bbexppHA)
summary(Exp1v2pHA)
Exp1v3pHA<-lmer(Exp1~Exp3*I(Time/24)+(1|Sample), data=bbexppHA)
summary(Exp1v3pHA)
Exp2v3pHA<-lmer(Exp3~Exp2*I(Time/24)+(1|Sample), data=bbexppHA)
summary(Exp2v3pHA)
#Biotic pH
Exp1v2pHB<-lmer(Exp2~Exp1*I(Time/24)+(1|Sample), data=bbexppHB)
summary(Exp1v2pHB)
Exp1v3pHB<-lmer(Exp1~Exp3*I(Time/24)+(1|Sample), data=bbexppHB)
summary(Exp1v3pHB)
Exp2v3pHB<-lmer(Exp3~Exp2*I(Time/24)+(1|Sample), data=bbexppHB)
summary(Exp2v3pHB)
#Abiotic cond.
Exp1v2condA<-lmer(Exp2~Exp1*Time+(1|Sample), data=bbexpcondA)
summary(Exp1v2condA)
Exp1v3condA<-lmer(Exp3~Exp1*Time+(1|Sample), data=bbexpcondA)
summary(Exp1v3condA)
Exp2v3condA<-lmer(Exp2~Exp3*Time+(1|Sample), data=bbexpcondA)
summary(Exp2v3condA)
#Biotic Cond.
Exp1v2condB<-lmer(Exp2~Exp1*Time+(1|Sample), data=bbexpcondB)
summary(Exp1v2condB)
Exp1v3condB<-lmer(Exp3~Exp1*Time+(1|Sample), data=bbexpcondB)
summary(Exp1v3condB)
Exp2v3condB<-lmer(Exp2~Exp3*Time+(1|Sample), data=bbexpcondB)
```

```
summary(Exp2v3condB)
#Abiotic DO
Exp1v2DOA<-lmer(Exp2~Exp1*I(Time/24)+(1|Sample), data=bbexpDOA)
summary(Exp1v2DOA)
Exp1v3DOA<-lmer(Exp3~Exp1*I(Time/24)+(1|Sample), data=bbexpDOA)
summary(Exp1v3DOA)
Exp2v3DOA<-lmer(Exp3~Exp2*I(Time/24)+(1|Sample), data=bbexpDOA)
summary(Exp2v3DOA)
#Biotic DO
Exp1v2DOB<-lmer(Exp2~Exp1*I(Time/24)+(1|Sample), data=bbexpDOB)
summary(Exp1v2DOB)
Exp1v3DOB<-lmer(Exp3~Exp1*I(Time/24)+(1|Sample), data=bbexpDOB)
summary(Exp1v3DOB)
Exp2v3DOB<-lmer(Exp2~Exp3*I(Time/24)+(1|Sample), data=bbexpDOB)
summary(Exp2v3DOB)
#Renaming rows for RDA Data Tables
row.names(NrmFldData)<- c("July","August","September-1","September-2","September-3",
"October-1","October-2","October-3","November-1","November-2", "November-3",
"December-1", "December-2", "December-3", "January-1", "January-2", "January-3", "February-
1", "February-2", "February-3")
row.names(NrmExpChemData)<- c("Exp1.Start1", "Exp1.Start2", "Exp1.Start3", "Exp1.End1",
"Exp1.End2", "Exp1.End3", "Exp2.Start1", "Exp2.Start2", "Exp2.Start3", "Exp2.End1",
"Exp2.End2", "Exp2.End3", "Exp3.Start1", "Exp3.Start2", "Exp3.Start3", "Exp3.End1",
"Exp3.End2", "Exp3.End3")
#Constructing RDAs
#Field Data RDA
library(vegan)
NewFldRDA<-rda(BBGenera.hell, NrmFldData, scaling=2)
summary(NewFldRDA)
plot(NewFldRDA, scaling=2)
#Experimental RDAs
#First clean the normalized experimental data into seperate tables due to missing data for
multiple RDAs
NrmExpChemData1<-NrmExpChemData[-c(4:6),]
NrmExpChemData1<-NrmExpChemData1[,-c(6)]
NrmExpChemData2<-NrmExpChemData[,-c(1:12)]
#Run Experimental RDAs
library(vegan)
NewExpRDA2<-rda(ExpGenera.hell, NrmExpChemData2, scaling=2)
summary(NewExpRDA1)
plot(NewExpRDA1, scaling=2)
NewExpRDA1<-rda(ExpGenera.hell, NrmExpChemData1, scaling=2)
summary(NewExpRDA2)
plot(NewExpRDA2, scaling=2)
```

```
#Adjusting R2 for all RDAs
#Rsquareadj() is located in the vegan package
NewFldRDAadjusted<-RsquareAdj(NewFldRDA)$adj.r.squared
NewExpRDA1adjusted<-RsquareAdj(NewExpRDA1)$adj.r.squared
NewExpRDA2adjusted<-RsquareAdj(NewExpRDA2)$adj.r.squared
#Testing RDAs for significance
anova.cca(NewExpRDA1)
anova.cca(NewExpRDA2)
anova.cca(NewFldRDA)
```

Mothur Script for Sequencing Analyses

#This file will use the batch name BBAll as an example for the scripts
#All files must be in the same folder as mothur.exe for these scripts. Can be done in another folder, but that was not the case for this project.
#Download SILVA reference files and RDP reference files from the mothur site for alignment. SILVA files are version 34 and RDP version 16.
#Prepare stability file for batch using forward and reverse reads received from the GSAF. Named BBAll.stability.files.txt.
#Oligos file prepared with primers from the GSAF's website. Named GSAF.oligos.txt.

Part 1: Cleaning Data and Organizing OTUs

#open mothur.exe
#First step pairs the sequences and set # of processers computer will use for downstream work. # of processers can be changed at any point. The more processers the faster it goes.

make.contigs(file=BBAll.stability.files.txt, processers=5)

#summary is used to view the current output. The command of current will use the most recent output fasta file. This is what will be used for most of the procedure with a few exceptions.

summary.seqs(fasta=current)

#Allows you to see sequences that fall of the desired range for the next step which is screening.
#Screening removes sequences that do not fall in the desired range and ambiguous bases. For the V4/V5 primer used by the GSAF the ideal range is 475-500 bases.

screen.seqs(fasta=current, group=current, maxambig=0, minlength=475, maxlength=500)

#view summary again to double check all bases now fall within desired range. The number of bases should drop from the previous summary view.

summary.seqs(fasta=current)

unique.seqs(fasta=current)
#Merges identical sequences assigns sequences to groups, and selects unique sequences.
#The output file BBAll.stability.files.trim.contigs.good.unique.fasta will be used down the line with SILVA alignment.

count.seqs(name=current, group=current)
#Counts the number of total and unique sequences to now display in summaries.
#Run a summary to see these numbers.

summary.seqs(count=current)

#Process the SILVA files. This was only done once for all batches as the same primer was used for all data received from the GSAF.
pcr.seqs(fasta=silva.bacteria.fasta, start=6388, end=25319)

#renamed the output file to something easier to use down the line

system(rename silva.bacteria.pcr.fasta silva.v34.fasta)

#can view the reference alignment dataset
summary.seqs(fasta=silva.v34.fasta)

#align previously edited sequences with the reference file
align.seqs(fasta=BBAll.stability.files.trim.contigs.good.unique.fasta, reference=silva.v34.fasta)

#check the results of the newly aligned sequences. Should be roughly around the same length. Note median range for use in next screen step.

summary.seqs(fasta=BBAll.stability.files.trim.contigs.good.unique.align,
count=BBAll.stability.files.trim.contigs.good.count_table)

screen.seqs(fasta=BBAll.stability.files.trim.contigs.good.unique.align,
count=BBAll.stability.files.trim.contigs.good.count_table, summary=
BBAll.stability.files.trim.contigs.good.unique.summary, start=6388, end=25316, maxhomop=8)

#max # of homopolymers set to 8, none any longer than 9 in the database. Can be changed if needed

#another summary to make sure all sequences now overlap
summary.seqs(fasta=current, count=current)

#filter removes overhangs, gap characters, and trump charaters
filter.seqs(fasta=BBAll.stability.files.trim.contigs.good.unique.good.align, vertical=T, trump=.)

unique.seqs(fasta=BBAll.stability.files.trim.contigs.good.unique.good.filter.fasta,
count=BBAll.stability.files.trim.contigs.good.good.count_table)
#takes out additional identical sequences after filtering
#Reduces number of unique sequences

#Next will de-noise sequencing by clustering sequences that have up to 4 differences (1 per 100 bp)
pre.cluster(fasta=BBAll.stability.files.trim.contigs.good.unique.good.filter.unique.fasta,
count=BBAll.stability.files.trim.contigs.good.unique.good.filter.count_table, diffs=4)

summary.seqs(fasta=current, count=current)
#number of unique sequences further reduced

#UCHIME algorithm to remove chimeras from the count file. Abundant sequences are the references. Dereplicate=t means that chimeric sequences will only be removed in the samples where they are found, whereas the default (dereplicate=f) will remove it from all samples.
chimera.uchime(fasta=BBAll.stability.files.trim.contigs.good.unique.good.filter.unique.precluster.fasta,
count=BBAll.stability.files.trim.contigs.good.unique.good.filter.unique.precluster.count_table, dereplicate=t)
#Chimeras removed from fasta file
summary.seqs(fasta=current, count=current)
#number of sequences should be reduced again

classify.seqs(fasta=BBAll.stability.files.trim.contigs.good.unique.good.filter.unique.precluster.pick.fasta, count=
BBAll.stability.files.trim.contigs.good.unique.good.filter.unique.precluster.denovo.uchime.pick.count_table, reference=trainset14_032015.rdp.tax, cutoff=80)
#Cutoff refers to bootstrap value for taxonomic assessment. 80% is stringent.

remove.lineage(fasta=BBAll.stability.files.trim.contigs.good.unique.good.filter.unique.precluster.pick.fasta,
count=BBAll.stability.files.trim.contigs.good.unique.good.filter.unique.precluster.denovo.uchime.pick.count_table,
taxonomy=BBAll.stability.files.trim.contigs.good.unique.good.filter.unique.precluster.pick.rdp.wang.taxonomy, taxon=Chloroplast-Mitochondria-unknown-Eukaryota)
#Removes unwanted DNA, unknown=domain level

cluster.split(fasta=BBAll.stability.files.trim.contigs.good.unique.good.filter.unique.precluster.pick.pick.fasta,
count=BBAll.stability.files.trim.contigs.good.unique.good.filter.unique.precluster.denovo.uchime.pick.pick.count_table,
taxonomy=BBAll.stability.files.trim.contigs.good.unique.good.filter.unique.precluster.pic.rdp.wang.pick.taxonomy, splimethod=classify, taxlevel=4, cutoff=0.15
#taxlevel=4 is order

make.shared(list=current, count=current, label=0.03)
#How many sequences are in each OUT at 0.03 cutoff (97%)

classify.otu(list=current, count=current, taxonomy=current, label=0.03)
#creates taxonomy of OTUs

Part 2: subsampling

#Rename the taxonomy files into something a little easier to find and understand

system(rename
BBAll.stability.files.trim.contigs.good.unique.good.filter.unique.precluster.pick.pick.an.unique_list.shared BBAll.stability.an.shared)

system(rename
BBAll.stability.files.trim.contigs.good.unique.good.filter.unique.precluster.pick.pick.an.unique_list.0.03.cons.taxonom BBAll.stability.an.cons.taxonomy)

#Count the number of groups in each sample. This will help us find the smallest to subsample to.
count.groups(shared=BBAll.stability.an.shared)

#Subsample to the lowest count, eliminate unusually low samples
sub.sample(shared=BBAll.stability.an.shared, size=1934)

Part 3: Running alpha diversity indices

collect.single(shared=BBAll.stability.an.shared, calc=chao-invsimpson, freq=100)

#information is in the output files
#rarefaction curve- output can be put into graphical software

rarefaction.single(shared=BBAll.stability.an.shared, calc=sobs, freq=100)
Output File Names:
stability.an.groups.rarefaction

#Table with # of sequences, sample coverage, # obs OTUs, simpson diversity in one file. subsample=T automatically selects smallest library

summary.single(shared=BBAll.stability.an.shared, calc=nseqs-coverage-sobs-invsimpson, subsample=1934)

Watershed Area in ArcGIS

1. Open a new map in ArcGIS and import the modified rivers and streams and DEM layers.
2. From the ArcHydro toolbar, select DEM reconditions from the Terrain Preprocessing and subsequent DEM Manipulation drop-down menus.
3. Type the stream and DEM file names into the pop-up window in the AGREE Stream and Raw DEM spaces respectively.
4. Set stream buffer to 5, smooth drop/raise to 10, and sharp drop/raise to 10.
5. Input the new file name the AGREE DEM space and then run the process.
6. Select Fill Sinks from the Terrain Preprocessing and Data Manipulation drop-down menus on the ArcHydro toolbar.
7. Input the filename from step 5 into the space labeled DEM in the pop-up window. Leave the other options unchanged and run.
8. A new layer will be added to the map. By default, this will be named Fill.
9. Select Flow Direction from the Terrain Preprocessing menu on the ArHydro toolbar.
10. Input the file name into the DEM space in the pop-up window. Presumably this is Fill, unless otherwise changed.
11. The output will be the Flow Direction Grid space. The default output file name is Fdr. Change this if you wish. Leave the Outer Wall Polygon space as null.
12. Run the process. The output will create a new layer which will be added to the map.
13. Select the Watershed tool within Hydrology and Spatial Analyst Tools.
14. Input the flow direction grid file and select the junction point. This will be where Blood Brook empties into the West Branch of the Pleasant River.

15. Run the process.
16. Select Raster to Polygon function in the Raster and Conversion Tools drop-down menu.
17. The output will be a polygon shapefile of the water shed. Select the Blood Brook watershed to view the polygon properties and obtain the watershed area.

BIOGRAPHY OF THE AUTHOR

Raymond Kahler III, better known as “Trey”, hails from the rural community of New Holland in Lancaster County, Pennsylvania. At a young age, he became fascinated with dinosaurs. He would dig for bones in the backyard, and spent countless hours watching and re-watching the Jurassic Park films. Michael Crichton’s message of man wielding science without regard for the consequences has always resonated with Trey. After graduating from Garden Spot High School in 2010, he attended the University of South Carolina for earth sciences, in the hopes of beginning a paleontology career. However, through the influences of Dr. Gene Yogodzinski and Dr. Ron Benner, Trey was encouraged to take his interest in biologic and geologic interactions into a more modern, and much smaller, setting. Upon graduation with a B.S. in 2014, Trey looked to the University of Maine to begin graduate work in biogeochemistry. He began his M.S. in the Fall of 2014 at UMaine under the tutelage of Dr. Amanda Olsen and Dr. Jean MacRae. In his free time, Trey continues to go on adventures with his wife Emily, and their cat TK, all while playing music, and enjoying video games with friends across the country. For the future, Trey looks to begin a career in environmental consulting with an emphasis on remediation. Trey is a candidate for the Master of Science degree in Earth and Climate Sciences from the University of Maine in December 2018.